



<https://theses.gla.ac.uk/>

Theses Digitisation:

<https://www.gla.ac.uk/myglasgow/research/enlighten/theses/digitisation/>

This is a digitised version of the original print thesis.

Copyright and moral rights for this work are retained by the author

A copy can be downloaded for personal non-commercial research or study,  
without prior permission or charge

This work cannot be reproduced or quoted extensively from without first  
obtaining permission in writing from the author

The content must not be changed in any way or sold commercially in any  
format or medium without the formal permission of the author

When referring to this work, full bibliographic details including the author,  
title, awarding institution and date of the thesis must be given

Enlighten: Theses

<https://theses.gla.ac.uk/>  
[research-enlighten@glasgow.ac.uk](mailto:research-enlighten@glasgow.ac.uk)

THE PRODUCTION OF CHARGED PIONS BY PHOTONS.

BY

W.R. HOGG

PRESENTED TO THE UNIVERSITY OF GLASGOW AS A THESIS FOR  
THE DEGREE OF DOCTOR OF PHILOSOPHY, NOVEMBER 1958.

ProQuest Number: 13850362

All rights reserved

INFORMATION TO ALL USERS

The quality of this reproduction is dependent upon the quality of the copy submitted.

In the unlikely event that the author did not send a complete manuscript and there are missing pages, these will be noted. Also, if material had to be removed, a note will indicate the deletion.



ProQuest 13850362

Published by ProQuest LLC (2019). Copyright of the Dissertation is held by the Author.

All rights reserved.

This work is protected against unauthorized copying under Title 17, United States Code  
Microform Edition © ProQuest LLC.

ProQuest LLC.  
789 East Eisenhower Parkway  
P.O. Box 1346  
Ann Arbor, MI 48106 – 1346

## Preface.

There are two investigations presented in this Thesis; both are concerned with the production of charged pions by photons. In the first study, which occupies the major part of the Thesis, the pions were produced by the irradiation of deuterium with photons; in the second, the target was calcium.

The preliminary considerations for the deuterium experiment had been taken before the author started his research in October 1954. It had been decided to use a liquid deuterium target, instead of the subtraction technique necessary for a deuterated hydrocarbon target, for example. From experience gained from an unsuccessful model, and with advice on low temperature techniques from Professor J.F. Allen of the University of St. Andrews, the author designed a liquid deuterium target under the guidance of Dr. E.H. Bellamy. The author was responsible for the supervision of the construction and vacuum testing of this target and of a second one, designed later, for use with liquid hydrogen only. The production and purification of the deuterium gas, necessary for the liquid target, was also part of the work of the author.

The development of a magnetic spectrometer for the deuterium investigation was at first under the supervision of Dr. E.H. Bellamy, but finally the author took full responsibility for the construction and testing of the counter telescopes, and participated in the production of the accompanying electronics. The magnet, designed by Drs. Bellamy, Robb and Rutherglen of this Laboratory, was an existing facility in the Laboratory when the present work commenced. The magnet fixed many of the parameters in the experimental arrangement of the deuterium investigation, so that the spectrometer was developed around the magnet.

The work of collection of the experimental data in the actual runs with the synchrotron beam was shared with other members of the Research Group. The analysis of the results and their interpretation were due solely to the author.

The photoproduction of charged pions from calcium was studied by an entirely different technique, namely detection with nuclear emulsions. The work was carried out in co-operation with D. Sinclair of the Nuclear Emulsion Group of this Laboratory, but the author was responsible for the present interpretation of the experimental results.

The author is greatly indebted to Dr. E.H. Bellamy for supervision and advice during the whole of this work. It is a pleasure to acknowledge the co-operation of Dr. W. McFarlane and his associates of the Synchrotron Group. The author acknowledges the assistance given by Professor J.F. Allen of the University of St. Andrews, in an advisory capacity, and for supplying liquid hydrogen during the early part of this research. For their interest and encouragement in the above research studies, the author wishes to express his gratitude to Professor P.I. Dee and Professor J.C. Gunn. Thanks are also due to the Workshop Staff and Technicians who contributed to this project, and in particular those who constructed the liquid targets, and those who assisted with the electronics. The author is indebted to the Department of Scientific and Industrial Research for the award of a Maintenance Grant which enabled him to carry out the research for the first three years, and to the University Court, Glasgow, for a Research Studentship for the final year.

## Contents.

Page.

Preface.

<u>Chapter I. Introduction.</u>	1
(a) Photoproduction of Pions from Hydrogen.	4
(b) Photoproduction of Charged Pions from Deuterium.	9
(c) Photoproduction of Charged Pions from Calcium.	14
<u>Chapter II. Review of Published Work.</u>	
(a) $\pi^-/\pi^+$ Ratio from Deuterium.	20
(b) Panofsky Ratio and the S-wave Scattering Lengths.	30
(c) $\pi^-/\pi^+$ Ratio from Calcium.	37
(d) Present Investigations.	39
<u>Chapter III. The Photoproduction of Charged Pions from Deuterium - Target.</u>	
(a) Introduction.	41
(b) Description of Targets.	43
(c) Performance of the Targets.	49
(d) Production of Deuterium Gas.	52
(e) Filling Procedure.	56

	<u>Page</u>
Chapter IV. The Photoproduction of Charged Pions from Deuterium - Detector System.	
<hr/>	
(a) Introduction.	59
(b) Detector System.	62
(c) Performance of the Detector System.	71
Chapter V. The Photoproduction of Charged Pions from Deuterium - Results.	
<hr/>	
(a) Experimental Details.	82
(b) Results.	87
Chapter VI. The Photoproduction of Charged Pions from Deuterium - Analysis and Discussion of Results.	
<hr/>	
(a) Threshold Behaviour of the $\pi^-/\pi^+$ Ratio.	92
(b) Threshold Relationship between $r_0$ , $P$ and $(\lambda_3 - \lambda_1)$ .	111
(c) Pion-Nucleon Coupling Constant.	118
Chapter VII. The Photoproduction of Charged Pions from Calcium.	
<hr/>	
(a) Experimental Arrangement.	121
(b) Collection of Data.	123
(c) Interpretation of Results.	126
(d) Discussion.	129
(e) Conclusions.	133

Appendices.

- (1) Derivation of the Panofsky Ratio P from the  $\pi^-/\pi^+$  Deuterium Ratio at Threshold and the S-wave Scattering Lengths. i
- (2) Absorption of Mesons. vi

Publications.

References.

... from production and ... the behaviour of ... about the properties ... the character of the ... nuclear interaction. ... it would be expected ... production of mesons from ... will ... the nature of ... mesons. ... production, ... characteristic ... the ... points of

## Chapter I

Introduction.

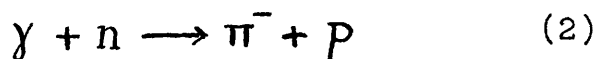
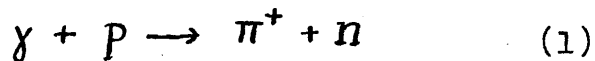
The first observations of the creation of charged pions in nuclear collisions of  $\gamma$ -rays were made at Berkeley by McMillan et al (1949) when a carbon target was irradiated with a bremsstrahlung beam of maximum energy of 335 MeV. It was not till later that charged pion photoproduction from protons was investigated, Steinberger and Bishop (1950). In general, a study of  $\pi$  meson production in heavy nuclei reveals more about the behaviour of nucleons in nuclei than it does about the properties of the  $\pi$  meson field and the character of the  $\pi$  meson-nucleon interaction. It would be expected that the production of mesons from free nucleons would yield the most information about the nature of mesons and their coupling to nucleons.

Before considering meson production, it is worthwhile to note some of the characteristics of the  $\pi$  meson; from the theoretical point of view, the most important properties of charged pions are that they have zero spin and odd parity (for a discussion of these and other properties see Bethe

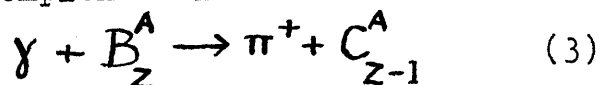
and de Hoffmann 1955). This implies that the charged mesons are pseudoscalar particles with respect to nucleons. The coupling of the meson to the nucleon is unknown but two forms are proposed - pseudoscalar and pseudovector. The main point to note about pseudovector coupling theory is that it cannot be renormalised. If pseudoscalar coupling is considered then the theory contains only one constant, namely the coupling constant giving the strength of meson-nucleon coupling. Therefore, there are two objectives of experiments - to evaluate the coupling constant, and to see if the theory based on this form of coupling is adequate. In the following, experiments involving only the photoproduction of mesons from nucleons will be considered.

The processes by which mesons can be produced by the interaction of photons on nucleons, referred to as photoproduction, can be expressed by the following reactions:

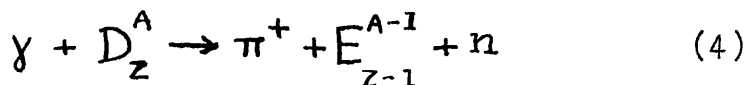
(i) From free nucleons



(ii) From complex nuclei - bound final state



- continuum final state



with similar equations for  $\pi^-$  meson production. In the reactions from complex nuclei, the product nucleus (C or E) may or may not be left in an excited state. In this Thesis, consideration will be given to only those reactions involving the photoproduction of charged mesons of energies such that the de Broglie wavelength of the meson (in the centre of mass system) is not small compared to the range of the interaction. This will include photons of energies up to about 350 MeV.

In the processes given above, (1) to (4), the photons are usually obtained from synchrotrons. Because the  $\gamma$ -ray spectrum from such accelerators is continuous, the energy of the photon responsible for a given event is generally not known. In the production from protons, however, a measurement of any two of the four parameters of the outgoing particles (nucleon and meson momenta and angles with respect to the direction of the photon beam) determines the kinematics, including the energy of the responsible photon. This one to one relationship between the energy of the incoming photon and the energy of the meson produced simplifies the study of the photoproduction of  $\pi^+$  mesons from protons. This is the most amenable of

of the reactions (1) to (4) to experimental investigation.

(a) Photoproduction of Pions from Hydrogen.

Since the first artificial production of positive pions from protons by Steinberger and Bishop (1950) and Bishop et al (1950), a considerable quantity of experimental data has accumulated. From measurements such as the low energy excitation function of both  $\pi^+$  and  $\pi^0$  production, information was obtained about the electromagnetic interaction of the incoming photon with the nucleon. At threshold, the  $\pi^+$  production cross-section was found to increase proportionally to  $(E_\gamma - E_0)^{\frac{1}{2}}$ , where  $E_\gamma$  is the photon energy and  $E_0$  is the threshold energy for the reaction. This energy dependence together with the fact that the angular distribution was almost isotropic near threshold indicated that there was a large s-wave contribution to the cross-section. Another feature of the experimental data was the maximum in the total cross-section at a photon energy near 300 MeV. In general, for comparison with theory the main characteristics of pion photoproduction are the shape and the energy dependence of the angular distributions, and the magnitude and the energy dependence of the total cross-sections.

The understanding of the elementary interactions of

the production and scattering of mesons at low energies has not kept pace with the knowledge of these phenomena. Theoretical work has endeavoured to produce a unified interpretation of the experimental results, but there has not yet been any complete theory for processes involving mesons. The theoretical treatments proposed to explain one or several experimental results can be divided into four groups; strong coupling theories, weak coupling theories, nonrelativistic theories, and phenomenological theories. These categories tend to overlap and some theories make use of ideas of several types. The characteristics of strong coupling (classical) theories are that the nucleons are treated nonrelativistically, that they have a finite size, and that both nucleons and mesons are treated classically (Brueckner and Case 1951, Watson 1952, Brueckner and Watson 1952). This theory gives only qualitative agreement with the observed  $\pi^+$  angular distribution, but the total cross-section predictions are good both for  $\pi^+$  and  $\pi^0$  production. While the meson-nucleon coupling constant is too small for a strict coupling approach, it is found that it is too large for the weak coupling theory to be effective. With this theory, at best, qualitative agreement is obtained (especially near threshold), /

but in general the results seldom compare well with experiment. However, the knowledge of such discrepancies has provided some guidance for a more empirical or phenomenological approach. (Weak coupling is discussed in Marshak 1952).

Considerable success, however, has been achieved with a phenomenological approach to the problems. In particular, great simplification of experimental data has been obtained by Gell-Mann and Watson (1954) who applied to pion reactions a phenomenological analysis. This model was based on the assumptions of charge independence, that the pion-nucleon interaction had a finite range, and that the p-state of the pion-nucleon system with total isotopic spin  $3/2$  and total angular momentum  $3/2$  was one of specially strong interaction. The concept of a resonance state with  $T = 3/2$  and  $J = 3/2$  was first suggested by Breuckner and Case (1951). As one example of the success of this model, the ratio of the contribution of the p-state to neutral and charged meson cross-sections was predicted as 2:1. At the resonance (about an energy of the photon of 300 MeV), the ratio was confirmed to have this value. (For example see the results of Tollestrup et al 1955, Walker et al 1955a, Oakley and Walker 1955 and Walker et al 1955b). This was in contrast to weak coupling

theory, for instance, which failed to give the observed shape of the angular distribution of  $\pi^+$  mesons at 250 MeV and which predicted a very small  $\pi^0$  cross-section, with respect to the  $\pi^+$  value, at all energies. On summing up, it was found that the three postulates of charge independence, finite interaction range, and the resonance hypothesis provided a successful and reasonably complete framework for describing the evidence for meson phenomena at low energies.

The applicability of nonrelativistic theories is limited to low energy pion physics, where this approach has met with considerable success. This has been due in part to the phenomenological elements used in the theories, that is elements which can be derived without recourse to any specific model. The exponents of the nonrelativistic theories are Chew (1953) and Low (1955). For each of the two couplings, pseudoscalar and pseudovector, a theory of pion-nucleon interactions can be established and studied by the perturbation method, that is the expansion of observable quantities in powers of the coupling constants. In pseudoscalar theory, the expansions turn out to be infinite, but by expressing the results in terms of the observed mass and charge of <sup>the</sup> electron (mass and charge renormalisation), the/

infinities are removed. However, this is not true in pseudovector theory. In his static cut-off pseudovector theory, Chew introduces the modification of a finite radius for the bare nucleon. The result of this is to cut off all integrals over virtual pion momenta at an energy which is an upper limit, and is of the order of the nucleon rest mass. This cut-off makes the theory nonrelativistic. In the cut-off pseudovector theory, the nucleons are treated as fixed, and all or most of nucleon recoil effects are neglected. This is the static approximation. The most important result of the static model approach to photomeson production (Chew and Low 1956) is that the main part of the low energy matrix element can be expressed as a function of the scattering phase shifts (obtained from either experiment or theory) and the static nucleon magnetic moments, and the remainder is given by the Born approximation. The approach taken by Low is different. This author redefines the nucleon state vectors (which are used in the calculation of the matrix element) to represent real nucleons, that is the particles in this theory are renormalised. While in Chew's theory, it is possible to calculate the matrix element for a nonrelativistic process, in the Low theory the mathematics

is complicated and it yields an integral equation, an explicit solution of which has not yet been obtained. There are, nevertheless, quite successful solutions calculated using phenomenological ideas. For example, Low's theory gives good quantitative agreement with observed results for charged pion production. This theory will be referred to later in the discussion of the deuterium experiment. It is found that even the crudest approximation to Low's nonrelativistic theory gives good agreement with the experimental data of the negative to positive pion ratio.

Recently, Chew et al (1957) have constructed a theory of meson-nucleon scattering and of meson photoproduction using dispersion relations. The numerical evaluation of this theory has not yet been published. It is, therefore, not possible at present to say whether agreement with experiments will be improved by this new approach.

(b) Photoproduction of Charged Pions from Deuterium.

In the production of mesons, the incident photon can interact with the currents of either the proton or the charged mesons. With this in mind, consider the other basic photoproduction process from neutrons;



For this reaction, the incident photon has two currents with which to interact, namely that carried by the recoil proton and that by the  $\pi^-$  meson. According to Breuckner and Goldberger (1949), in the production of the  $\pi^-$  meson there is constructive interference between the contribution of the current of the meson and that of the recoil proton. In the positive meson production, the recoil particle is a neutron and, therefore, does not contribute to the current. Hence it would be expected that  $r$  would be greater than unity, where  $r$  is defined as

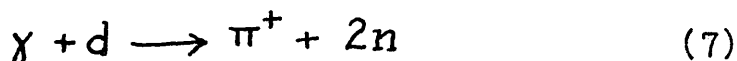
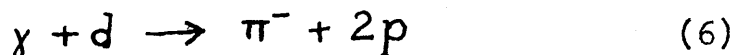
$$r = \frac{\sigma(\gamma + n \rightarrow \pi^- + p)}{\sigma(\gamma + p \rightarrow \pi^+ + n)} \quad (5)$$

The study of the photoproduction of mesons from neutrons is not possible directly but some information may be obtained from photoproduction from deuterium.

Meson production from deuterium is of interest on account of the data it yields about the dependence of the reaction on the charge and spin of the nucleons. The charge dependence is revealed in the ratio of the cross-sections of negative to positive mesons, and the spin dependence in the ratio of positive mesons from protons and from deuterons.

Investigations of meson production processes from the deuteron present difficulties from the viewpoint of

both theory and experiment. This results basically from the fact that in dealing with this, the three body problem is encountered, and the presence of the second nucleon greatly complicates the phenomenon. For example, the angle and energy of a single reaction product in either of the reactions:



does not uniquely define the energy of the incident photon responsible for the reaction.

In order to compare theories of photomeson production with experiment, it is desirable to investigate the production from free neutrons as well as from free protons. As already stated, the deuteron is the simplest system involving neutrons, hence it is necessary to understand how the observed pion production from a bound nucleon in deuterium is related to that from a free nucleon. There are various ways of tackling this problem; one may study positive pion production from both hydrogen and deuterium to compare the free and the bound proton. Alternatively, it is possible to measure the hydrogen to deuterium neutral pion production. Finally, the negative to positive ratio of pion photo-production can be used to give an insight into this problem. These last two experiments include pion

production from bound neutrons. As this last ratio from deuterium forms the main topic of this Thesis, it will be discussed more fully.

There are several reasons, both experimental and theoretical, why it is profitable to study the ratio of the cross-sections of the two basic photoproduction reactions,  $r$ . There is the trivial reason that it is not possible to measure (2) directly. In order to overcome this, one might use experiments from various complex nuclei and develop a theory to derive the ratio  $r$  from the measured  $\pi^-/\pi^+$  ratio from the complex nuclei. However, it is easier to select deuterium as the example of the complex nucleus and apply a correction factor specifically calculated for deuterium to obtain the ratio  $r$ . This factor - the Coulomb correction - will be dealt with later. Experimentally, it is easier to make relative measurements, such as a ratio, since the efficiency of the measuring technique may be eliminated. On the theoretical side, it is reasonable to think that when a ratio is considered, some features of the theory might cancel out, thereby simplifying the treatment. As an example, the coupling constant in the lowest order perturbation theory drops out in the ratio  $r$ .

In the investigations presented here, the measured quantities were the relative yields of negative and positive photomesons from deuterium, expressed as the ratio R where

$$R = \frac{\sigma(\gamma + d \rightarrow \pi^- + 2p)}{\sigma(\gamma + d \rightarrow \pi^+ + 2n)} \quad (8)$$

For deuterium, the  $\pi^-/\pi^+$  ratio is not the same as for free nucleons, because of Coulomb effects and because of the possible interaction of the charged mesons with the product nucleons before the pions escape from the range of their interaction. Near threshold, some of these effects are negligible, but the strongest influence of the Coulomb force would be expected at forward pion angles because of the lower velocities of the corresponding recoiling nucleons.

The main interest of this work is at pion threshold, and this is twofold; firstly, there is a theoretical prediction of 1.3 (see Chew et al 1957) for the value of the ratio r at threshold

$$r_0 = \left\{ \frac{\sigma(\gamma + n \rightarrow \pi^- + p)}{\sigma(\gamma + p \rightarrow \pi^+ + n)} \right\}_{\text{threshold}} \quad (9)$$

so that the relationship between the measured ratio R from deuterium and that for free nucleons r is of special

importance. Secondly, a relationship exists between  $r_0$ , the Panofsky ratio  $P$ , and the difference of the s-wave scattering lengths of the ( $\pi$ , p) system ( $\lambda_1 - \lambda_3$ ), Anderson and Fermi (1952). Here the Panofsky ratio  $P$  is defined as the ratio of the charge exchange scattering rate and the radiative transition rate of negative pions on protons, Panofsky et al (1951). Also,  $\lambda_1$  and  $\lambda_3$  are the s-wave scattering lengths (in units of  $\hbar/\mu c$  where  $\mu$  is the pion mass) corresponding to the states of isotopic spin of 1/2 and 3/2 respectively. By definition,  $\lambda = \alpha/q$  where  $\alpha$  is the s-wave scattering phase shift and  $q$  is the pion momentum in the centre of mass system. The values of  $\lambda_1$  and  $\lambda_3$  can be obtained from a phase shift analysis of the elastic scattering of negative pions on protons. The second point of interest in this work can be re-stated in the form that the Panofsky ratio can be used to connect the positive energy s-wave cross-sections for pion-proton scattering and pion photoproduction.

(c) Photoproduction of Charged Pions from Calcium.

The production by photons of charged pions from a complex nucleus, calcium (the last stable even - even nucleus), was also studied. The reactions can best be

described in terms of the relative yields of  $\pi^-$  and  $\pi^+$  mesons from the calcium nucleus. The problem in this case, as compared to the deuterium experiment, was more complex due to the presence of the other nucleons in the calcium nucleus, but it was possible to interpret the results in terms of the basic reactions (1) and (2) from free protons and neutrons.

We are considering a photoproduction process from a nucleus as distinct from a nucleon. Such a modification cannot be effected without complicating the theoretical treatment of the problem. For one thing the simplicity of the kinematics is lost. If, however, the production from a complex nucleus can be regarded as an interaction of the photon with a single nucleon, then certain conclusions can be drawn when a comparison is made between this single nucleon reaction and the production from a free nucleon. This is based on the observation that, with a given incident photon energy and at a given angle, there is in general a broad spectrum of mesons produced from a complex nucleus. As a result of the spread in momenta of nucleons in the complex nucleus, there exists no unique photon energy corresponding to a given energy and angle of emission of the pion. Instead, there corresponds a band of

photons available for meson production. Secondly, for a given energy and angle of emission of the meson, the average energy of the photons available for production from a complex nucleus is different from that from a free nucleon. This difference depends on the binding energies of the nucleons in the nucleus, and the interactions of the recoiling nucleons and mesons with the product nucleus, including the Coulomb interaction.

In other words, the reactions from nuclei differ from the free nucleon processes in other than kinematic aspects. This can be illustrated further; in the case of charged production, the processes turn one of the protons in the nucleus into a neutron or vice versa. This involves changes in energy which have to be taken into account. Also, in the supposed interaction of the meson on its way out of the nucleus, it might undergo charge exchange and thereby change the observed emission angle and energy. It is clear that the treatment of photoproduction from complex nuclei is in general a complicated joint problem of pion physics and nuclear physics. It is, therefore, not very useful for yielding information about processes which cannot be observed

directly from free nucleons. Alternatively, it would be anticipated that photoproduction from complex nuclei would give more data about nuclear properties than about basic meson interactions.

Following the earlier work of Lax and Feshbach (1951), the production of charged mesons from heavy nuclei has been considered theoretically by Butler (1952). The two main experimental observations in this field are as follows:

- (i) The meson yields per nucleon from complex nuclei are less than the yields from free nucleons.
- (ii) The total yield for  $\pi^-$  and  $\pi^+$  mesons together exhibit an  $A^{2/3}$  dependence, where A is the mass number.

This last result would suggest that only nucleons on the surface of the nucleus contribute to meson production. In his calculations, Butler (1952) considers only surface production. From this, it would appear that the relative densities of protons and neutrons at the surface of the nucleus are important.

As already noted from the argument involving the interactions of currents, a comparison of the fundamental reactions (1) and (2) led to the conclusion that the

$\pi^-/\pi^+$  ratio,  $r$ , would be expected to have a magnitude greater than unity.

In general, the foregoing can be summarised to give the following factors which might be considered important in influencing the value of the  $\pi^-/\pi^+$  ratio from complex nuclei.

- (i) The position in the bremsstrahlung spectrum of the band of photons responsible for the production of  $\pi^-$  mesons and  $\pi^+$  mesons.
- (ii) Limitations on the final states of the recoil nucleon.
- (iii) Coulomb field effects.
- (iv) The variation of the effective neutron to proton ratio at the nuclear surface.
- (v) The intrinsic reduction of  $\gamma + p \rightarrow \pi^+ + n$  relative to  $\gamma + n \rightarrow \pi^- + p$ .

In the field of photoproduction from heavy nuclei, the main lines of investigation have been the variation with atomic number of the ratio of negative and positive mesons, and the same variation with the total number of charged mesons. Littauer and Walker (1952) made extensive measurements of pion yields from many nuclei. For symmetrical nuclei, they found that the  $\pi^-/\pi^+$  ratio decreased steadily with atomic number. This could

be explained in terms of the increasing Coulomb repulsion leading to lower binding energies for the protons. It was thought that the last symmetrical nucleus, calcium, was an interesting one in which to study the trend of the  $\pi^-/\pi^+$  ratio with pion energy at a given angle of emission. This was the subject of the second investigation.

## Chapter II

Review of Published Work.

This is a review of previous measurements in the fields introduced in the foregoing Chapter, and also includes a brief description of the present studies.

(a)  $\pi^-/\pi^+$  Ratio from Deuterium.

The early measurements of the ratio of negative to positive pions from deuterium gave a value close to unity, and independent of pion energy. These results were obtained using bremsstrahlung beams of maximum energies around 300 MeV. The mesons detected had energies in the range 40 to 130 MeV, and they were emitted at angles between  $45^\circ$  and  $180^\circ$  (in the laboratory system) to the direction of the photon beam. Both types of detector systems of nuclear plates and counter telescopes (with and without magnetic analysis) were used in conjunction with the following types of targets:

- (i) Subtraction technique (for example, heavy water - light water, or deuterated hydrocarbon - carbon targets), as used by Lebow et al (1952), Littauer and Walker (1952), Palfrey et al (1953), and Jenkins et al (1954).

- (ii) Cooled high pressure gas target. See White et al (1952).

The statistical accuracy of this early work was poor, as can be seen from figures 1, 2 and 3.

Of the above groups working in this field, the technique which was most interesting was that of Jenkins et al (1954), since it was not unlike the one adopted in the present work, differing mainly in the type of target used. The Cornell group made measurements of the yields of charged pions produced from light water and heavy water targets by bremsstrahlung beams of maximum energies of 200, 235, and 265 MeV. The pions were deflected through collimating slits by a  $90^\circ$  double focusing magnet, which had external foci, and they were detected in a counter telescope of three proportional counters. Altogether three different angles of emission of the pions were investigated, but the results suffered from poor counting statistics, the best being about 16%.

Recent results which were more statistically significant are shown in figures 4, 5, 6 and 7, which give the California Institute of Technology (Cal. Tech.) and the Rome - Illinois measurements. The authors were Sands et al (1954), Carlson-Lee et al (1955), and Beneventano et al (1954), (1956) and (1956s). At the Cal. Tech. laboratory, the mesons were produced in a

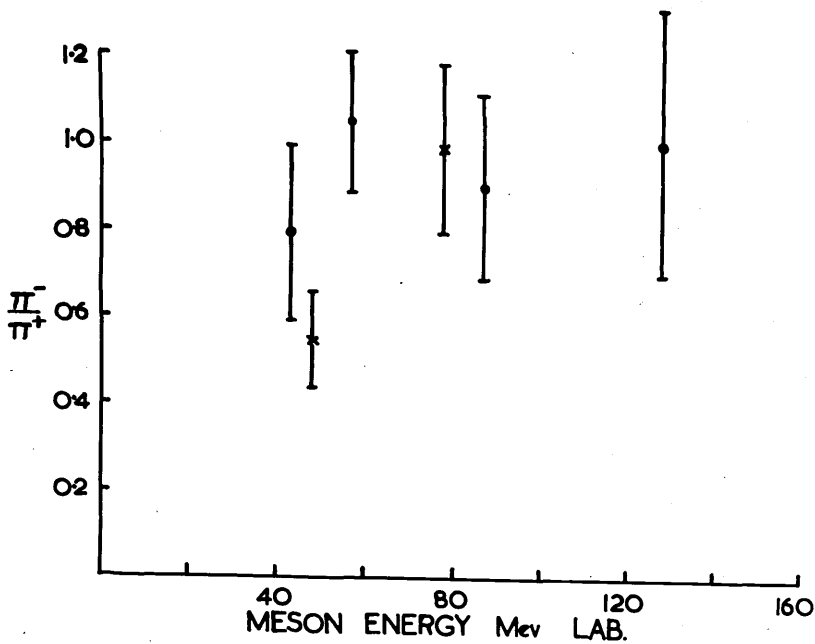


Figure 1. 45°

• White et al (1952), x Jenkins et al (1954).

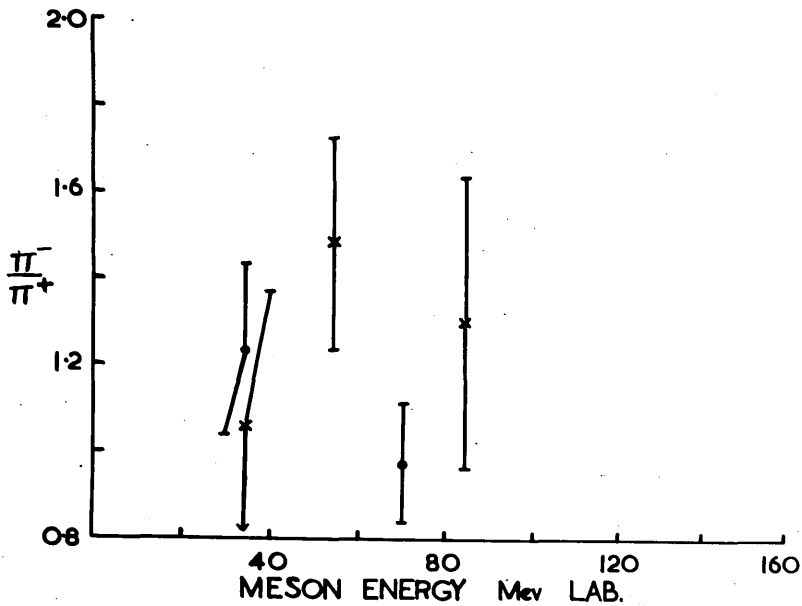


Figure 2. 90°

• White et al (1952), x Jenkins et al (1954).

$\pi^-/\pi^+$  ratio from deuterium as a function of meson energy, angles measured in the laboratory system.

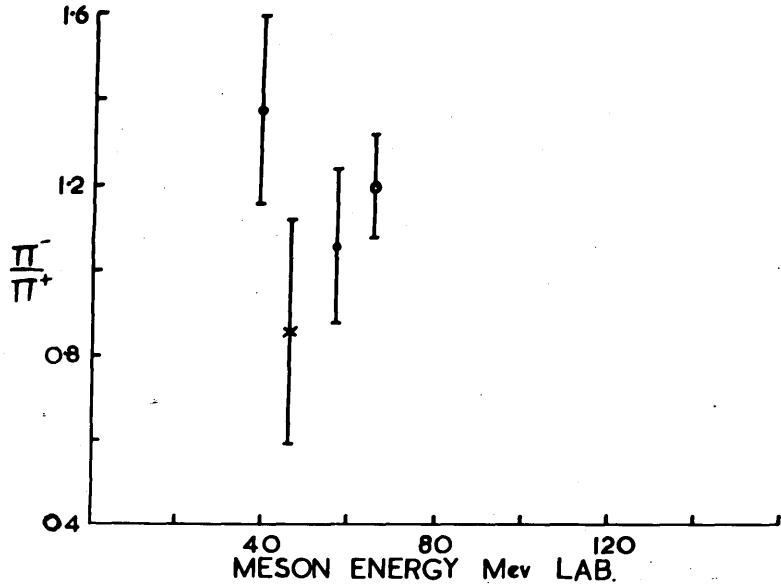


Figure 3.

- 135° White et al (1952), × 180° Jenkins et al (1954),
- 135° Littauer and Walker (1952).

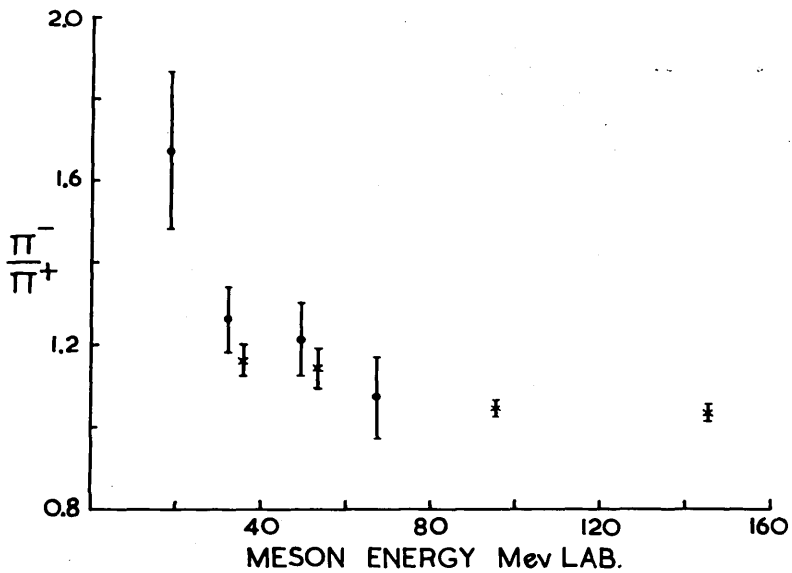


Figure 4.

- × 29° Sands et al (1954),
- 45° Beneventano et al (1956).

$\pi^-/\pi^+$  ratio from deuterium as a function of meson energy, angles measured in the laboratory system.

high pressure cooled deuterium gas target by a bremsstrahlung beam of maximum energy of 500 MeV. The yields of the  $\pi^-$  and  $\pi^+$  mesons were measured in the laboratory system at angles of  $29^\circ$ ,  $73^\circ$  and  $140^\circ$  for several meson energies, by a detection system consisting of a magnet and a counter telescope. A later report gave measurements made at  $104^\circ$  in the laboratory system, Watson et al (1956). The magnet was wedge-shaped and could focus mesons of energies up to 300 MeV. After the magnetic analysis, the pions were focused into a coincidence telescope of two large liquid scintillators with lead absorber between the scintillators, as described by Walker et al (1955a). Corrections were made for background counts from the empty target, for decay in flight of the pions, for the fraction of  $\mu$  mesons counted, and for the electron contamination of the total counts. The results indicated that the value of the  $\pi^-/\pi^+$  ratio was near unity for forward angles and high meson energies, but rose steeply for angles backward of  $90^\circ$  at these energies. Near threshold, however, the ratio tended to a visual extrapolated value of 1.4 as indicated by the measurements at the four angles. At backward angles, it is seen that

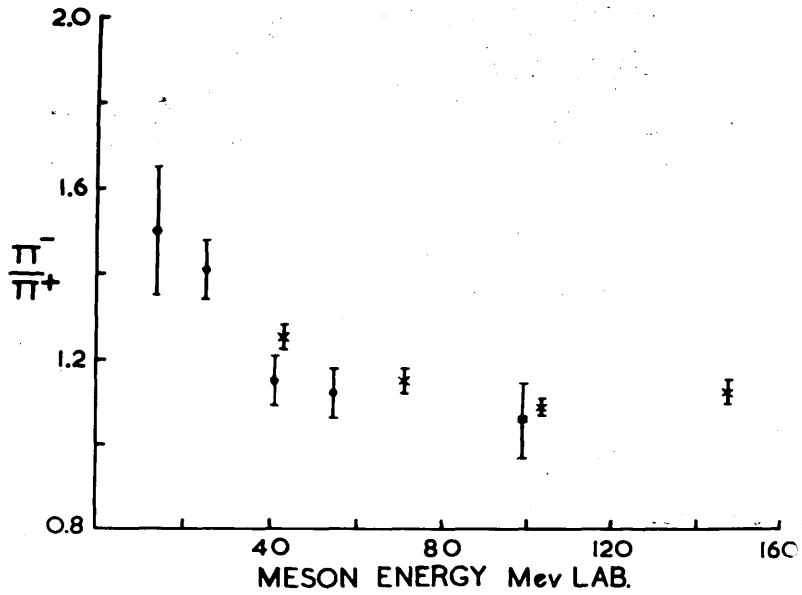


Figure 5.  
 x 73° Sands et al (1954),  
 ● 75° Beneventano et al (1956),  
 ■ 73° Land (1956).

$\pi^-/\pi^+$  ratio from deuterium as a function of meson energy,  
 angles measured in the laboratory system.

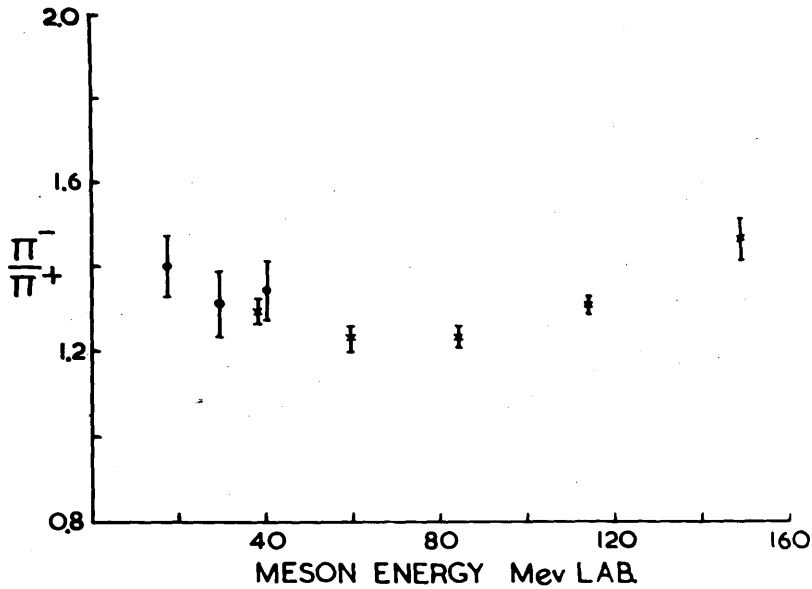


Figure 6.  
 × 104° Sands et al (1954),  
 • 105° Beneventano et al (1956).

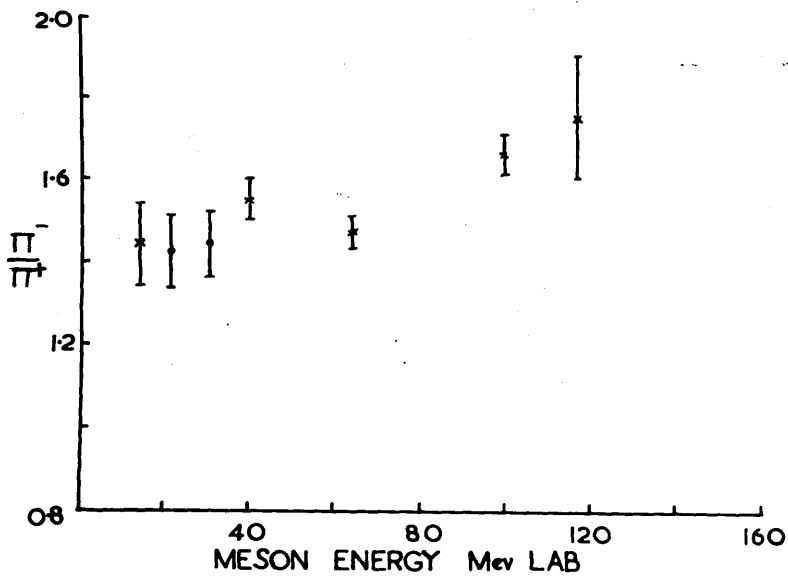


Figure 7.  
 × 140° Sands et al (1954),  
 • 150° Beneventano et al (1956).

$\pi^-/\pi^+$  ratio from deuterium as a function of meson energy,  
 angles measured in the laboratory system.

production of pions was greater from neutrons than from protons. Two points worth noting about these results are firstly the good statistics obtained; except for the results at  $140^\circ$  in the laboratory system, most of the points had statistical errors between 2 and 5 per cent. Secondly, the lower limits of the pion energy detected varied from 30 MeV at  $140^\circ$  lab., to about 50 MeV at  $29^\circ$ . In other words, there was no attempt to reach low pion energies.

The second work quoted is that of the Illinois and Rome laboratories who used the 300 MeV Illinois betatron and a liquid deuterium target, with nuclear pellicles as detectors, for their investigation; the production of charged pions from deuterium was measured at photon energies between 195 and 300 MeV at angles of  $45^\circ$ ,  $75^\circ$ ,  $105^\circ$  and  $150^\circ$  in the laboratory system. In the comparison of the Cal. Tech. and the Rome - Illinois results, figures 4 to 7, the latter were reduced to values of the  $\pi^-/\pi^+$  ratio as a function of the kinetic energy of the pion. The pion energies were determined on the assumption that the nucleons were initially at rest. As indicated in the figures, the trend of the  $\pi^-/\pi^+$  ratio at threshold was towards a value close to 1.6.

In a later analysis of these results, Beneventano et al (1956) obtained a value of  $r$  at threshold at  $90^\circ$  in the centre of mass system (c.m.s.) to be  $r_0 = 1.87 \pm 0.13$ . The derivation of this threshold ratio was based on the results of the photoproduction angular distribution of positive pions from hydrogen. This value was obtained from measurements at  $90^\circ$  c.m.s. where the influence of binding and Coulomb forces was presumed to be small. This extrapolation to zero momentum and general analysis will be discussed in a later Chapter.

The Rome - Illinois work was reported in four papers over a period of two years, the final publication, Beneventano et al (1956), embracing most of the previous accounts. This last paper is a review of results of charged photopion production from hydrogen and deuterium, giving the experimental techniques, results, corrections applied to these results, and the methods of analysis. It is difficult to criticise the procedure adopted to obtain the deuterium  $\pi^-/\pi^+$  ratio from the observed quantities, and to estimate the reliability of the results. The scanning efficiency was high, around 99% and never below 97%. Stripped nuclear emulsions were

used and samples from the sea of emulsion were scanned, thereby eliminating edge effects. All obvious corrections were made to take into account decay in flight, nuclear interactions of the pions before ending in the emulsion, and the background from the target walls, these corrections amounting to less than 15% with an error of about 20%. Hence, it is evident that the identification of the pions was investigated in great detail.

In the nuclear emulsion detection technique for pions, there is always the problem of identification of one-pronged stars. If it is impossible to see the decay positron in the scheme  $\pi^+ \rightarrow \mu^+ \rightarrow e^+$ , then it is not certain whether a given track of mesonic nature with a one-pronged secondary is a  $\pi^+$  or a  $\pi^-$  meson. In such circumstances, the one-pronged events are usually analysed in terms of previously established work in the prong frequency analysis of  $\pi^-$  mesons. The Rome - Illinois group adopted this method, and in particular they carried out a control experiment with a beam of magnetically focused negative mesons from the Illinois betatron and detected the mesons in Ilford G5 (600 microns) nuclear plates, obtaining over

1500  $\pi^-$  events. In this exposure, the decay positron tracks were visible so that the one-pronged stars could be divided with certainty into  $\pi^-$  and  $\pi^+$  groups simply from the scanning of the emulsion. The results of this control experiment were analysed in terms of the prong frequency of  $\pi^-$  mesons, and a comparison with results of the deuterium experiment expressed in the same coefficients showed close agreement. It is obvious that there was internal consistency in the Rome - Illinois work. However, if the coefficients of the  $\pi^-$  meson prong frequency of this work are compared with other results in this field (these coefficients are given in Table 1), there is no longer consistency. Only those results which were obtained with the same convention for the length of a track were considered. When the more statistically significant, and more recent, of these are compared to the Rome - Illinois coefficients, the tendency is to decrease the values of the  $\pi^-/\pi^+$  ratios obtained by the Rome - Illinois group by a factor of about 10%.

Apart from the detection technique, the main difference between the Cal. Tech. and the Rome - Illinois experimental arrangements was the maximum energy of the bremsstrahlung used to irradiate the

Reference	Number of Prongs					Track Length	Pions Observed
	N <sub>0</sub>	N <sub>1</sub>	N <sub>2</sub>	N <sub>3</sub>	N <sub>4</sub>		
Cheston and Goldfarb (1950)	35.2	23.3	16.5	16.1	7.0	1.9	429
De Sabbata et al (1953)	27 +3	32.3 +2.2	19.2 +1.7	14.2 +1.4	6.1 +0.9	1.2 +0.4	500
Demeur et al (1956)	39 +3	24.4 +1.2	16.7 +1.0	12.3 +0.8	6.1 +0.6	1.4 +0.3	576
Beneventano et al (1954)	30.2 +2.1	32.4 +1.3	18.4 +1.0	12.8 +0.8	5.5 +0.6	1.0 +0.2	1634
	30.5 +1.5	31.6 +2.0	19.4 +1.5	12.9 +1.3	5.0 +0.8	0.6 +0.3	

Prong Frequency of  $\pi^-$  Mesons in Nuclear Emulsions

Table 1.

targets, namely 500 MeV and 300 MeV respectively. Due to the availability of higher energy quanta for producing pions, it is not unreasonable to consider the case of a high energy pion, at creation, which is scattered in the nucleus and is detected as a lower energy pion. The general result of such nuclear scattering would be to make the observed  $\pi^-/\pi^+$  ratio less steeply dependent on the pion energy, especially where the  $\pi^-/\pi^+$  ratio differed most from unity. This effect would be more pronounced in the Cal. Tech. results, but the magnitude of such an effect on the ratio is difficult to estimate.

In conclusion, a summary of the main points of the above two reviews can be made as follows:

- (1) The Cal. Tech. and the Rome - Illinois groups together have made the most important contribution to date to the knowledge of the behaviour of the  $\pi^-/\pi^+$  ratio from deuterium with pion energy and angle of emission.
- (2) While the more statistically significant results were those of Sands et al, unfortunately there were no measurements in the interesting low energy region.

- (3) Beneventano et al made the first measurements of the  $\pi^-/\pi^+$  ratio at pion energies near to threshold, but there was no significant overlap with the results of Sands et al at high energy, so that it was not certain whether there was consistency in the two separate measurements.
- (4) The two sets of results gave on analysis threshold values of the  $\pi^-/\pi^+$  ratio which differed by as much as 30%.
- (5) There is need to establish accurate  $\pi^-/\pi^+$  ratios at pion energies which go down to at least 10 MeV but yet overlap the Cal. Tech. energy region. This would confirm whether the existing results were experimentally consistent or not. If there was consistency, then it would be necessary to examine carefully the methods of analysis and the interpretation of the previous results to decide which, if any, was based on sound theoretical arguments, and thereby elucidate the above discrepancy.

A preliminary report was given at the C.E.R.N. Symposium, Geneva (1956) of work being done by Land at M.I.T. to measure the  $\pi^-/\pi^+$  ratio from deuterium.

The technique adopted was to analyse the pions magnetically and to select them by range measurements in a telescope of six counters. Two angles of emission of the pion, viz.  $73^\circ$  and  $120^\circ$  (lab.), were chosen and the maximum energy of the bremsstrahlung beam was varied between 223 MeV and 307 MeV. For some of the measurements a bremsstrahlung spectrum was used, and for others two such spectra were subtracted to give the  $\pi^-/\pi^+$  ratio for pions produced by a narrow band of photons. The results obtained by the subtraction method were not statistically different from those obtained from the single bremsstrahlung spectrum. In general, no disagreement was found with values of the ratio found by other observers.

It has also been reported that Carlson-Lee (1958) at Illinois was making  $\pi^-/\pi^+$  ratio measurements. Pions from a liquid deuterium target were detected in a nuclear emulsion stack. The result quoted was  $R = 2.10 \pm 0.17$  for an average pion energy of 9.2 MeV at an angle of  $90^\circ$  in the centre of mass frame. This ratio was corrected for Coulomb effects to give a value of  $1.83 \pm 0.15$ . No further details are known.

## (b) Panofsky Ratio and the S-wave Scattering Lengths.

Originally Panofsky et al (1951) found that the charge exchange rate of capture of  $\pi^-$  mesons from the K shell in hydrogen

$$\omega (\pi^- + p \rightarrow \pi^0 + n) \quad (10)$$

was comparable with the radiative capture rate

$$\omega (\pi^- + p \rightarrow \gamma + n) \quad (11)$$

That is  $P = \frac{\omega (\pi^- \rightarrow \pi^0)}{\omega (\pi^- \rightarrow \gamma)} = 0.94 \pm 0.20$ .

The  $\gamma$ -ray from the process (11) is monoenergetic, having energy of 130 MeV, whereas the  $\gamma$ -rays from the  $\pi^0$  decay in (10) have a distribution of energies centred on 70 MeV, due to the Doppler shift produced by the motion of the  $\pi^0$ . The experiment was carried out using a conventional pair spectrometer to determine the energy distribution of the  $\gamma$ -rays from  $\pi^-$  capture in a cooled high pressure hydrogen gas target. With this experimental arrangement, the energy resolution was good but the detection efficiency was very low. This accounts for the poor statistical accuracy of the measurement.

Later, two determinations of P were carried out at Liverpool; Keuhner et al (1956), using a  $180^\circ$

focusing pair spectrometer, obtained the value  $P = 1.60 \pm 0.17$ . The other measurement was made by Cassels et al (1957) simultaneously, but this group used a total absorption spectrometer to give  $P = 1.50 \pm 0.15$ . The relative intensities of the gamma radiation from the absorption of stopped negative pions in a liquid hydrogen target were measured by a Cerenkov counter. In this case, the efficiency of detection was high but the energy resolution was poor. Hence, the combined Liverpool results should be reliable since the one technique was complementary to the other.

More recently, by the technique of a total absorption Cerenkov spectrometer, Fischer et al (1958) at Chicago made a measurement of the capture of  $\pi^-$  mesons in liquid hydrogen. This resulted in the determination  $P = 1.87 \pm 0.10$ . The surprising observation is that this was the technique used by Cassels, and yet the difference in the results amounts to over 20%. This would suggest that there might exist a systematic error in one or other of these experiments. However, other results, not yet published, indicate agreement more with the Liverpool results than with Chicago. The low value of the original measurement is difficult to explain, but it may be indicative of

the method used, and how the improved techniques and more intense pion beams now available can lead to more accurate results. If one accepts the errors of the four experimental values of P, the weighted mean of the combined results is  $P = 1.65 \pm 0.10$ .

Now to a consideration of the s-wave scattering lengths  $\lambda_1$  and  $\lambda_3$ . The results of experiments on the elastic scattering of  $\pi^+$  and  $\pi^-$  on protons can be expressed in terms of real phase shifts characterising partial waves. For very low energy scattering, only two parameters need be considered namely  $\alpha_1$ , which is the phase shift corresponding to the isotopic spin state  $I = 1/2$ , and  $\alpha_3$  that for  $I = 3/2$ . If Coulomb effects are neglected, then one may write for s-wave scattering:

$$\begin{aligned} \sigma(\pi^+, \pi^+) &= 4\pi \lambda_c^2 \lambda_3^2 \\ \sigma(\pi^-, \pi^-) &= \frac{4\pi}{9} \lambda_c^2 (\lambda_3 + 2\lambda_1)^2 \end{aligned} \quad (12)$$

and 
$$\sigma(\pi^-, \pi^0) = \frac{8\pi}{9} \frac{v_0}{v_-} \lambda_c^2 (\lambda_3 - \lambda_1)^2$$

where  $\lambda_c$  is the pion Compton wave length,

$\lambda$  is the scattering length i.e.  $\lambda = \frac{\alpha}{q}$  where

$\alpha$  is the phase shift,

$q$  is defined as the pion momentum, in units of  $\mu c$ , in the centre of mass frame,

$v_0$  is the velocity of the outgoing  $\pi^0$ ,  
and  $v_-$  is the velocity of the incoming  $\pi^-$ .

The above expressions indicate which scattering length(s) is (or are) obtained from a given scattering process.

There have been many determinations of these parameters  $\lambda_1$ ,  $\lambda_3$ , and some of the earlier results are given in Table 2. Orear (1956) published values of  $\lambda_1$  and  $\lambda_3$  obtained from a least squares determination of reported data for all low energy pion-nucleon scattering results containing s-wave scattering phase shifts for pion energies up to 60 MeV. This analysis was based on the assumption that the s-wave scattering lengths showed a linear dependence on the c.m.s pion momentum.

The results are  $\lambda_1 = 0.167 \pm 0.012$  (13)

and  $\lambda_3 = -0.105 \pm 0.010$

It is observed that Leiss et al (1955) suggested that  $|\lambda_1 - \lambda_3|$  might not be expected to depend linearly on  $q$  right down to low pion energies. This was the criticism of the Orear extrapolation to threshold which was stated in the paper by Cini et al (1958) (to be published). This will be discussed in Chapter VI.

Recently at Rochester, Barnes et al (1958) measured pion-proton scattering cross-sections at 41.5 MeV at

Reference. 1.	2.	3.	Result. 4.
Bodansky et al (1953)	a	58	$\lambda_3 = -.10 \pm .02$
Perry and Angell (1953)	a	40	$\lambda_3 = -.146$
Orear et al (1954a)	a	45	$\lambda_3 = -.138 \pm .03$
Bodansky et al (1954)	c	65	$\lambda_1 - \lambda_3 = .3$
Orear et al (1954b)	b	26	$2\lambda_1 + \lambda_3 = .152 \pm .087$
Tinlot & Roberts (1954) (adjusted by Bethe and de Hoffmann 1955)	c	40	$\lambda_1 - \lambda_3 = .266 \pm .025$
Spry (1954)	c	20	$\lambda_1 - \lambda_3 = .25 \pm .03$
(as quoted by Orear 1954)	c	30	$\lambda_1 - \lambda_3 = .26 \pm .03$
Rinehart et al (1955)	b	2.5-30	$2\lambda_1 + \lambda_3 = .25 \pm .05$
Whetstone & Stork (1956)	a	21.5	$\lambda_3 = -.098 \pm .014$
Alston et al (1956)	a	10-35	$\lambda_3 = -.130 \pm .035$
Nagle et al (1957)	b	10-30	$2\lambda_1 + \lambda_3 = .231 \pm .033$

2 - Scattering Process; a  $\pi^+ + p \rightarrow \pi^+ + p$   
 b  $\pi^- + p \rightarrow \pi^- + p$  c  $\pi^- + p \rightarrow \pi^0 + n$ .  
 3 - Pion Energy, MeV.

S - Wave Scattering Lengths.

Table 2.

six angles for  $\pi^+$  mesons and five for  $\pi^-$  mesons. A phase shift analysis of these results, together with other measurements made in the same laboratory at energies of 24.8 MeV, 31.5 MeV and 60 MeV determined the phase shifts  $\alpha_3$  and  $\alpha_1$  to an accuracy of 4% and 8% respectively. These results together with others were included in those quoted by Puppi at the C.E.R.N. Conference (1958):

$$\lambda_3 = -0.110 \pm 0.004 \text{ and } \lambda_1 = 0.173 \pm 0.011 \quad (14)$$

which are valid in the pion energy range 25 to 60 MeV.

The derivation of the relationship between all the above threshold processes, that is photoproduction, scattering and capture of pions is given in Appendix 1. For the present discussion, it is sufficient to note that the following equality holds at zero energy:

$$P = 6.35 \times 10^{-27} \left\{ \frac{(\lambda_3 - \lambda_1)^2}{r_0 \cdot \sigma_+^s / q} \right\}_{\omega=1} \quad (15)$$

where  $\sigma_+^s$  is the s-wave  $\pi^+$  photoproduction cross-section extrapolated to pion threshold and  $\omega$  is the c.m.s. pion energy. The constant factor was derived mainly from kinematical relationships, and it can only introduce negligible sources of error. This expression for P is only valid at zero pion momentum and it is this requirement/

that causes the difficulty. This can be seen when it is remembered that  $\sigma_+^s$  and  $(\lambda_3 - \lambda_1)$  are measured for positive energy pions while the capture data, in the direct derivation of P, involves pions at small negative energies. Thus, the main problem in this analysis involves the step in going from energies different from zero to threshold. This extrapolation will be dealt with in full later, since the only point in introducing the threshold relationship here was to emphasise the importance of having accurate and reliable experimental information to insert into the above formula.

If the following experimental values are assumed:

$$P = 1.50 \pm 0.15 \quad \text{Cassels et al (1957)}$$

$$(\lambda_1 - \lambda_3) = 0.28 \pm 0.01 \quad \text{Puppi (1958)}$$

$$\sigma_+^s/q = (1.43 \pm 0.02) \times 10^{-28} \text{ cm}^2 \quad \text{Orear (1956)}$$

then the indirect calculation of P from positive energy data is:

$$P = 1.86 \quad \text{for } r_0 = 1.87$$

$$\text{or } P = 2.82 \quad \text{for } r_0 = 1.24$$

where the two values of  $r_0$  were those obtained by the Rome - Illinois group and the Cal. Tech. group, respectively, from their measurements on deuterium.

(The errors in the derived values of P are of the order

of 20%). It is noteworthy that the value of  $P$  in less disagreement with the experimental value of 1.50 was the one calculated from  $r_0 = 1.87$ . This is a value of  $r_0$  which is difficult to reconcile with the theoretical prediction of 1.3.

Hence, it is concluded that there exists a discrepancy between the negative energy result of the Panofsky ratio measured from capture data and that predicted from positive energy results of pion scattering and photoproduction. There are at least two alternative explanations of this disparity; either the solution lies in the inaccuracy of the experimental data and in the neglect of possible corrections which should be used in deriving the relationship between them, or else there is a flaw in the basic physics of the problem. This latter view was adopted by Baldin (1958) who looked on the discrepancy in the values of the Panofsky ratio as one of the reasons for thinking in terms of the two component  $\pi^0$  meson field hypothesis.

However, when one considers the statistical errors of each of the experimental data involved in the scheme linking pion scattering and photoproduction, as well as overall uncertainties (e.g. the value of  $\sigma_+^s$  is subject to beam calibration measurements), it is apparent

that the problem of the s-wave pion-nucleon interaction may still be solved by making more accurate experimental measurements in all branches of the field. Even before Baldin's hypothesis was put forward, it was obvious that there was a need for further measurements of the  $\pi^-/\pi^+$  ratio from deuterium especially near to threshold, and at  $90^\circ$  in the centre of mass frame (c.m.s.) where the experimental data are more amenable to analysis. Before the present results were obtained, there were only five values of the  $\pi^-/\pi^+$  ratio at  $90^\circ$  c.m.s. below a pion energy of 60 MeV, figure 5, and it was difficult to decide whether these values were experimentally consistent. On the other hand, there was a definite contradiction of the final results of the analysis of the two sets of results, the difference amounting to about 30%. It was for these reasons that an investigation of the  $\pi^-/\pi^+$  ratio from deuterium at low pion energies was undertaken.

(c)  $\pi^-/\pi^+$  Ratio from Calcium.

In this field, two laboratories have published results:

(i) Littauer and Walker (1952) at Cornell measured the  $\pi^-$  and  $\pi^+$  meson yields from a number of different

nuclei. Their results were obtained by detecting pions with energies of  $65 \pm 15$  MeV at an angle of  $135^\circ$  to a photon beam of maximum energy of  $310 \pm 10$  MeV. Particles emitted from the target were analysed in a two magnet system, so that the particles detected satisfied conditions of momentum and charge. After this selection, the mesons were detected in a triple coincidence telescope of three trays of Geiger counters. Because of overall uncertainties the measurements were normalised to that of  $\pi^+$  mesons from hydrogen. The observed value of the  $\pi^-/\pi^+$  ratio was  $0.58 \pm 0.06$ .

Also at Cornell, Waters (1957) has measured the photoproduction cross-sections of positive and negative pions from calcium using the bremsstrahlung beam of the 1 BeV strong focusing synchrotron. This work was published after the present study, reported in this thesis, was completed. Mesons emitted at  $35^\circ$  to the direction of the photon beam of maximum energy of 800 MeV were detected by means of a double focusing magnet and a three counter telescope. For pions of energy of 40 MeV, the measured  $\pi^-/\pi^+$  ratio was  $0.92 \pm 0.11$ .

(ii) At Stanford, Motz et al (1955a) obtained a value of  $0.70 \pm 0.03$  for the  $\pi^-/\pi^+$  ratio for calcium,

observing mesons in the energy range 43 to 63 MeV at an angle of  $75^\circ$  in the laboratory frame. The linear accelerator was used at an electron beam energy of  $300 \pm 15$  MeV to produce a bremsstrahlung spectrum. The detection technique involved magnetic analysis and identification of the pions by observing the decay positrons and electrons in delayed coincidence, using a beam of short duration. Both  $\pi^-$  and  $\pi^+$  mesons were detected in this way, only those  $\pi^-$  mesons which decayed in flight being counted. The Stanford  $\pi^-/\pi^+$  ratio for carbon was normalised to that observed by Littauer and Walker, so that the Stanford results could be directly compared to those obtained by these authors.

(d) Present Investigations.

The deuterium experiment was carried out using a liquid deuterium target, and the charged pions were detected in proportional counter telescopes, after being magnetically analysed. Pions, in the energy range 10 to 50 MeV, were selected by the magnet after being emitted from the liquid target at an angle of  $75^\circ$  to the bremsstrahlung beam, of maximum energy of  $240 \pm 5$  MeV, of the Glasgow electron synchrotron. The relative yields of  $\pi^-$  and  $\pi^+$  mesons were obtained as

a function of their kinetic energy. With a liquid target, the subtraction of background counts, due to mesons from the target walls, was small, thereby giving better counting statistics. The spectrometer enabled both  $\pi^-$  and  $\pi^+$  mesons to be detected with an identical experimental set-up by simply reversing the magnetic field. Further, by using more than one telescope at a time, a few different pion energy ranges could be measured simultaneously so that  $\pi^-/\pi^+$  ratios could be determined for these energy intervals during a time in which experimental conditions were kept almost constant. In this way the present experimental technique was superior to previous methods.

The second study describes measurements made of the yields of negative and positive pions from a calcium target. Mesons emitted at  $90^\circ$  to the photon beam with energies between 60 and 120 MeV were detected in nuclear plates. Previous work referred to one energy range of the pion at a given angle of emission, whereas the present experiment was designed to determine the dependence of the  $\pi^-/\pi^+$  ratio on pion energy. This was the significant difference from other investigations in this field.

Chapter III.The Photoproduction of Charged Pions from  
Deuterium - Target.

## (a) Introduction.

In studying the production of pions by photons from deuterium four types of targets can be used.

- (i) Subtraction technique e.g. heavy water -light water subtraction, as used by Littauer and Walker (1952), Jenkins et al (1954) and Crowe et al (1955).
- (ii) High pressure gas target which is cooled to liquid nitrogen temperature - see White et al (1952) and Sands et al (1954).
- (iii) Liquid deuterium target - Beneventano et al (1956).
- (iv) Nuclear plates loaded with heavy water - Adamovich et al (1956).

In order to obtain good counting statistics (for example 5%) and to avoid undue use of accelerator time, it is necessary to have a target which will yield a workable flux of mesons, about one per minute for a given detector system. If it is required to select low energy particles by the detector, the thick walls of a high pressure gas target eliminate this type. In general, the subtraction technique tends to give poor results statistically, so that for the related reasons

of making best use of machine time and of yielding good counting statistics, a liquid target is preferred, even although this type can present many constructional difficulties. As an illustration of this preference, consider a liquid deuterium target 4 cm long in a beam of photons of intensity of  $10^9$  equivalent quanta per minute. Let it be assumed that the detection system counts mesons of energy of 50 MeV in a 5 MeV energy interval and accepts a solid angle of  $1/50$  steradian. Then the counting rate is about one meson per minute. Further, if there is a background counting rate of 10% of the total, (due to mesons coming from the containing walls of the target etc.) then to obtain 4% counting statistics about thirty four hours of accelerator time would be required. On the other hand, if a subtraction technique using deuterated paraffin is chosen, and if all things are equal (including the same target thickness of deuterons), 5% statistics would be obtained in a time increased by a factor of about five, and the energy resolution would be worse. This indicates the advantages of a liquid target, which gives a concentrated source of deuterons.

(b) Description of Targets.

For the photoproduction investigation from deuterium, two liquid targets were built; one was designed for hydrogen (or helium), and the other for deuterium. In the literature, many liquid targets have been described; at Berkeley, Cook (1951), and Leonard and Stork (1954). At Columbia, Lindenfeld et al (1953), and Bodansky et al (1954). At Chicago, Nagle (1955). At Illinois, Whalin and Reitz (1955), and Nicolai (1955). At Harvard, Swenson and Stahl (1954). Finally at Cornell, Littauer (1958). In basic design, the cryostats of the present targets resembled the Columbia one. However, many modifications and improvements were included in the new design. This was obtained from experience gained from an unsuccessful model, and from advice given by Professor J.F. Allen of St. Andrews University on the low temperature aspects of the problem. The liquid targets built were essentially thin walled vessels, containing the liquefied target gas, in thermal contact with liquid hydrogen. This assembly was placed in a large metal double-walled Dewar, the middle wall being a radiation shield at liquid nitrogen temperature ( $77.3^{\circ}\text{K}$ ). The vacuum jacket and the nitrogen container were common to the

two targets, but separate central reservoirs with the target assembly attached were required for each target.

(i) Deuterium Target.

A section of the liquid deuterium target is shown in figure 8. The target chamber itself was a copper cylinder, of wall thickness of 1 mil, and of diameter of 1.5 inches. Above the target chamber and connected to it by a thin walled capillary tube was the deuterium reservoir. This had a volume greater than the target chamber. This reservoir was filled through the deuterium intake tube, entering near the top of the cylinder. There was also an exhaust tube in the target chamber. The purpose of the deuterium reservoir was to enable background counting rates to be measured from the empty target chamber while there was still liquid deuterium in the system. This was achieved by closing off the deuterium exhaust tube and by supplying heat to the liquid in the target chamber. This forced the liquid up the capillary tube into the deuterium reservoir where it remained so long as heat was supplied.

The deuterium reservoir was in thermal contact with the base plate of the hydrogen reservoir, figure 8. In this target, the deuterium reservoir and the target

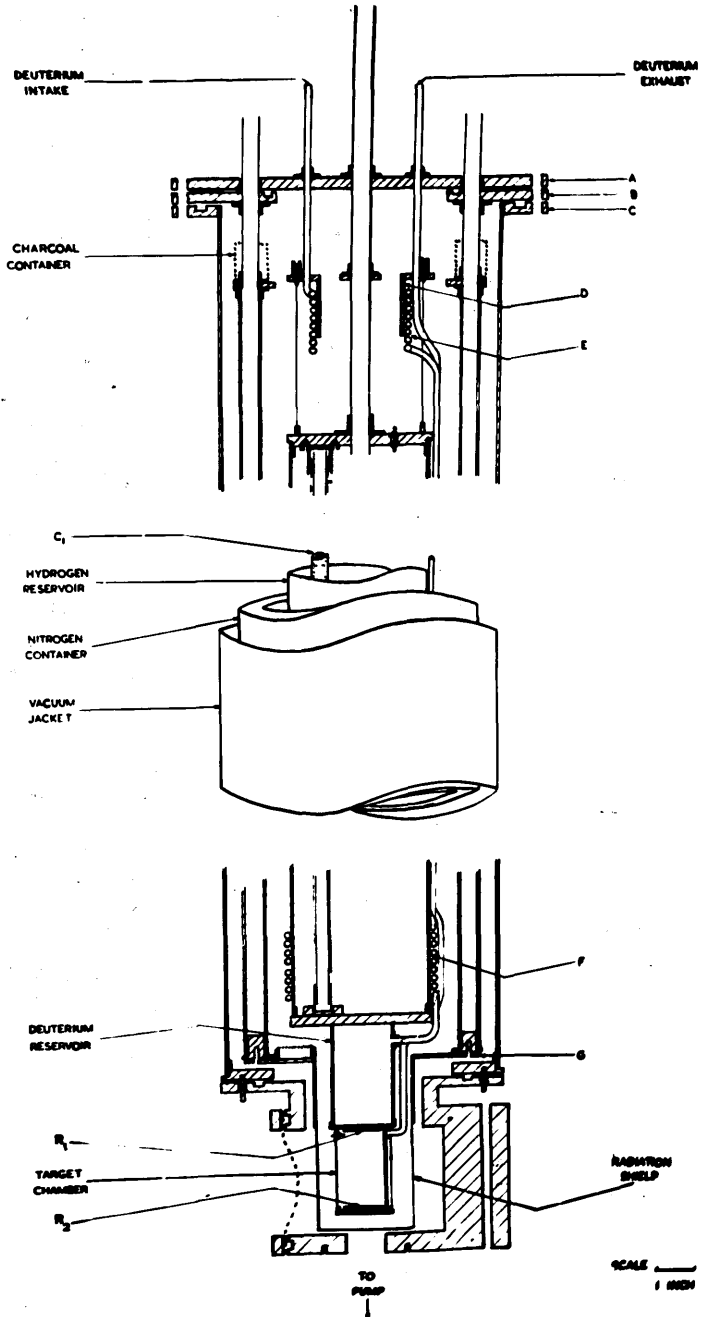


Figure 8.  
Cross-section of the liquid deuterium target.

chamber constituted one system, and the hydrogen reservoir another. Thermal contact was obtained by compressing a ring of indium wire (16 gauge) between the two plates. The hydrogen reservoir was a brass cylinder 25 cm long and 1.5 litres volume. It was filled through a 12 mm diameter tube, to which was attached the transfer tube from the liquid hydrogen storage Dewar. Near the top of this central filling tube, there was a brass plate, D of figure 8, which was in thermal contact with the surrounding nitrogen container when the whole target was assembled. By this means, liquid hydrogen was conserved at the expense of liquid nitrogen. In the process of liquefying the deuterium gas, the first stage was to cool it to  $77^{\circ}\text{K}$  in coil E, and then to  $20^{\circ}\text{K}$  in the heat exchanger F where the gas finally condensed into the deuterium reservoir. In order to reduce conduction losses, the hydrogen reservoir was suspended from the plate A by tubes of low conductivity material. The liquid hydrogen filling tube, the deuterium intake and exhaust tubes, and one dummy support tube were all copper - nickel alloy tubes (composition 40% copper and 60% nickel) of 1/4 mm wall thickness. These were found to be best for their low thermal conductivity property, mechanical strength and

and the ease with which they could be soldered.

Resistive type level indicators,  $R_1$  and  $R_2$  of figure 8, were used to show when the target was full and empty respectively. The principle of this type of level indicator depended on the difference of thermal conduction from the resistor, when a current flowed in it, when it was in the liquid deuterium and when it was in the cold vapour above the liquid, thereby producing a measurable change in resistance. The change in current through the resistor (68 ohm high stability type) was measured in a bridge circuit, and for the arrangement used an out of balance current of about 10 microamps was obtained. A general discussion of liquid gas level indicators has been given by Edwards (1956).

In the hydrogen reservoir, on the other hand, the liquid level was given by a capacitor type indicator, a cylindrical condenser being used,  $C_1$ . This type made use of the change in capacity produced when the gas between the condenser cylinders was replaced by liquid, causing about a 12% increase. The capacitor (about 100 pF) was part of a tuned circuit fed from a Pierce crystal oscillator of 2.7 Mc/s frequency, and the resonant current was measured through a cathode follower output.

The hydrogen reservoir and target chamber are shown

in figure 9, while figure 10 illustrates plate A on which the hydrogen filling tube, the deuterium intake and exhaust tubes, and the terminal board for the level indicators can be seen.

The nitrogen container was an annular volume of 3.5 litres, constructed from 5 and 6 inches diameter brass cylinders, and completely surrounded the hydrogen reservoir. Attached to the base of the nitrogen container there was a 1 mil aluminium foil radiation shield which entirely enclosed the deuterium reservoir and the target chamber, thermal contact with the main vessel being maintained by a indium wire seal. The liquid nitrogen could be filled through any of three tubes on the top of the container. At different places on this container, there were baskets of activated charcoal which, at liquid nitrogen temperature, maintained a good vacuum (less than  $10^{-5}$  mm Hg) when the whole assembly was isolated from the diffusion pump.

The parts of the target described above were enclosed in a vacuum jacket which was a copper tube of 7 inches diameter and 30 inches long, flanged at the top C. A vacuum seal between plates A, B and C was achieved with O-ring neoprene gaskets. The target base was attached to the bottom of the vacuum jacket. The base had a jaw-like structure as seen from figures 11

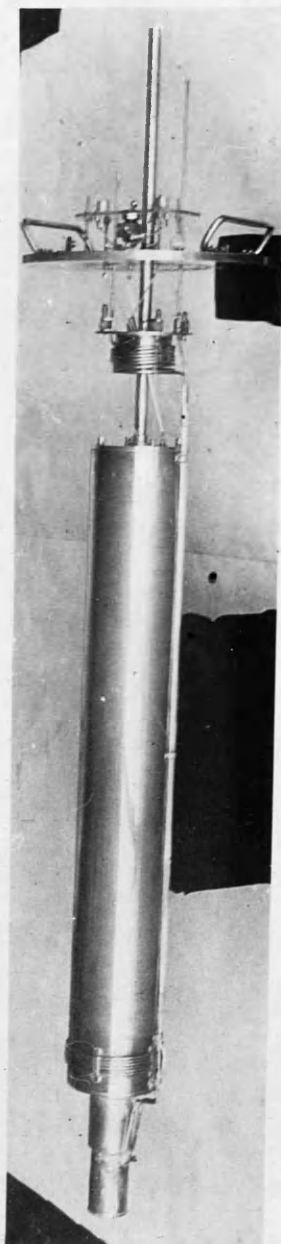


Figure 9.  
The cryostat of the liquid  
deuterium target.

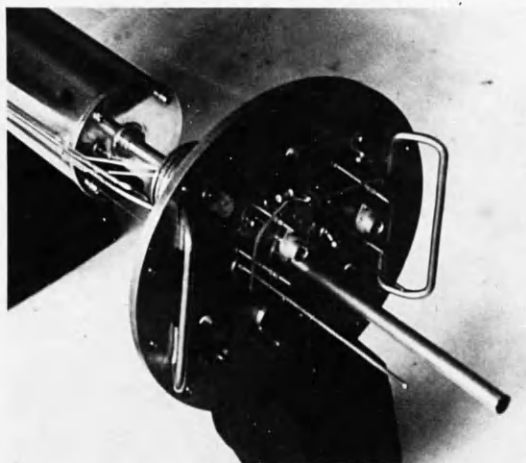


Figure 10.  
The top plate A of the target,  
showing the hydrogen filling  
tube, the deuterium intake and  
exhaust tubes, and the terminal  
board for the level indicators.

and 12. The vacuum wall was a 5 mil Mylar window, and a vacuum seal was obtained by clamping this foil over an O-ring which extended round the circumference of the jaw. The target assembly was continuously pumped by a 50 litres per second oil diffusion pump to give a pressure better than  $5 \times 10^{-6}$  mm Hg, as measured by an ionisation gauge placed on the top plate A.

From this, it is seen that before the photon beam reached the liquid deuterium, it must traverse 5 mil Mylar, 1 mil aluminium and 1 mil copper. It was estimated that the background from these foils would contribute about 10% of the total number of counts. This will be discussed later.

(ii) Hydrogen Target.

A second target was constructed for liquids which had the same refrigerant as the liquefied gases themselves, for example hydrogen and helium. The basic difference between this and the deuterium target was that the reservoir for the refrigerant, the target reservoir and the target chamber made up only one system. This facilitated the process of obtaining a liquid hydrogen target since it was only necessary to transfer the liquid hydrogen from its Dewar into the target. This was distinct from the deuterium target where it was necessary

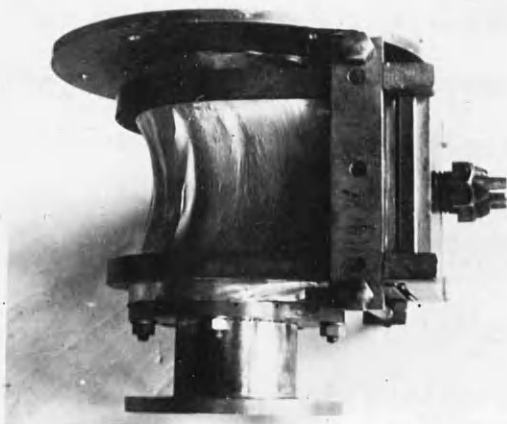


Figure 11.  
Target base : assembled.



Figure 12.  
Target base : dismantled.

to liquefy the deuterium gas in the target cryostat.

In the hydrogen target, the reservoir had a volume of three litres. It was suspended from the top plate by the central filling tube and three dummy support tubes. Again resistive level indicators were used in the target chamber, and a cylindrical condenser indicated the volume of liquid hydrogen in the reservoir. The target chamber was of the same design as that of the deuterium target.

(c) Performance of the Targets.

The main practical difficulty in the construction of the liquid targets was obtaining good vacuum seams at low temperature. Before this present work was started a liquid target had been made, but after a short time this model was rejected because of vacuum trouble. An improved design was obtained and from this the two targets described above were constructed.

From the point of view of the design of liquid targets, the greatest problem is the conservation of the liquefied gases in their containers. The processes by which heat enters the system are thermal conduction, radiation, convection and gaseous conduction. Of these, gaseous conduction and convection contribute least since these methods are almost eliminated by having the liquefied gas reservoirs in high vacuum. It was estimated that

gaseous conduction added to the evaporation rate of liquid hydrogen by less than ten per cent when the pressure was  $10^{-5}$  mm mercury.

The two other factors of thermal conduction and radiation heat input contributed to the evaporation rate approximately equally and together accounted for most of the loss of liquid. Thermal conduction down the filling tubes was minimised by using low conductivity tubes throughout the construction of the targets. The conduction losses could be calculated, but there was an uncertainty introduced in the value assumed for the thermal conductivity of the copper - nickel alloy of these tubes at low temperatures. However, if a value of 0.05 cal/sec.cm.deg was used (which was not unreasonable in view of values quoted by Squire 1953), then the loss of liquid hydrogen due to conduction, from the hydrogen target was estimated as 22 ml/hour, and from the deuterium target as 10 ml/hour. The corresponding figure for a helium target would be 100 ml/hour. Under the same assumptions, the liquid nitrogen would evaporate at a rate of 90 ml/hour. One final factor not taken into account in these estimations was the cooling effect of the evaporated gas as it escaped up the exhaust tubes, so that there was not a linear temperature gradient down the tubes. This

had the effect of making these quoted figures as upper estimates.

The heat input into the cryostat due to radiation was reduced by having the surfaces of the containers at low temperature highly polished, whereby making the emissivity of the absorbing surfaces small. If a value of 0.1 was assumed for the emissivity, the radiation losses of liquid hydrogen from the hydrogen target and from the deuterium target were estimated as 10 ml/hour and 5 ml/hour respectively, while the corresponding figure for liquid nitrogen was 25 ml/hour.

One further loss not yet considered was that due to the conversion of ortho- to para-hydrogen. This released energy of the order of magnitude of the latent heat, and hence if the conversion took place in the hydrogen reservoir, there would be a loss of liquid hydrogen due to boiling. This loss was difficult to estimate since it depended on the age of the liquid hydrogen, which in turn determined the equilibrium mixture. A rough estimate of this heat input was of the order of 10 ml/hour.

Hence on summing up, the estimated total evaporation rates of liquid hydrogen from the hydrogen target and from the deuterium target were 45 and 15 ml/hour respectively while nitrogen losses were 190 ml/hour.

If helium occupied the hydrogen reservoir, the total loss would be 125 ml/hour.

As a comparison, measurements made on the evaporation rates of the liquid hydrogen from the hydrogen target and from the deuterium target showed a loss of 50 and 25 ml/hour respectively. The liquid nitrogen loss was 150 ml/hour. The lower hydrogen loss from the deuterium target was mainly due to the longer conduction path from the liquid hydrogen container, and also due to the smaller volume and hence surface area of this vessel. It was advantageous to have the small evaporation loss of liquid hydrogen as it allowed constant use of the targets for one and a half to two days without requiring to recharge the cryostat.

#### (d) Production of Deuterium Gas.

The deuterium target was obtained by liquefying deuterium gas, unlike the hydrogen target which could be made by transferring liquid hydrogen directly from the Dewar into the hydrogen reservoir of the target. Since deuterium gas was not available commercially, it was necessary to manufacture it in the laboratory. The deuterium was produced by electrolysing heavy water and purifying the gas evolved. The method adopted for the purification process was that of adsorption by activated

charcoal cooled to liquid nitrogen temperature. Other methods were tried, including the separation of deuterium (and hydrogen) from its impurities by diffusion through a hot nickel leak (Landecker and Gray 1954) but this was abandoned in favour of the simplicity of the first method. Deuterium gas can also be obtained from heavy water by passing heavy steam over hot magnesium (see Rogers and Lederman 1957), but the electrolysis method was preferred in view of the facilities available in the Laboratory.

Since it was necessary to obtain about 110 litres of deuterium at N.T.P., some effort was spent trying out different types of electrolytic cells and electrolytes to obtain a system with a high rate of gas yield. The final design, due to Mr. J.T.Lloyd and constructed by Mr. I. White, is shown in figure 13. The cell was made from five concentric Pyrex glass tubes; the innermost was the inlet for the cooling water which circulated down the outside of this tube and up the annular volume of the outer water jacket to the outlet. The electrodes were helices of platinum wire, the anode being partitioned from the cathode by the middle glass tube. The whole electrode structure and the two gas outlets could be removed from the water jacket, the air-tight seal being achieved by an O-ring gasket. The overall

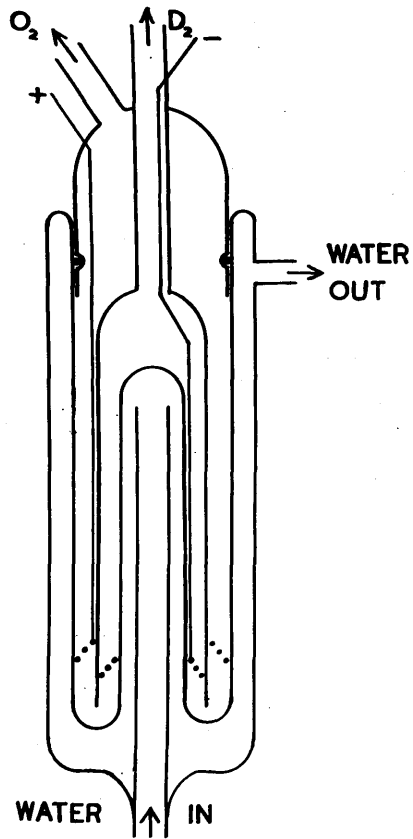


**Figure 13.**  
**Electrolytic cell, used in the production of deuterium gas.**  
**( Not to scale ).**

length of the cell was 23 cm. and the width was 4.8 cm. The gas was collected through mercury valves, made with sintered glass diaphragms. This type of valve made it possible to collect the deuterium gas up to a total pressure exceeding atmospheric pressure.

The heavy water of 99.5% purity was obtained from Norst Hydro, Norway. The electrolyte chosen was sodium hydroxide (in the form of dried pellets) and the initial concentration was two per cent. Due to the efficient cooling system used, it was possible to operate the cell at an electrolysis current of four amps. The limiting factor was turbulence produced by the high rate of gas evolution, but at this current no back - streaming of the gas bubbles was observable.

The system for purifying and collecting the deuterium is shown schematically in figure 14. After leaving the electrolyser, the deuterium gas (with a high water content) was passed through a glass cold trap from which heavy water was recovered. Thereafter, the gas entered an all metal system starting with a cold trap which had a slow pumping speed and a large surface area (greater than 2500 cm<sup>2</sup>) exposed to the gas. After that stage, it was assumed that the gas was dry so that the remainder of the system was designed to remove

impurities, mainly oxygen and nitrogen. Other impurities included hydrogen and HD, as analysed spectroscopically (kindly carried out by Dr. I.R. Reed of the Chemistry Department). This purification was achieved by adsorbing the impurities in cold charcoal traps; these were U-traps filled with 150 gm. of granular charcoal and immersed in liquid nitrogen. The charcoal-filled traps were continuously evacuated (backing - pump pressure) for a few days while they were electrically heated to a temperature around 300°C. This activated charcoal at liquid nitrogen temperature adsorbed the impurities in preference to hydrogen and deuterium (see for example, Dunoyer 1926, Chapter IV). The cleaned gas was finally collected in a 110 litre steel cylinder which had been previously outgassed. This storage cylinder was filled to a pressure of 80 cm mercury.

Due to adsorption of some of the evolved deuterium on to the charcoal, and to vacuum trouble, the overall efficiency of the operation was only 80%, where the efficiency was taken as the volume of deuterium gas collected to that possible from the mass of heavy water electrolysed. About 125 gm. of heavy water were required to complete the manufacture of the gas, and the whole process occupied about twelve days.

(e) Filling Procedure.

When the target system had been assembled, the pressures inside the vacuum jacket, the hydrogen reservoir, and the target chamber were reduced to a few microns of mercury with rotary pumps. The vacuum jacket pressure was further reduced to the order of  $10^{-6}$  mm with a two inch oil diffusion pump, this pressure being obtained after filling up the nitrogen container with liquid nitrogen. About twenty-four hours were allowed for the whole assembly to come to equilibrium temperature. (This was confirmed by using the hydrogen reservoir as a constant volume gas thermometer). During normal operation of the target, liquid nitrogen was fed continuously into the container from a Dewar, about 150 ml of liquid nitrogen being transferred automatically per hour. At this stage, the target was prepared for the filling operation.

To obtain a hydrogen target, the hydrogen reservoir was firstly filled with dry hydrogen gas to one atmosphere and then connected to the liquid hydrogen Dewar by a vacuum jacketed transfer tube. The liquid hydrogen was finally transferred by exerting a positive pressure of 10 cm Hg of dry hydrogen gas on the liquid in the hydrogen Dewar. Gravity filled the target

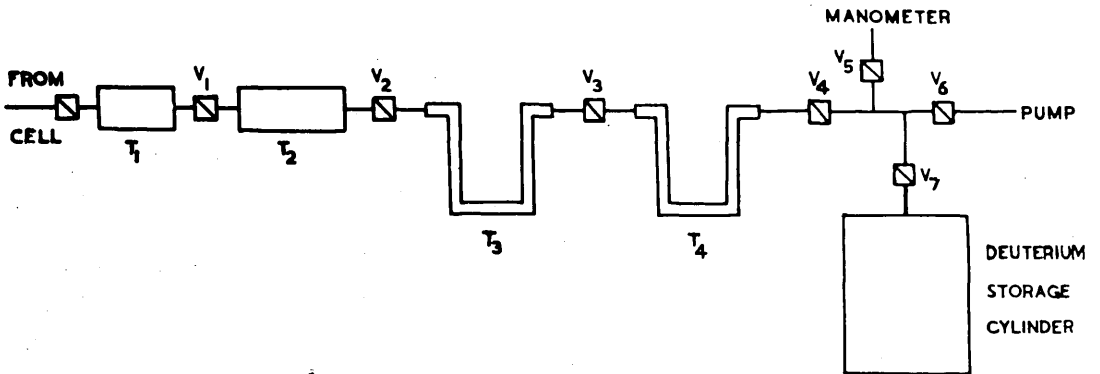


Figure 14.  
Purifying system for the deuterium gas.  
V - valves,  $T_1$  - glass cold trap,  $T_2$  - metal cold trap,  $T_3$  and  $T_4$  - charcoal filled U-traps.

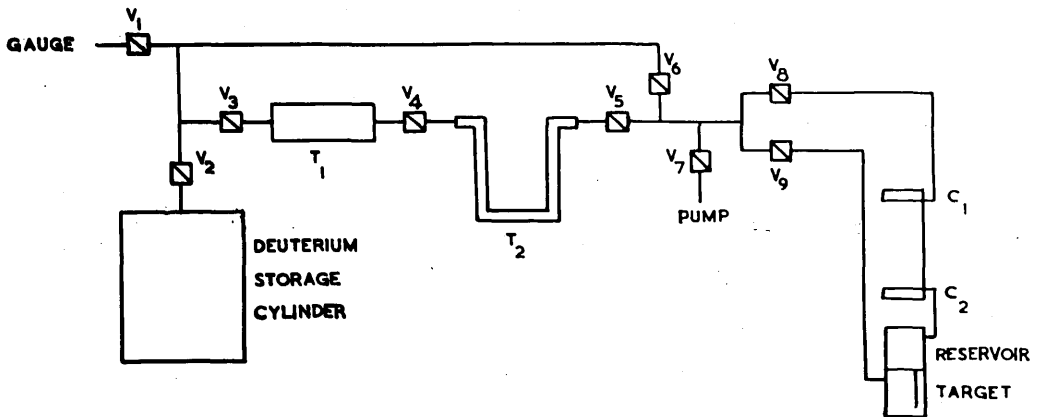


Figure 15.  
Flow diagram for the deuterium target.  
V - valves,  $T_1$  - metal cold trap,  $T_2$  - charcoal filled U-trap,  $C_1$  and  $C_2$  - heat exchangers corresponding to coils E and F of figure 8.

chamber after the reservoir had been cooled to the temperature of liquid hydrogen ( $20.4^{\circ}$  K at 760 mm Hg). The evaporated hydrogen gas escaped through an exhaust tube to the atmosphere outside the building. When in use the hydrogen reservoir was filled up at least every thirty-six hours, the evaporation loss being less than  $1\frac{1}{4}$  litres of liquid hydrogen per day.

The flow diagram for the liquid deuterium target is shown in figure 15; initially all the valves, except  $V_2$ ,  $V_8$  and  $V_9$ , were opened and the system was evacuated to backing pump pressure while liquid hydrogen was transferred to the hydrogen reservoir of the deuterium target in a manner similar to that described for the hydrogen target. The apparatus was then ready for filling in the deuterium gas from the storage cylinder; with  $V_6$  and  $V_7$  closed, the gas was slowly passed through the cold trap  $T_1$  to remove moisture and through the U-trap  $T_2$  (containing activated charcoal immersed in liquid nitrogen) to remove impurities. The cleaned gas was cooled to  $77^{\circ}$  K in coil  $C_1$ , maintained at liquid nitrogen temperature, and finally it condensed in coil  $C_2$  which was in thermal contact with liquid hydrogen. The liquefied deuterium filled the target chamber by passing through the capillary tube

from the deuterium reservoir. To fill the target completely, the liquefying process took about 30 minutes. When the target was full, as shown by the resistive level indicators, the traps were isolated and the by-pass tube was used to connect the target to the storage cylinder. The closed system was in liquid-vapour equilibrium at about 263 mm mercury pressure for  $20.4^{\circ}$  K equilibrium mixture of deuterium. As estimated from the vapour pressure, the temperature of the liquid deuterium was determined. The target thickness in nuclei of deuterium per  $\text{cm}^2$  was obtained from the data of Woolley et al (1948).

## Chapter IV.

The Photoproduction of Charged Pions from  
Deuterium - Detector System.

## (a) Introduction.

In the production of charged pions by photons, several methods are available for the detection of the particles which define uniquely the reaction under observation.

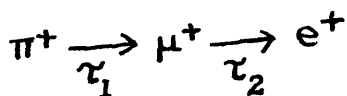
## (i) Nuclear Plates.

Both  $\pi^-$  and  $\pi^+$  mesons may be simultaneously counted using nuclear emulsions, each type of pion being distinguished by their track and track endings. It is found that more than 99% of all  $\pi^+$  mesons exhibit a decay scheme  $\pi^+ \rightarrow \mu^+ + \nu$ ,  $\mu^+ \rightarrow e^+ + \tilde{\nu} + \nu$ . Consider the ideal case of a typical meson track in an emulsion which comes to a stop and produces a one-pronged track of mesonic characteristic. If this also stops in the emulsion and gives rise to a lightly ionising particle, the event can be attributed to a positive pion. On the other hand,  $\pi^-$  mesons can give rise to n pronged stars where  $n = 0, 1, 2, 3$  etc. As stated in Chapter II, one of the difficulties of this detection technique is the identification of one-pronged events, that is whether a given event is a  $\pi^+ - \mu^+$  decay or a  $\pi^-$  star with one visible track. Such events, however, can be analysed

analysed in terms of previously established results of the prong frequency of  $\pi^-$  mesons in emulsions. This will be discussed in the analysis of the calcium experiment in which this detection technique was used. Beneventano et al (1956), and Adamovich et al (1956) made use of nuclear emulsions as pion detectors.

(ii) Counter Telescope.

Again, this system is based on the decay scheme for  $\pi^+$  mesons



where  $\tau_1 = 2.56 \times 10^{-8}$  sec. and  $\tau_2 = 2.22 \times 10^{-6}$  sec. (Crowe 1957). Therefore, a scintillation counter telescope and delayed coincidence technique can define the positive meson. For example, it may be observed that a particle travelling in a given direction has stopped in a crystal, using a coincidence anticoincidence device, and a delayed coincidence may be observed in a time  $\tau_1$  or  $\tau_2$ , due to either the  $\mu^+$  or  $e^+$  respectively, whereby defining the particle to be a positive pion. The detection of positive mesons on the basis of their  $\pi-\mu$  decay was first demonstrated by Jakobson et al (1951). This technique can also be applied to detect  $\pi^-$  mesons, but in this case only those that decay in flight can be counted, (see for example Motz et al 1955a).

Another way in which a scintillation counter can be used is in the time of flight technique; in such a method either the pion or a recoil particle is used to open a fast gating circuit by passing through the first crystal of the telescope, and only those particles are accepted which reach and stop (or lose a given fraction of their energy) in a second crystal within a pre-determined time, depending on the type and energy of the particle.

It is also possible to identify an observed particle as a pion by measuring energy loss and range, by either scintillation or gas counters.

(iii) Magnetic Analysis.

A magnet system (of one or two magnets) along with a counting device which measures either the energy loss or range or time of flight of the particle to be detected, can be used to identify both  $\pi^-$  and  $\pi^+$  mesons.

This method has the main advantage of selecting by momentum the particles under study, so that at least one condition must already be satisfied by the particles before they enter any counter system. The most obvious use of this technique is the detection of pions in a large electron background. On comparison with the technique of nuclear plates, a magnetic spectrometer can be used

to produce results quickly, unlike the inherently slow process of scanning. The disadvantages include selection of one energy range at a time, and acceptance of a small solid angle. This detection technique was used in the deuterium experiment and will be described in this Chapter.

(b) Detector System.

With the type of magnet used, particles from an external point were focused along a plane approximately coinciding with one boundary of the magnetic field. The main advantage of this, despite the small solid angle involved, was that at least three different meson intervals could be studied simultaneously. Since the particle detector had effectively to be placed in the field, and if scintillation counters were to be used, it was necessary to remove photomultipliers from regions of high magnetic fields by means of light guides. Unfortunately, from the point of view of the mechanical arrangement of such a system, it was considered impracticable when it was envisaged that at least two counters would be required for each of three telescopes. Hence, it was necessary to use gas counters.

(i) Magnet.

The magnet employed in the spectrometer was of the

fringe focusing type. By making use of the fringing field produced by shaping the pole pieces at the entrance slit, double focusing was achieved in the vertical and radial planes. The pole pieces, 104 cm long and 61 cm wide, were spaced 15 cm apart, and fields homogeneous within a few per cent could be produced up to values of 15 kilogauss. The magnet, weighing twenty tons, was water cooled, and during normal operation the power required was of the order of twenty kilowatts. Apart from some preliminary work with an electrolytic tank to find magnetic field homogeneities, and putting into working order safety cut-out devices in the electrical circuit of the magnet, the author had no part in the design of the magnet which was due to Drs. Bellamy, Robb and Rutherglen of this Laboratory.

For a given value of the current through the magnet coils, it was possible to accept mesons within the energy range of 10 to 60 MeV (using a field of 8.5 kilogauss). A slit at the front of the magnet defined the angular acceptance of the system, a gap 6" x 6" being used to give a solid angle of 0.027 steradian. The magnet was calibrated with a search coil and fluxmeter; this method gave an accuracy of at least

one per cent after calibrating the search coil, in turn, with a magnet used in nuclear magnetic resonance work, this field being known to three parts in  $10^4$ . Momentum trajectories of pions were traced out using the current carrying wire technique. From this, for a given value of the magnetic field, the relationship between meson energy and linear distance along one long edge of the pole piece was derived. This relationship was used to position the counters to accept the required pion momentum interval. Typical momenta trajectories are shown in figure 16. It was found that the remanence of the magnet was negligible when the field was reversed to transmit particles of the opposite charge.

(ii) Counter Telescopes.

As it was proposed to study at least three energy groups of mesons simultaneously, it was expedient to have the simplest workable counter system. In the first instance, this principle appeared practicable since the momentum resolution already obtained by magnetic selection enabled pions to be separated from other particles. The detection system, however, could not be so apparently straight-forward since the pions had to be counted in the presence of a large photon and electron background. Further, it was found that

64a

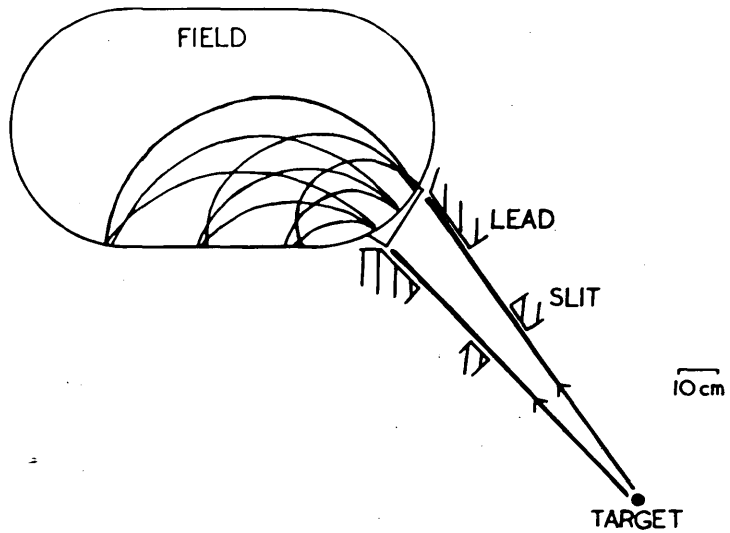


Figure 16.  
Magnetic spectrometer - collimator and pole piece.  
Typical momentum trajectories are also shown.

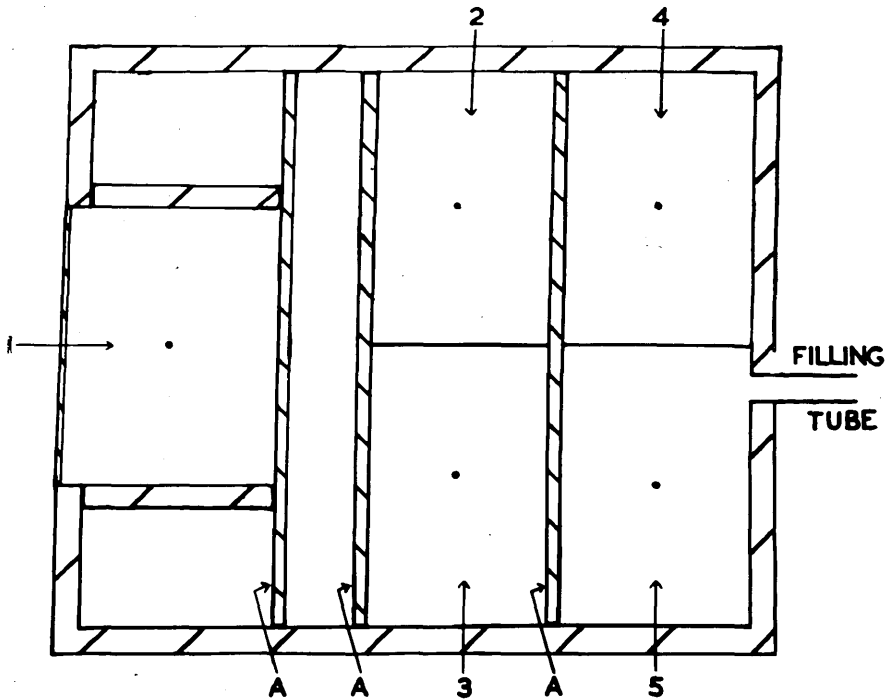


Figure 17.  
Section of a proportional counter telescope.  
1 - front coincidence counter, 2 and 3 - coincidence  
counters, 4 and 5 - anticoincidence counters,  
A - copper absorber.

fast electrons of the same momentum as the pions produced slow electrons in the counter walls, and these secondaries spiralled in the fringing field of the magnet to produce pulses indistinguishable from those due to mesons.

Therefore, it was obvious that a telescope of two counters in coincidence was necessary, and it was found that a gas counter had to be used because of the sensitivity of a scintillation counter to the high  $\gamma$ -ray background. In the telescopes used, proportional counters were chosen not for their proportional characteristics but because they had no dead time and were insensitive to neutrons. In fact, the information yielded from the counters was merely whether a pulse above a given minimum amplitude was obtained or not, and the discrimination was carried out electronically.

Each telescope consisted of five proportional counters; the first along with the second and third in series were in coincidence, and the fourth and fifth together in anticoincidence, as shown in figure 17. Between counters 1 and (2 + 3) there was copper absorber to slow down the mesons before entering (2 + 3) and to define the lower meson energy limit accepted by the telescope, while absorber between (2 + 3) and (4 + 5) defined the upper energy limit. In this way the pions

were detected by their range rather than momentum. The counters were designed to accept about a five MeV meson interval as defined by the momentum trajectories. Unfortunately, for particles leaving the external focus, the magnet focused these along a plane which did not quite coincide with the boundary of the pole piece, with the result that some trajectories were over-focused and others under-focused as they crossed the edge of the field. This caused, at a few inches from this edge, widely diverging paths for some of the trajectories, so that it was necessary to have a coincidence counter (i.e. the 2 + 3 counter) which was wider than the front counter, and similarly for the anticoincidence counter (4 + 5).

In order to reduce the number of accidental counts due to electrons which penetrated the coincidence counters but not into the back counters (this effect was most noticeable in the telescope for low energy pions), the distribution of absorber before counters (2 + 3) was such that most of the copper was placed between 1 and (2 + 3) rather than before the front counter. The bias levels of the discriminators were also raised slightly in the low energy counters where the energy losses of the mesons would be expected to be greater

than twice minimum ionisation loss.

However, due to the small energy loss of the mesons (less than 100 Kev) in the gas of the counter, the Landau effect was large (Landau 1944, and see also Igo and Eisberg 1954). The result of this was to limit the setting of the discriminator levels below the calculated average energy loss of a given pion traversing the counter. The high background counting rate was reduced by approaching the problem from another way altogether. A further proportional counter was placed at the entrance to the magnetic field, and this counter was taken in coincidence with each of the telescopes. This defined the pion trajectory such that the particle had to come from the target through the collimator into this counter, and then have the correct energy to enter the telescope. The walls of this counter, through which the pion passed, were made of one mil Mylar with a coating of aluminium evaporated on to the inner surface which was connected to the same potential as the rest of the case. This additional counter was made up of two counters of three inch square cross-section, each six inches high.

The counters could be filled simultaneously to the same pressure each time, the filling mixture being argon plus 7% of methane to a total pressure of one atmosphere.

Two mil pure tungsten wire was used, and during normal operation a potential of about two kilovolts positive was required, with the case at earth. In order to keep the counter gas dry, phosphorus pentoxide traps were used continuously during operation of the counters.

Therefore, as a summary of the above, the mesons were identified by having charge and momenta such that the magnetic field would deflect them into a given counter telescope, and by having sufficient range to penetrate into counters (2 + 3) but stop in the absorber before counters (4 + 5). Protons and other heavy particles of the same momenta as the mesons could not reach counters (2 + 3). Electrons similarly (and positrons) of high energy (greater than 40 MeV), coming from a target at the focus of the magnet, would pass through the telescope and would not therefore be counted.

### (iii) Electronic Circuitry.

The pulses from the proportional counters were sent through White cathode followers into I.D.L. Wide-Band Amplifiers. It was found that, for a given set-up, minimum ionising particles gave 3 volt pulses while slow electrons produced pulses of amplitude between 30 and 40 volts. Hence, it was necessary to design a pulse selector which would accept all pulses above a given/

minimum amplitude level and yet not be troubled, by pick-up into other channels (for example) by large pulses which only had a nuisance value. Also, because of the geometry of the proportional counters (rectangular 3" x 2" x 6") used, it was estimated that a maximum collection time of one microsecond was not unreasonable. Therefore, for a charged particle going through the telescope, the pulse from any one counter might lead or lag the pulses from one of the others by a time up to one microsecond. Therefore, to obtain a true coincidence-anticoincidence rate, it was decided to shape all pulses such that their width was two microseconds, to delay all pulses in counters 1 and (2 + 3) by two microseconds, and to lengthen the pulses from counters (4 + 5) to six microseconds. With this arrangement there was only a negligible probability of missing an anticoincidence pulse by expanding these pulses to six microseconds, since the pulse rate in any one of the counters was never greater than about two or three per millisecond.

The delaying and clipping of the pulses was achieved by lumped networks, the discrimination by flip-flop trigger circuits, and the coincidence - anticoincidence circuits were of the cathode follower

type. The selected pulses were gated so that only coincidence pulses were counted which occurred within a period of two milliseconds, the start of which was determined by a trigger pulse from the synchrotron. The timing of this latter pulse could be altered such that the bremsstrahlung beam of approximate width of one millisecond was maintained in the middle of the gate. This further pulse selection was obtained by a cathode follower linear gate circuit. The block diagram for the low energy telescope circuitry is given in figure 18.

Since the running time at a given angle of detection was of the order of a few weeks machine time, the circuitry had necessarily to be stable over such working periods; to achieve this, some effort was spent in circuit design and in ensuring that components and valves were not being overloaded. Stabilised power supplies with long term voltage stabilities of better than one per cent were used throughout. As far as possible, all trigger circuits were designed so that they depended on valve characteristics rather than the stability of components. The chassis lay-out was arranged so that there was no interference among the three channels of a given telescope, and such that there

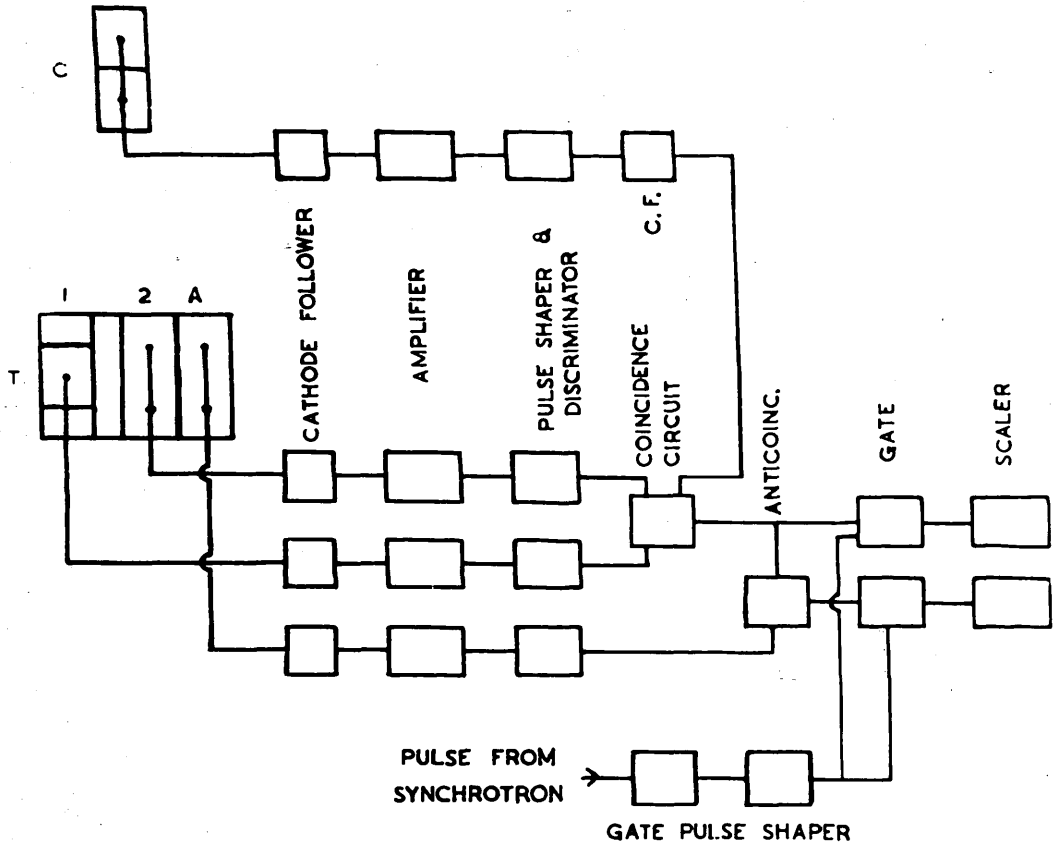


Figure 18.  
Block diagram of the electronics required for one telescope, T. C is the thin walled counter.

was facility in servicing and testing any part of the circuit before or during each run. In general the performance and reliability of the circuitry was satisfactory, even over a period of three weeks.

(c) Performance of Detector System.

The purpose of the detector system described in the previous section was to identify charged pions in a background of electrons, protons,  $\gamma$ -rays and neutrons. The following method was adopted to test the technique; a given energy range of the pion was selected, and with a counter telescope placed at the calculated position in the magnet as governed by the momentum of the pion, the variation in coincidence rate with magnetic field was observed. The expected result of such an operation would be a maximum in the counting rate at the field corresponding to the momentum of the pion which was acceptable as far as defined by the range in the absorber of the telescope.

Before any quantitative measurements could be made with the set-up, it was necessary to be sure that the overall gain of each counter or group of counters of the telescopes remained constant. This gain could be affected by numerous factors; one of these was loss of pulse amplitude in the proportional counters due to

poison of the gas with time - this was kept to a minimum by changing the filling gas frequently. Another factor was the change in the potential applied to the wire of the counter. This in turn was almost eliminated both by using stabilised E.H.T. units which had long term voltage stability of better than five volts per day, and by adding methane to the filling gas thereby causing the gas multiplication to be less steeply dependent on the applied voltage. Finally, another factor was the change in gain of the main amplifiers. This last fluctuation together with the previous two could be taken into account by monitoring the amplitude of the pulses at the output of the amplifiers. The reference pulses were those from fast electrons (i.e. minimum ionising particles). These could be made to enter the telescopes, after being produced in a thin lead target, by reducing the magnetic field to about one kilogauss. The variation in the current through the magnet coils was produced by controlling the exciter field of the D.C. generator supplying the magnet. If the pulse amplitude produced by minimum ionising particles was known, then the bias levels of the discriminators could be set to accept pions of known average ionisation loss. Hence, at the

start of each run, fast electrons were deflected into the telescopes, and the overall gain of each of the ten channels was adjusted to give three volt pulses. Then a pulse generator was used both to set the discriminator levels at this value and to check the remainder of the electronics.

Before the deuterium experiment was started, some considerable effort was expended in testing the detector system under various conditions. In this preliminary work, four different targets were used, namely carbon, polythene, lead and liquid hydrogen.

Because of the facility with which solid targets (as distinct from liquid hydrogen for example) could be obtained, carbon and polythene were used in the first instance. These targets were useful in the sense that the pion counting rate was high, compared to liquid hydrogen, so that statistically significant results could be obtained quickly. The spectrum of counting rate (two-fold coincidence, anticoincidence) versus field showed a maximum at the expected field value, but the background rate on either side of the peak was disappointingly high, amounting to about 30% of the total, figure 19. It was at this stage the extra coincidence counter (thin walled type) was considered.

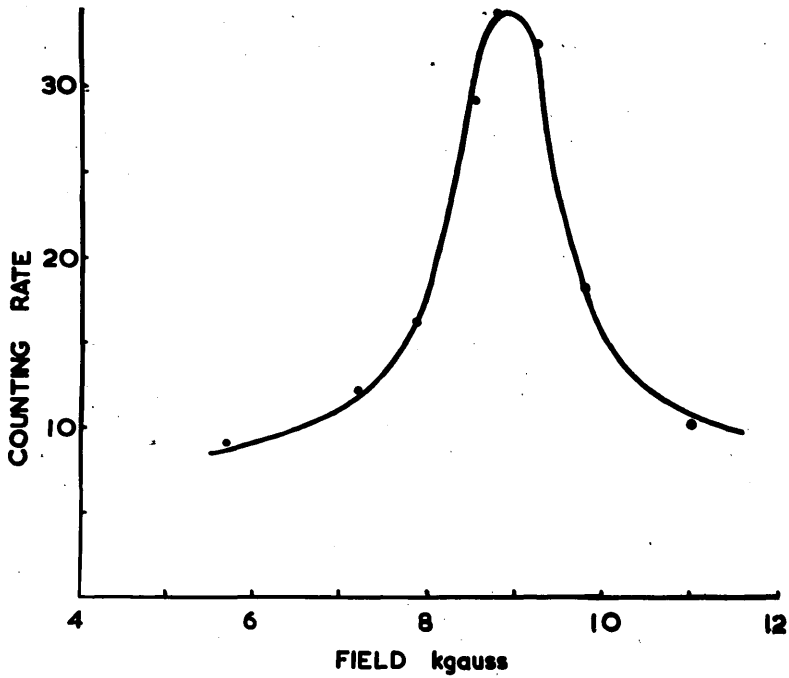


Figure 19.

$\pi^-$  spectrum from carbon.  
(double coincidence and anticoincidence).

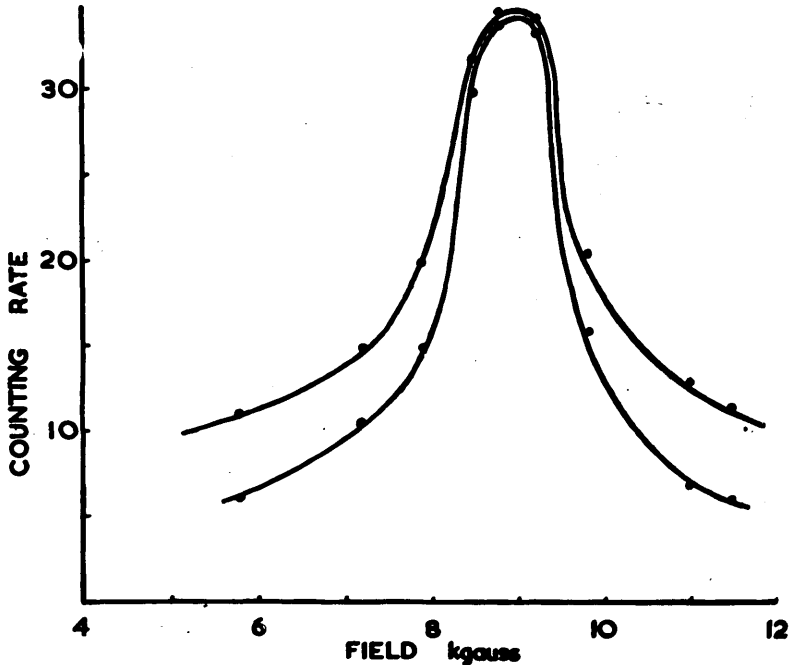


Figure 20.

Efficiency of the slit counter G.  
Top curve - double coincidence and anticoincidence,  
Bottom curve - three-fold coincidence and anticoincidence.

While the carbon and polythene targets produced quite a high yield of pions (about 100 pions per hour for the experimental arrangement used) they suffered from the disadvantage of contributing a large number of electrons to the observed counting rate. This was distinctly noticeable after the slit counter was introduced, when the counting rate in this counter exceeded more than one pulse per ten microseconds. With this pulse rate frequency, it was doubtful if the pulse shaping circuitry could handle this without being troubled with pile-up, for example. It was felt that although there was an appreciable diminution of the background counting rate, this counter would operate more efficiently when liquid hydrogen or deuterium was irradiated since the electron contribution would be much less. The efficiency of this counter for removing accidental counts by demanding that the particle, which registered in the telescope, should traverse the slit at the entrance to the magnetic field was obtained, and it is shown in figure 20.

The performance of the detector system, when a large number of electrons was emitted from the target, was observed by irradiating a lead plate. It was possible to deflect electrons from the lead target into the

telescopes when the field was adjusted to a low value. A typical spectrum is given in figure 21, where it is seen that the electron peak fell steeply, the counting rate at 4 kilogauss being only 3% of that at the peak.

Considerable time was devoted to the study of the behaviour of the meson detection system using a liquid hydrogen target. This work was an estimation of the reliability of the technique to detect pions when both the pion counting rate (about 30 per hour) and the background rate were low. This part of the work can be conveniently divided into three sections.

(i) Due to the high background counting rate of electrons from the carbon and polythene targets, the effect of the slit counter was not as marked as might be expected (see figure 20). With liquid hydrogen, however, as the source of pions it was found that the counting rate in this counter was on the average less than one pulse per thirty microseconds. The accompanying electronics could deal with this pulse rate. When the three-fold coincidence was demanded, the background from hydrogen decreased to less than 10% of the total observed counting rate, as illustrated in figure 22. This typical spectrum was obtained with a  $1\frac{1}{2}$ " cylinder of liquid hydrogen in the bremsstrahlung

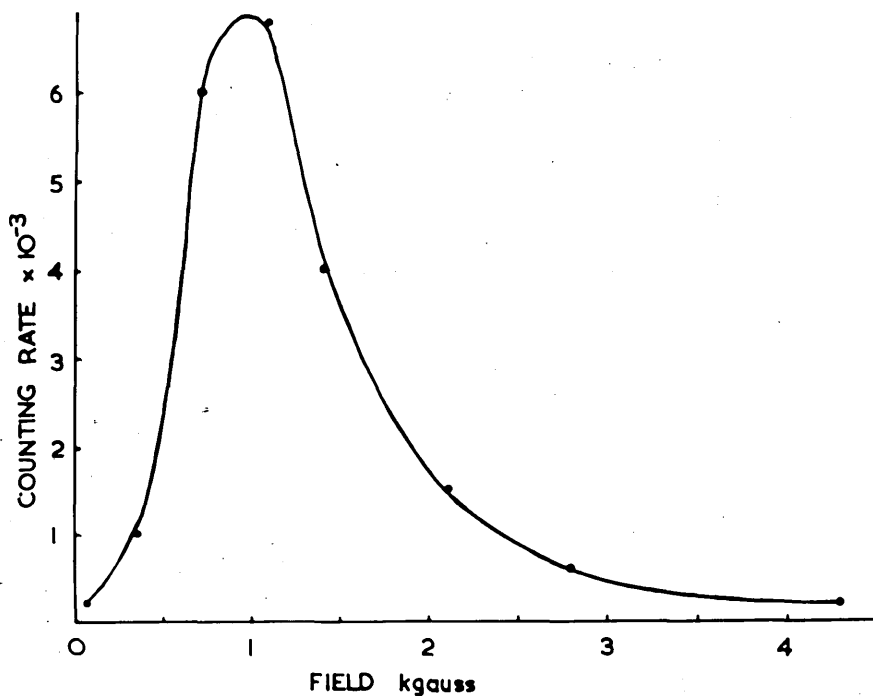


Figure 21.  
Electron spectrum from lead.

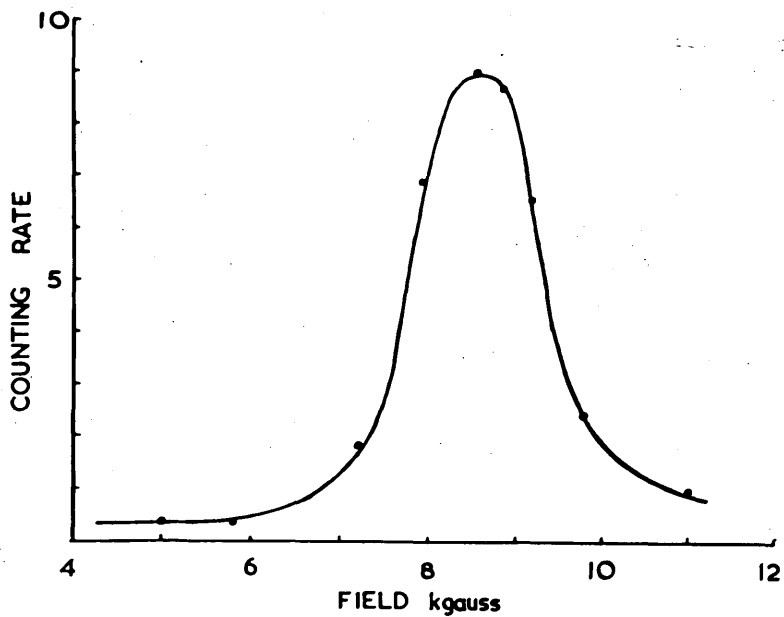


Figure 22.  
 $\pi^+$  spectrum from hydrogen.  
(three-fold coincidence and anticoincidence)

beam of maximum energy of 330 MeV. The slit counter was placed at the entrance to the field at<sup>a</sup>/distance of one metre from the target. The angle of emission of the  $\pi^+$  mesons was  $75^\circ$  in the laboratory frame, and the telescope accepted pions in a 25 MeV interval centred on 45 MeV. With a beam intensity of the order of  $10^9$  equivalent quanta per minute, the observed counting rate, as stated above, was about one per two minutes so that the spectrum of figure 22 was obtained in about one day of accelerator time. The spectrum from liquid hydrogen shows the resolution of the detector system, as measured by the relative counting rates at the meson peak and on either side, under conditions which would be similar to those expected when liquid deuterium was irradiated. In figure 22, the calculated maximum of the  $\pi^+$  meson peak was 8.5 kilogauss, and this was observed. The energy interval accepted by the telescope, as defined by the range of the pions in the copper absorbers, was greater than that defined by the momentum condition (which was determined by the geometry of the front counter). Also, spectra (such as figure 22) were obtained by deflecting pions of energy between 10 and 80 MeV (corresponding to fields of 4 to 12 kilogauss respectively) through the telescope. For these two

reasons, the pion spectrum would be expected to exhibit two definite cut-off values. One of these would be at the low energy end. This was calculated to be at 7.1 kilogauss, where it is seen that there was experimental agreement. On the other hand, 9.8 kilogauss was the expected value of the high energy limit where there was evidence of a tail to the spectrum. This was assumed to be due to  $\mu$  mesons coming from the decay in flight of  $\pi$  mesons.

(ii) There were two ways in which the meson detection system could be used, depending on the material irradiated; if the target was a substance of low atomic number (and hence the electron production would be relatively small except at forward angles of emission), then it might be unnecessary to use the anticoincidence counters. Alternatively, if these counters were used, it would be required to measure the efficiency of the telescopes for detecting  $\pi^+$  mesons. This would be the technique adopted for targets of high atomic number. Consider this second case; the original design of the telescopes with two coincidence channels and one anticoincidence at the back was made to eliminate high energy electrons of the same momentum as the observed pions, since these electrons (or positrons) would traverse all three

counters of the telescope and be rejected by the anticoincidence circuit. The following case, however, must be considered; a  $\pi^+$  meson might stop in the absorber between the second coincidence and the anticoincidence counters, and decay to a positron in just over two microseconds. If this positron was emitted in the same direction as the parent pion and entered the anticoincidence counter, it would be doubtful if the original meson would be counted. The reason for this is the fact that the time resolution of the set-up could not distinguish this decay positron from a high energy positron (for example) which was produced in the target and was transmitted by the magnet into the telescope. If the pulse from such a positron (that is, one which traversed the telescope) was delayed in the last counter due to slow collection of ions in a volume of low field, and since there was no pulse amplitude analysis in the coincidence counters (which ideally could distinguish a pion from a fast positron), then the electronic circuitry could not always distinguish these two cases. Therefore, it was necessary to know the fraction of  $\pi^+$  mesons which the telescopes missed when the anticoincidence counters were in use.

This efficiency could be obtained from a liquid hydrogen target in the following way; when the

anticoincidence was demanded, a fraction of the total number of  $\pi^+$  mesons emitted from the target, and all the  $\pi^-$  mesons from the walls of the target would be counted respectively at the two different polarities of the magnetic field. This neglected the  $\pi^-$  star products which were emitted forward into the anti-coincidence counter, but this must be a small effect since the total number of  $\pi^-$  mesons itself was about 10% of the  $\pi^+$  meson counting rate, from liquid hydrogen. When only coincidences were used, on the other hand, all the  $\pi^+$  mesons and the positrons, and all the  $\pi^-$  mesons and electrons from the target would be counted. If it was assumed that the numbers of positrons and electrons from the target were equal (this was not unreasonable when the pair production origin of these particles was considered), then the fraction of  $\pi^+$  mesons counted with the anticoincidence counter in circuit could be calculated. Hence, the  $\pi^+$  meson counting efficiency was established.

(iii) For the case of a target of low atomic number, for example liquid deuterium, it might be expected that the contamination of the observed pions by electrons would be very small. If this was proved true (that is, less than 10% of the total) and if this fraction was

measurable, then it would not be necessary to use the anticoincidence counters. Therefore, it would not be required to measure the efficiency of the system for detecting  $\pi^+$  mesons. When liquid hydrogen was irradiated it was experimentally found that the background was indeed small (see figure 22). The problem remaining was the estimation of this quantity. It was not sufficient merely to measure the counting rate from the empty liquid target (when liquid deuterium was being investigated, for instance) since there would be an unknown contribution of electrons from the liquid deuterium itself. While it would be expected that this would be small, it was a better method to measure the background when the magnetic field was set to transmit negatively charged particles coming from a full liquid hydrogen target. This measured the number of electrons from the liquid hydrogen as well. If it was assumed that the number of electrons from the hydrogen was the same as would be expected from deuterium, then it was this background measurement which was the fraction to be subtracted from the total observed counting rate. Hence, this would be measured by using a liquid hydrogen target.

The spectra shown in Figures 19, 20, 21 and 22, were obtained with experimental arrangements which had

the following factors in common; a bremsstrahlung beam of maximum energy of 330 MeV was used to irradiate the various targets. The pions were emitted at  $75^\circ$  to the photon beam into a total angular aperture of  $10^\circ$  in the plane of the beam, and the counter telescope was positioned to accept pions of an average energy of 45 MeV in a range 25 MeV wide. The relative numbers of target nuclei in the photon beam to give these results were about 45: 275: 500: 1000 for lead, hydrogen, polythene, carbon respectively. The curves drawn in the figures represented the best visual fits to the observed counting rates which were known to better than 10% statistically. The counting rates were normalised to that of hydrogen which was expressed in units of  $10^{10}$  equivalent quanta, approximately.

In conclusion, from the evidence given here it was plain that the detection technique for mesons would operate satisfactorily when liquid deuterium was used, since its behaviour was well known when pions from liquid hydrogen were detected, and since the background (which could be the worst problem to overcome) from deuterium would be expected to be of the same order of magnitude as that observed from hydrogen.

## Chapter V.

The Photoproduction of Charged Pions from  
Deuterium - Results.

## (a) Experimental Details.

## (i) Synchrotron.

In all the work described here, the source of photons was the bremsstrahlung beam of the Glasgow electron synchrotron. This machine has been described elsewhere by McFarlane et al (1955).

At present, the peak electron energy available is 340 MeV. The photon beam is produced by the accelerated electron beam striking a tungsten target which is a wire, 1/16 inch diameter, placed normal to the median plane of the synchrotron. The bremsstrahlung beam is emitted in the forward direction with respect to the electron beam, and it passes out of the vacuum chamber through a thin window in the ceramic wall of the donut. The beam emerging from the machine shows rather a wide intensity distribution across its diameter, with an angular width of about a half of a degree at half maximum.

The  $\gamma$ -ray beam passes through an aperture in the wall of the synchrotron chamber into a separate beam room so that the nearest point to the machine at which experiments can be conveniently carried out is about

six metres from the tungsten target. At this position the diameter of the beam (at half maximum intensity) is just under two inches. Because it was desirable to have a beam which was well defined in cross-section and position, it was necessary to introduce a collimation system. This has been described by Atkinson et al (1957) in connection with an expansion chamber investigation. The effect of the collimation was to reduce the beam angular divergence to a cone of  $1/5$  degree and the width to about  $7/8$  inch at the point six metres from the target. The collimator and beam tube are illustrated in figure 23 (by kind permission of Atkinson et al).

The position of the liquid deuterium target was two metres from the exit port of the pair spectrometer, figure 23. For half of this distance, the beam was enclosed in a three inch diameter tube, so that the beam was in vacuum from the collimator to within one metre of the liquid target. Further shielding was achieved by placing a six inch thick steel screen between the pair spectrometer and the deuterium target, the beam tube passing through a central hole in this screen.

During the deuterium experiment, the maximum energy of the bremsstrahlung beam required was 240 MeV, and

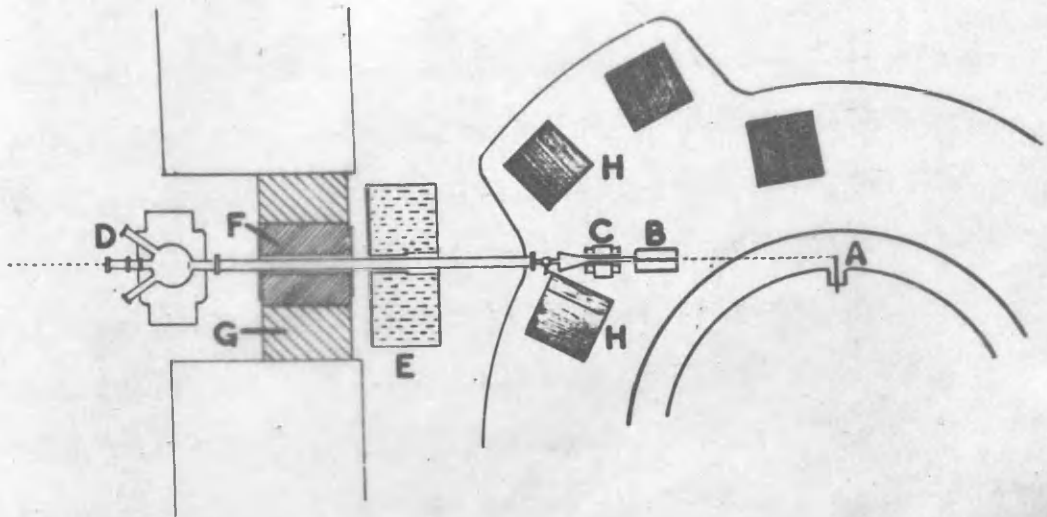


Figure 23.

Collimator and beam tube.

- A - synchrotron target, B - collimator, C - scrubbing magnet,  
 D - pair spectrometer, E - water tank, F-lead shielding,  
 G - barytes loaded concrete, H - part of magnet yoke.

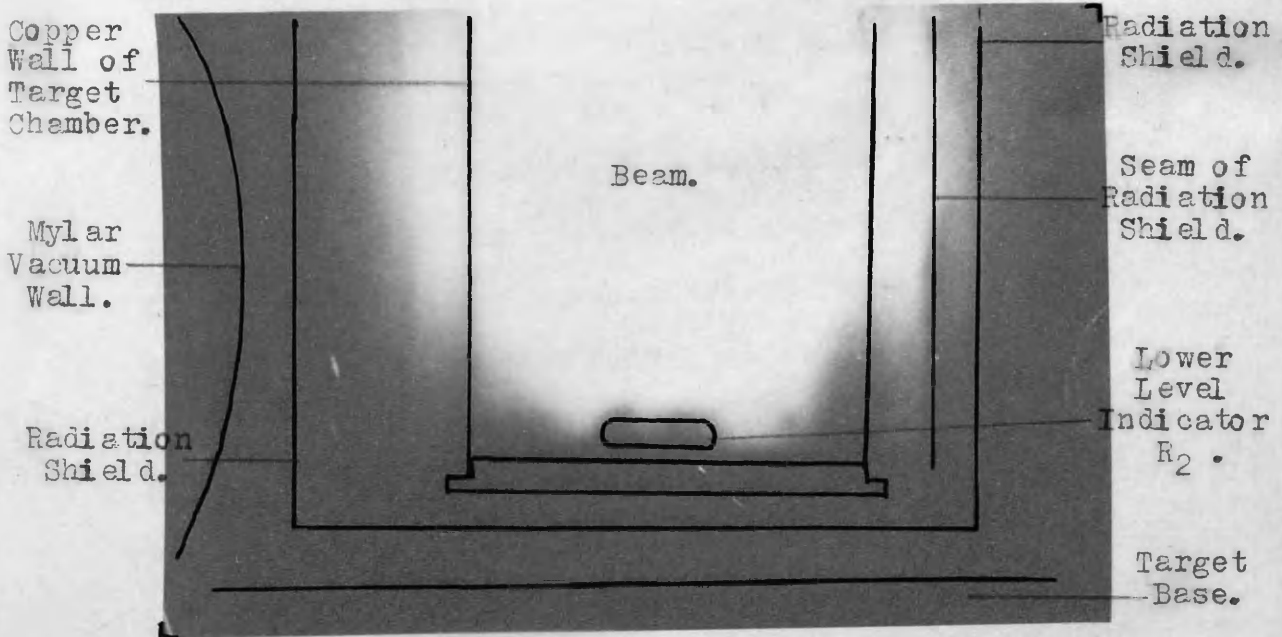


Figure 24.

Taken from an X-ray film ; showing the position of  
 the photon beam in the target.  
 ( Enlarged by a factor of 5/3 )

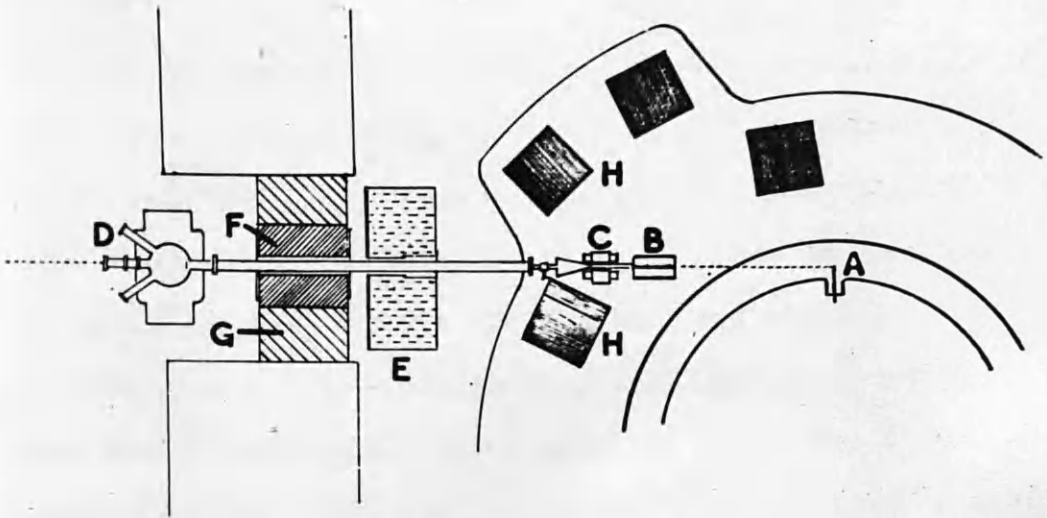


Figure 23.

Collimator and beam tube.

- A - synchrotron target, B - collimator, C - scrubbing magnet,  
 D - pair spectrometer, E - water tank, F-lead shielding,  
 G - barytes loaded concrete, H - part of magnet yoke.



Figure 24.

Taken from an X-ray film ; showing the position of  
 the photon beam in the target.  
 ( Enlarged by a factor of 5/3 )

the machine was used continuously running, that is every eleventh or twelfth cycle of mains frequency. The bremsstrahlung beam was monitored by a Cornell type ionisation chamber which was placed at the end of the beam room, about 12 metres from the pair spectrometer. By this means, the intensity of the beam was determined. The maximum energy of the bremsstrahlung beam was known to within 5 MeV, from pair spectrometer measurements.

(ii) Deuterium Experiment.

From a consideration of the previous results published for the  $\pi^-/\pi^+$  ratio from deuterium for pion energies below 60 MeV at  $90^\circ$  c.m.s., figure 5, it was decided to make measurements of the ratio from as low an energy as practicable and yet overlap the Rome - Illinois and the Cal. Tech. ratios. The present results were obtained in two periods of machine time, occupying a total of six weeks. The counter telescopes were arranged to accept the following five ranges of pion energies: 10 to 15 MeV, 15 to 22 MeV, 23 to 29 MeV, 35 to 43 MeV and 46 to 53 MeV. These were the intervals of pion energy defined by momentum only, and not the energies of the pions at creation.

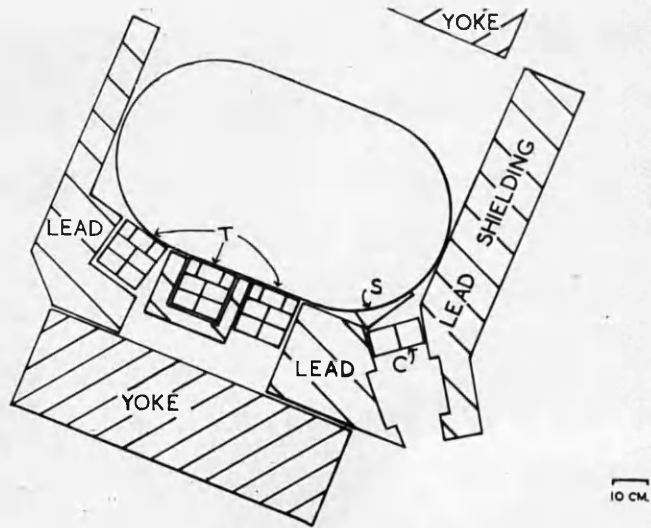
The position of the 1.5 inch diameter liquid

target was about eight metres from the synchrotron target. At this distance the collimated beam diameter was about three cm. This can be seen from figure 24 which is an electron scattering photograph used for the alignment of the liquid target in the photon beam. The angle of emission of the pions with respect to the direction of the photon beam was  $75^\circ$ , this being known to within two degrees. Mesons, which were emitted into an angular width of  $10^\circ$  in the plane of the beam, were accepted. This angular width was defined by a collimator of two lead slits. The solid angle subtended by the entrance slit to the magnet at the target was 0.027 steradian. The corresponding solid angle for the telescopes was a fraction of this. The fraction was a complex factor to evaluate but for the measurements of the  $\pi^-/\pi^+$  ratio it was not required, since it applied to both the denominator and the numerator of the ratio.

It was necessary to shield the telescopes from background radiation produced from the target and from air in the path of the beam. This was done by enclosing the counters on three sides with lead, and by screening both front and back of the magnet with more lead. Such precautions were necessary when the

counting rate of real events was as low as that experienced in this work. The general lay-out of the experiment is given in figure 25, while figure 26 displays the experimental position of the deuterium target and the magnet in the beam room.

In the deuterium experiment, the anticoincidence counters were not used since the background was found to be low. This was about 12% of the total observed counting rate for telescopes accepting pions of energies above 20 MeV, approximately, and about double this value for measurements made below this energy. These background counting rates were established with liquid hydrogen in the deuterium target, by detecting negatively charged particles which satisfied the three-fold coincidence condition. This counting rate consisted of contributions of  $\pi^-$  mesons from the target walls, radiation shield and vacuum jacket, and electrons from these materials and from the liquid hydrogen. It was assumed that the background of positrons was the same as that of electrons, and that both these backgrounds were the same from liquid deuterium. The basis of these assumptions was the reasoning that the origin of the electrons and positrons was pair production, and that the negative to positive ratios of mesons for copper, aluminium and Mylar were unity



PHOTON  
 ← BEAM ————— TARGET

Figure 25.

Experimental lay-out of the deuterium experiment.  
 T - counter telescopes, C - thin walled counter, S - shim  
 on pole pieces to produce fringe field focusing.

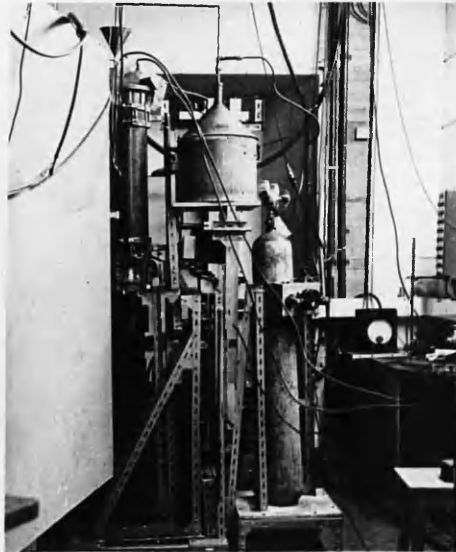


Figure 26.

Liquid target and magnet in the beam room.

in each case. This could introduce an error, but this must be of the order of a few per cent of the total background counting rate. As a check, background counting rates from the empty deuterium target were taken and it was found that there was no statistical difference from the rate of negative particles from liquid hydrogen ( $7\% \pm 15\%$  of total background). In other words, the contribution to the background of electrons from the liquid hydrogen itself was negligibly small. The same cryostat and target chamber were used with liquid deuterium or liquid hydrogen as required, so that conditions were maintained the same throughout the operations described above.

(b) Results.

In the first part of the deuterium work, the energy intervals of the pions selected were 10 to 15 MeV, 23 to 29 MeV, and 46 to 53 MeV. On the other hand, in the second period, only two ratios could be determined, since the pions accepted by the high energy telescope were produced by photons very near the cut-off of the 240 MeV bremsstrahlung spectrum. Here the ratio would become sensitive to small fluctuations in the maximum energy of the bremsstrahlung, and also the

number of available photons for producing the high energy pions would be very small. In both allocations of machine time, the maximum energy of the machine was maintained at the same value, namely  $240 \pm 5$  MeV, and the counters were also kept in the same positions in the magnet. The two different sets of energy ranges of pions measured were obtained by increasing the magnetic field from 8.5 to 10.3 kilogauss. The current through the magnet windings could be varied by the control unit, mentioned earlier. Over a period of twelve hours, the drift in magnet current amounted to about a one per cent variation in the value of the field.

The data from which the  $\pi^-/\pi^+$  ratios were calculated are given in Table 3. The two columns (5) and (6) are the observed counting rates for negative and positive mesons, after normalising for exposure to the same number of equivalent quanta. The errors quoted are standard deviations. In order to obtain the true negative to positive ratio for deuterium, these observed rates must be corrected for background, for impurities in the liquid target, for absorption of mesons, for decay in flight of the pions, and for spread in the energies of the pions due to target thickness. By far the largest correction

(1)	(2)	(3)	(4)	(5)	(6)	(7)	(8)	(9)
10 - 15	15	829	695	12.11 +0.42	9.52 +0.36	3.03	1.28	1.40 +0.10
15 - 22	20	818	662	14.60 +0.51	11.40 +0.44	1.95	1.27	1.34 +0.08
23 - 29	27.5	661	572	8.73 + 0.34	7.73 +0.32	1.10	1.13	1.15 +0.08
35 - 43	40	834	694	14.90 + 0.52	11.77 +0.45	1.21	1.27	1.29 +0.07
46 - 53	50	649	554	8.87 + 0.35	7.80 +0.33	1.23	1.14	1.16 +0.08

(1) Pion energy interval, MeV. (2) Mean energy of pion at creation, MeV.  
(3) Total number of negative pions observed. (4) Total number of positive pions observed. (5)  $\pi^-$  counts normalised for photon flux. (6)  $\pi^+$  counts normalised for photon flux. (7) Background normalised. (8)  $\pi^-/\pi^+$  ratio uncorrected. (9)  $\pi^-/\pi^+$  ratio corrected for background.

Experimental Data of Deuterium Experiment.

Table 3.

factor is that of background. The magnitude of these counting rates can be seen from column (7) of Table 3.

The purity of the liquid deuterium was estimated by a mass spectrographic analysis of the deuterium gas. A troublesome impurity which might be present in the liquid target would be hydrogen, but it was established that the contamination of the deuterium gas by hydrogen was negligibly small. The effect of this would be to cause an increase in the  $\pi^-/\pi^+$  ratio from deuterium by an amount never greater than 1%.

Another correction factor which must be considered is the absorption of the pions; the materials traversed by the pions include liquid deuterium, the aluminium, copper and Mylar foils surrounding the deuterium, the air path from the target to the telescopes, the Mylar windows of the slit counter C (figure 25) as well as the argon filling gas, and finally the copper walls and absorbers of the counters. Unfortunately, there is little pertinent information about the absorption of  $\pi^-$  and  $\pi^+$  mesons in copper, aluminium and Mylar in the pion energy range of interest, i.e. up to about 60 MeV. For aluminium, for example, it is found (for pion energies above 50 MeV) that the quantity  $(\sigma^- - \sigma^+) = 100$  m.barns

with a 50% error, where  $\sigma$  is the total absorption cross-section, and the superscripts refer to the charge of the pions. (Chedester et al 1951, Tracy 1953, and Martin 1952). There is also a lack of data for copper (this is considered in Appendix 2 in the correction of the  $\pi^-/\pi^+$  ratio from calcium). For pion energies above 70 MeV, there is no statistically significant difference in the absorption cross-sections for negative and positive mesons in deuterium. In conclusion, it was felt that there was not sufficient experimental evidence to show a difference in the mean free paths for  $\pi^-$  and  $\pi^+$  mesons in the materials concerned. Therefore, no correction for absorption was applied to the  $\pi^-/\pi^+$  ratio from deuterium.

Decay in flight of the pions could affect the results in two ways; the first concerns the number of pions which decay in the trajectory from the target to the counters. This is easily calculated if the length of the flight path is known. As this correction applies symmetrically to both  $\pi^-$  and  $\pi^+$  mesons, it cancels out in the evaluation of the ratios. The second factor is more complex, as it involves the number of pions which decay to  $\mu$  mesons which enter the corresponding telescope, and those muons which enter

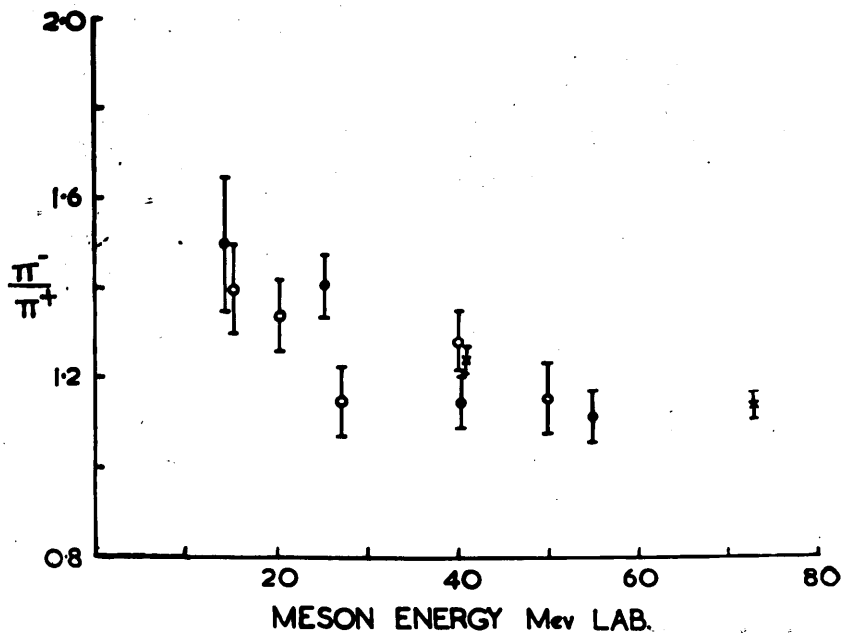


Figure 27.  
 × 73° Sands et al (1954),  
 • 75° Beneventano et al (1956),  
 ● 75° Present Results.

$\bar{\pi}/\pi^+$  ratio from deuterium as a function of meson energy, angles measured in the laboratory system.

a different telescope from that which the original pion would have entered if there had been no decay. From a knowledge of the trajectories of the pions and of the kinematics of the decay in flight of the pion, it is possible to obtain a rough estimation of this effect. In the worst case, for the low energy telescope, the estimate was 5%, while a value of 3% was obtained for the higher energy pions, the correction tending to lower the value of the ratio.

The final correction applies to the energy of the pions detected; this is due to the energy loss of pions, in the liquid deuterium and the other materials, before they reached the telescopes.

In order to see the effect of such corrections, the  $\pi^-/\pi^+$  ratios were calculated with and without subtracting the background, which contributed the most. The final values of the corrected ratios along with all other measurements are shown in figure 27. The most important conclusion to be drawn from this is that the present results have established that the previous independent measurements are experimentally consistent. This would suggest that the existing discrepancy in the values of the extrapolated ratio to threshold is in the interpretation of the observed results.

## Chapter VI.

The Photoproduction of Charged Pions from Deuterium -  
Analysis and Discussion of Results.(a) Threshold Behaviour of the  $\pi^-/\pi^+$  Ratio.

The negative to positive pion ratios from deuterium are obtained at positive pion energies, whereas the important theoretical predictions apply to pion threshold. Therefore, the object of the experimental work is to establish reliable and accurate values of the ratio, especially at low pion energies. These experimental results can then be analysed to give an extrapolated ratio, at zero pion momentum, which can be compared with the theoretical value. At this point, it will be assumed that reliable experimental  $\pi^-/\pi^+$  ratios are available, and the analysis and interpretation of such data will now be considered.

The Cal. Tech. experimental data of photopion production have been analysed by Watson et al (1956) in terms of s- and p-waves of the final pion-nucleon system. The approach was phenomenological, and the model used was that of Gell-Mann and Watson (1954), referred to in Chapter I. This treatment gave a simple explanation of the gross features of the observed results, but it failed to exhibit the detailed features.

With the aid of this model, the  $\pi^-/\pi^+$  ratio as a function of pion energy and angle was calculated. When a comparison was made with experiment, it was found that there was fair agreement at forward angles for all pion energies, but disparity at backward angles. The extrapolated  $\pi^-/\pi^+$  ratio at threshold was 1.24, assuming that Coulomb effects were negligible.

The Rome - Illinois analysis was also based on a phenomenological approach. A semi-empirical equation was derived for the energy dependence of the  $\pi^-/\pi^+$  ratio near threshold. The coefficients of the angular distribution of positive pions from hydrogen as well as experimental  $\pi^-/\pi^+$  ratios from deuterium were used to extrapolate the ratio to zero momentum. It was assumed that the angular distribution (in the centre of mass system, c.m.s.) of pion production could be expressed in the form:

$$\frac{d\sigma^\pm}{d\Omega} = A^\pm(\omega) + B^\pm(\omega) \cos\theta + C^\pm(\omega) \cos^2\theta \quad (16)$$

where, if p-wave recoil effects were neglected,

$$\begin{aligned} A^+(\omega) &= \chi(\omega) \left[ a_{0S}^+(\omega) + a_{0p}(\omega) \right] \\ B^+(\omega) &= -2 \chi(\omega) \operatorname{Re} \left[ a_{0S}^+(\omega) K(\omega) \right]^{1/2} \\ C^+(\omega) &= \chi(\omega) \left[ K(\omega)^2 - a_{0p}(\omega) \right] \end{aligned} \quad (17)$$

In these coefficients,

$$\left. \begin{aligned} a_{0s}^+ & \text{ is the s-wave contribution,} \\ a_{0p} & \text{ is the p-wave, non spin flip contribution,} \\ K(\omega) & \text{ is the p-wave, spin flip part,} \\ W(\omega) & = \frac{q \omega}{\left(1 + \frac{\omega}{M}\right) \left(1 + \frac{k}{M}\right)}, \quad \chi(\omega) = \frac{W(\omega)}{\omega k} \end{aligned} \right\} (18)$$

The units used are:

$$\left. \begin{aligned} q & - \text{ the meson momentum} \\ \omega & - \text{ the total meson energy} \\ k & - \text{ the photon energy} \end{aligned} \right\} \begin{array}{l} \text{in the c.m.s. and in} \\ \text{units of } \mu \end{array} \quad (19)$$

$M$  - the nuclear rest mass in units of  $\mu$

$\mu$  - the pion rest mass

$\hbar = c = 1.$

Each of the quantities (18) was assumed to be real at low pion energies. If the three coefficients of the angular distribution were known at each energy, then the three s- and p-wave components could be obtained.

The purpose of such a treatment was to compare the observed data with theoretical values derived using various approximations.

One of the basic points of this treatment was the dependence on pion momentum of the coefficient  $\frac{A^+}{W}$ . It was found experimentally, that this coefficient was constant in the photon energy range 170 MeV to 265 MeV,

with a further measurement at 156 MeV. On this basis, Beneventano et al extrapolated the coefficient linearly to pion threshold. This would appear to be a reasonable assumption in view of the experimental evidence alone. With this information, together with the angular distribution coefficients and four observed  $\pi^-/\pi^+$  ratios from deuterium, an empirical formula for the  $\pi^-/\pi^+$  ratio at  $90^\circ$  c.m.s. was derived. The results obtained from this analysis are the following:

- (i) The threshold value of the  $\pi^-/\pi^+$  ratio at  $90^\circ$  c.m.s. from deuterium was  $1.87 \pm 0.13$ .
- (ii) The pseudovector coupling constant was evaluated to be  $f^2 = 0.067 \pm 0.003$ .
- (iii) The form of the recoil term was such that it was found to decrease with increasing energy.

The striking feature of the above results was the high value of the extrapolated  $\pi^-/\pi^+$  ratio. It was remarked that this estimate disagreed with that predicted by perturbation theory (about 1.3) which should be correct at low energy, according to threshold theorems (for example the Kroll-Ruderman theorem). Again Coulomb effects were taken to be small (less than 5%). Also, the above value of the pion-nucleon coupling constant was low by about 20% compared to the

magnitude obtained from scattering, for example. Further, theory predicted that the recoil term should be an increasing function of energy. It was observed by the authors that this high threshold ratio was compatible with that predicted from the values of the s-wave scattering lengths and the Panofsky ratio existing at that time. (This will be dealt with in the next section). In other words, there was the suggestion that a real discrepancy existed between the predicted and the observed  $\pi^-/\pi^+$  ratio at threshold. At this point, let it be clearly stated that the experimental information yielded by the Rome - Illinois work is not doubted, but rather it is the form of analysis and interpretation of these results which is contradicted in this Thesis.

An interesting observation is that the highest value of the measured ratios was  $1.50 \pm 0.15$  at  $75^\circ$  (lab. system) for a photon energy of 170 MeV. Hence, the extrapolation to pion threshold had to show a steep dependence on energy if a value of  $r_0 = 1.87$  was to be obtained. It is found that the method of predicting the threshold value of the ratio is not unambiguous. This has been pointed out by Moravcsik (1958). An extrapolated curve of the form of Beneventano's can be

made to show a flatter dependence on energy by applying small justifiable corrections to parameters in the original analysis. As an illustration, the original extrapolated curve (dotted) of Beneventano et al (1956) and one derived from it (dashed) by including some of these adjustments, are shown in figure 28 along with all the recent experimental data. This modified curve (dashed), taken from Moravcsik (1958), was assumed to have the form:

$$R = \left[ \frac{a}{\sqrt{\omega k}} (1 + \sqrt{R_0}) - \frac{2\lambda}{\sqrt{a_0}} \left( \frac{b}{\sqrt{\omega k}} - \sqrt{\omega k} \right) \right]^2 - 2 \left[ \frac{a}{\sqrt{\omega k}} (1 + \sqrt{R_0}) - \frac{2\lambda}{\sqrt{a_0}} \left( \frac{b}{\sqrt{\omega k}} - \sqrt{\omega k} \right) \right] \left( 1 + \frac{a_2}{a_0} \right)^{1/2} + 1$$

where  $a$  and  $b$  are constants,  $R$  and  $R_0$  as in Chapter I,  $\omega$  and  $k$  as in (19), and  $a_0$  and  $a_2$  are the coefficients  $A/W$  and  $C/W$  of equation (17). The dashed curve was drawn for  $R_0 = 1.60$ , and the correction was the inclusion of the factor  $\lambda$  (part of the s-wave recoil term) which Beneventano et al took as being negligibly small, but in this case it was given a value of 5%. The energy trend of these two curves of figure 28 gave support to the view that Beneventano's extrapolation showed too great an energy dependence near threshold, and that a better fit to the experimental points was the curve of Moravcsik. Assuming the form of this

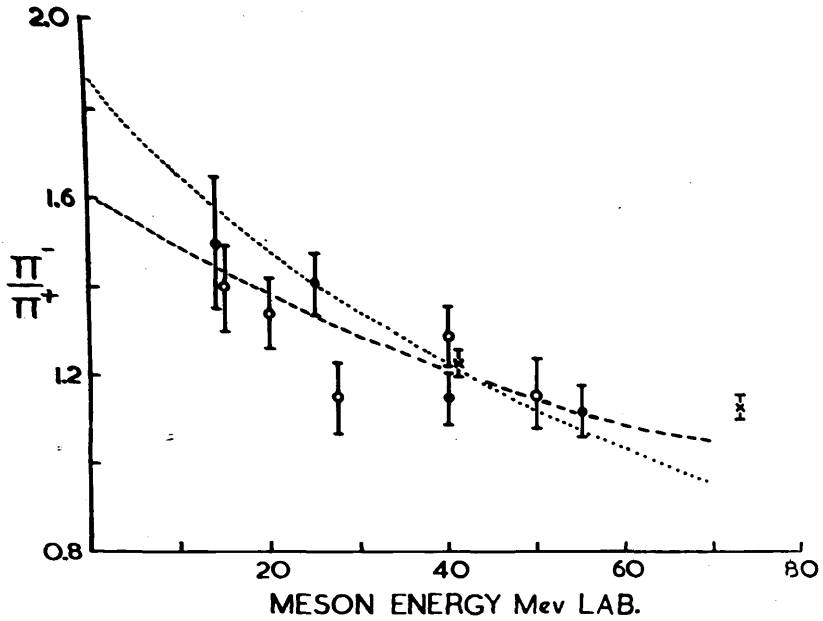


Figure 28.

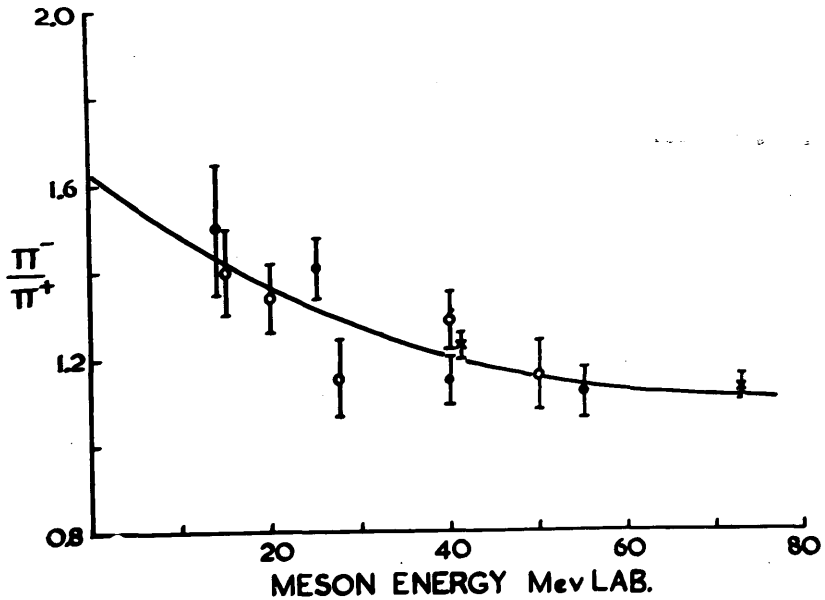


Figure 29.

$\pi^-/\pi^+$  ratio from deuterium as a function of meson energy, angles measured in the laboratory system,  
 x  $73^\circ$  Sands et al (1954),  $\bullet$   $75^\circ$  Beneventano et al (1956),  
 $\circ$   $75^\circ$  Present Results.

Dotted curve - extrapolation of Beneventano et al,  
 dashed curve - modified curve from Moravcsik,  
 solid curve - visual fit.

modified curve, a visual fit to the eleven observed ratios measured at  $90^\circ$  c.m.s. for pions of energies up to 70 MeV can be obtained, as shown in figure 29.

Because of the doubt cast on the extrapolation to threshold, it was decided to abandon the method of analysis of Beneventano et al in favour of a more rigorous treatment. As this approach made use of the ratio of the cross-sections from free nucleons, a correction factor was required to convert this ratio to that for bound nucleons in deuterium. Such a factor was considered by both Watson et al (1956) and Beneventano et al (1956) in their analyses, but the effect of the correction was assumed to be negligibly small, as already stated. This deuterium correction will now be considered.

What is required is a factor C which can be applied to the  $\pi^-/\pi^+$  ratio from deuterium, R, to give the free nucleon ratio, that is  $r = CxR$ , or vice versa. If charge symmetry was assumed, it would seem likely that purely nuclear effects in the final state would cancel. Therefore, the correction factor involves only Coulomb effects. There are no Coulomb interactions in the final state in positive pion production. However, there are three charged particles in the final state of the negative pion process, so that clearly such a factor applies only in this case. There are three such

interactions; the pion-proton interaction giving rise to a correction  $C_1$ , and the proton-proton interaction giving a correction  $C_2$ . There is also the interaction of the meson with the nucleon from which it was created,  $C_3$ . In the  $\pi^-$  production, if it is assumed that the photon interacts with only the neutron in the deuteron, then this neutron becomes a proton with a small recoil velocity when the pion is produced. Thus, it will also have a fairly small relative velocity (compared to the total phase space available) with respect to the spectator proton, and its wave function in the final state will be accordingly suppressed as compared to the  $\pi^+$  case. This effect is difficult to calculate, but a suppression of about 30% was obtained when  $2\pi x (e^{2\pi x} - 1)^{-1}$  was used for the s-state Coulomb penetration factor, where  $x = e^2/\hbar v$ , (Machida and Tamura 1951). A similar result was found by Saito et al (1952). Various estimates of the Coulomb effect have been made, but these have mainly dealt with the proton-proton interaction which does not give an appreciable contribution near threshold. Orear (1956) assumed a Coulomb correction of  $10 \pm 10\%$ . It has been reported by both Beneventano et al (1956) and Moravcsik (1957a), that Chew and Low have given a better treatment of these Coulomb interactions. These are given in Table 4.

Photon Energy MeV	185	205	225
Coulomb Factor %	7	4	3

## Coulomb Correction (Chew and Low)

Table 4.

The Coulomb correction factor is defined as the ratio of the corrected count rate to the uncorrected count rate. It is usually expressed as a percentage. The factor is used in the calculation of the activity of a source. It is obvious that the application of this factor to the curve of figure 29, for example, would give a result almost equivalent with energy.

The whole problem of the interpretation of photo-production from deuterium bound nucleons has been dealt with by Baldin (1958). After a rigorous treatment of the Coulomb correction, the conclusions reached by this author were that  $C_1$  was a negative correction, increasing in magnitude as the pion energy decreased below about 25 MeV, and that  $C_2$ , a positive correction, only became important for pion energies greater than 25 MeV. Baldin gave an explicit expression for the correction  $C_1$  in terms of the momentum vectors of the photon and the meson. Because of the three body problem in the final state and because a bremsstrahlung beam is used in the experimental investigation of such processes, the values of these momentum vectors cannot be determined uniquely. However, in the expression for the Coulomb correction, the meson momentum vector term dominates, and also it is the pion energy which is usually observed, so that a good approximation can be used in the evaluation of this correction factor. It is obvious that the application of these corrections to the curve of figure 29, for example, would tend to give a ratio almost constant with energy, in qualitative agreement with theory.

There have been several attempts to derive the  $\pi^-/\pi^+$  ratio from free nucleons. From the point of

view of charge independence, it might be thought, in the first instance, that this ratio would be unity. However, charge independence cannot be applied directly to photoproduction, since isotopic spin is not conserved in processes involving photons. A classical argument was given by Brueckner and Goldberger (1949) to explain the  $\pi^-/\pi^+$  ratio in terms of a current interaction of the form  $\underline{j}\cdot\underline{A}$ , where  $\underline{A}$  is the vector potential. For the process  $\gamma+n\rightarrow\pi^-+p$  the incident photon can interact with the two currents of the meson and the recoil proton. In the positive pion reaction, there is only the meson current. If these currents are associated with the movement of the particles, then one obtains:-

$$\begin{aligned} \frac{\sigma^-}{\sigma^+} &= \frac{(\underline{j}\cdot\underline{A})_{\pi^-} + (\underline{j}\cdot\underline{A})_p}{(\underline{j}\cdot\underline{A})_{\pi^+}} \\ &= \left[ 1 - \frac{\omega}{M} (1 - v \cos \theta) \right]^{-2} \end{aligned} \quad (20)$$

where  $\omega$  and  $M$  are defined in (19),  $v$  is the velocity of the pion, and  $\theta$  is the laboratory angle between the pion and the photon. This function is plotted in figure 30 which was calculated for  $\theta = 75^\circ$ . It is seen that equation (20) predicts much larger ratios than those observed, the disparity being more marked as the energy increases. Even at moderate energies,

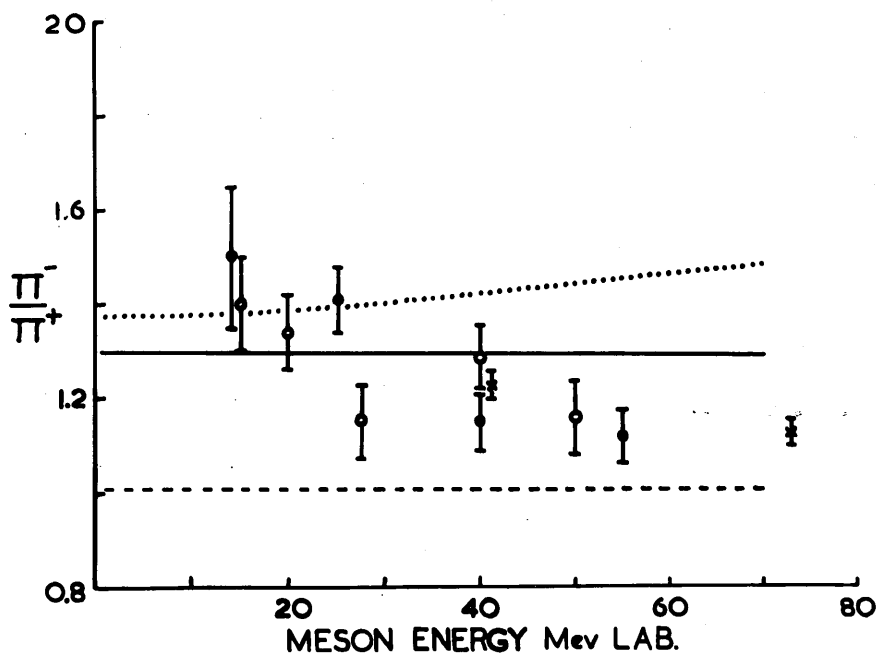


Figure 30.

Dotted curve - from Brueckner and Goldberger (1949),  
 dashed curve - from Brueckner (1950),  
 solid curve - drawn for  $r = 1.30$ .

$\pi^-/\pi^+$  ratio from deuterium as a function of meson energy,  
 angles measured in the laboratory system.  
 x 73° Sands et al (1954), • 75° Beneventano et al (1956),  
 o 75° Present Results.

the disagreement is outside the experimental error. This argument was expanded by Brueckner (1950) by including in the current  $\underline{j}$ , the magnetic moment also. If the meson - nucleon interaction is suppressed, and if the interaction through the magnetic moments is taken to be predominant, the prediction for the ratio is too small, yielding about 1.06 for all energies at 90° c.m.s. (figure 30). Similar results were obtained by Kaplon (1951). None of the above theories, therefore, gives a good fit to the experimental data. What is required is a theory which includes the two types of interactions in the correct proportion, as it were, to give the observed ratio.

Using a perturbation theory approach, Klein (1955) calculated the threshold ratio  $r_0$  assuming only s-wave production by electric dipole absorption of the photon. If Coulomb effects were neglected, the resulting ratio was:

$$r_0 = \left( 1 + \frac{\mu}{M} \right)^2 = 1.32$$

While this gives the expected threshold value of the ratio, it was decided to obtain a treatment of the energy dependence of the ratio which would include automatically the threshold value.

In general, nonrelativistic theories of pion

photoproduction give a differential cross-section which can be expressed as (see Chew and Low 1956, or Moravcsik 1957a) :

$$\frac{d\sigma}{d\Omega} = K \left[ a \underline{\sigma} \cdot \underline{\epsilon} + b \frac{\underline{\sigma} \cdot (\underline{k} - \underline{q}) \underline{q} \cdot \underline{\epsilon}}{(\underline{k} - \underline{q})^2 + 1} + c \left[ i \underline{q} \cdot (\underline{k} \times \underline{\epsilon}) - (\underline{\sigma} \cdot \underline{k} \underline{q} \cdot \underline{\epsilon} - \underline{\sigma} \cdot \underline{\epsilon} \underline{q} \cdot \underline{k}) \right] + d \left[ 2i \underline{q} \cdot (\underline{k} \times \underline{\epsilon}) + (\underline{\sigma} \cdot \underline{k} \underline{q} \cdot \underline{\epsilon} - \underline{\sigma} \cdot \underline{\epsilon} \underline{q} \cdot \underline{k}) \right] + e \left[ \underline{\sigma} \cdot \underline{k} \underline{q} \cdot \underline{\epsilon} + \underline{\sigma} \cdot \underline{\epsilon} \underline{q} \cdot \underline{k} \right]^2 \right] \quad (21)$$

where  $K$  is an energy dependent constant (including phase space factors),  $a \dots e$  are constants to be determined from various theories,  $\underline{\sigma}$  is the nucleon spin and  $\underline{\epsilon}$  the photon polarisation, and the rest of the symbols have been defined in (19). The purpose of theories is the evaluation of the constants  $a \dots e$ . For example, in the phenomenological theory used by Watson et al (1956), discussed earlier, these coefficients were obtained from experimental data.

If the discussion is now restricted to low photon energies (less than 200 MeV), then the important terms of (21) which contribute to the photomeson production amplitude are the first two alone. The first term in the square brackets is a pure s-wave term, arising from the requirement of gauge invariance. The second term of equation (21) takes into account the interaction of the electromagnetic field with the meson current.

This term contains all angular momentum states with strengths which decrease slowly with angular momentum. The direct interaction term does not depend on a particular meson theory, appearing in all the theories mentioned in Chapter I. With the inclusion of this term, the angular distribution of pion photoproduction can now be written:

$$(1 - \nu \cos \theta)^2 \frac{d\sigma}{d\Omega} = A + B \cos \theta + C \cos^2 \theta + D \cos^3 \theta + E \cos^4 \theta \quad (22)$$

The importance of this term has been pointed out by Moravcsik (1956) and (1957b). If the positive meson angular distribution is expressed thus, the behaviour of the experimental data at small forward angles can be accounted for, (for example, see Knapp et al 1957, and Malmberg and Robinson 1958). In other words, not only is the direct interaction term based on sound theoretical arguments, but the necessity to include it in the theory has also been demonstrated experimentally.

An examination of the first two terms of equation (21) shows that the form is symmetrical for both positive and negative pion production, that is a  $\pi^-/\pi^+$  ratio of unity. This is in disagreement with both experiment and other theoretical predictions. The same difficulty was met by Moravcsik (1957a). This author finally

used a model which was a combination of contributions of a perturbation s-wave and of higher angular momenta of the type obtained from Low's nonrelativistic theory. By this approach, it was possible to predict the angular distributions of the  $\pi^-/\pi^+$  ratio (from free nucleons) for photon energies between 170 and 400 MeV. In particular, it was estimated that the value of the ratio was 1.3 at an angle of  $75^\circ$  (laboratory system) for the photon energy interval 170 to 230 MeV. The uncertainty, introduced by choosing different approximations in the theory, in this determination was about 5%. Coulomb field effects were neglected since these were reckoned to amount to less than 10%, which was the magnitude of the average error of the experimental data. The same type of solution was adopted in the present treatment.

The expression (21) is derived from a consideration of the interaction between the pion field and a single fixed nucleon. In order to take into account the finite nucleon mass, nucleon recoil terms must be added. This includes effects of the order  $V/c$  where  $V$  is the nucleon velocity. Kinematical effects give rise to a factor  $(1 + \frac{\omega}{M})^{-2}$  in the cross-section, applying to both charged pion production processes. A simple

classical approach to the type of photoproduction mechanism expected, leads to the conclusion that the transition is electric dipole at threshold. The matrix element for  $\pi^+$  photoproduction corresponding to an electric dipole transition with the production of an s-wave pion is given by a term proportional to  $\underline{\sigma} \cdot \underline{\epsilon}$ . This term can be corrected for recoil effects by considering the currents of the particles involved in the two charged production processes. This introduces a difference in the matrix elements for the two processes, which can be expressed by a factor  $(1 \pm \frac{\omega}{2M})$ , the positive and negative signs corresponding to  $\pi^-$  and  $\pi^+$  mesons respectively.

Therefore, the differential cross-section for charged pion production can now be written :

$$\frac{d\sigma^{\mp}}{d\Omega} = 2 \frac{e^2 f^2}{\mu^2} \frac{q\omega}{(1 + \frac{\omega}{M})^2} \sum \left| \frac{1}{\sqrt{\omega k}} \left[ (\underline{\sigma} \cdot \underline{\epsilon}) \left(1 \pm \frac{\omega}{2M}\right) + 2 \frac{\underline{\sigma} \cdot (\underline{k} - \underline{q}) q \cdot \underline{\epsilon}}{(\underline{k} - \underline{q})^2 + 1} + F(\omega) \right] \right|^2 \quad (23)$$

where the sum implies the average over nucleon spin and photon polarisation,  $e^2 = 1/137$ ,  $f^2$  is the pion - nucleon renormalised coupling constant,  $F(\omega)$  is a term including all p-wave contributions, and the other quantities are the same as for equation (19). In the energy region under consideration,  $F(\omega)$  would be expected to add only a few per cent to the photoproduction cross-section at  $90^\circ$  c.m.s. Support for the validity

of the form of the recoil term (  $1 \pm \frac{\omega}{2M}$  ), and for only considering the first two terms of (21) can be obtained from a consideration of the low energy theorems. One of these, due to Kroll and Ruderman (1954), states that to the lowest order in  $\mu/M$ , the s-wave photoproduction contribution to the cross-section is correctly given by the lowest order perturbation result. Kroll and Ruderman found that there was a small difference between  $\pi^-$  and  $\pi^+$  photoproduction :

$$\begin{aligned} \frac{d\sigma^-}{d\Omega} &= S \left[ 1 + b \frac{\mu}{M} + O\left(\frac{\mu^2}{M^2} \log \frac{M}{\mu}\right) \right] \\ \frac{d\sigma^+}{d\Omega} &= S \left[ 1 - b \frac{\mu}{M} + O\left(\frac{\mu^2}{M^2} \log \frac{M}{\mu}\right) \right] \end{aligned} \quad (24)$$

where S is the perturbation cross-section for electric dipole production of s-wave pions

$$\frac{d\sigma^S}{d\Omega} = 2 \frac{e^2 f^2}{\mu^2} v \quad (25)$$

where v is the velocity of the outgoing pion (Chew 1954). Equations (24) can be expressed in the form (if higher order terms are neglected):

$$\frac{d\sigma^\mp}{d\Omega} \sim 1 \pm f(\omega) \quad (26)$$

where  $f(\omega)$  is of the order of  $\mu/M$ . A similar theorem can be established for the meson current contribution to the cross-section, Klein (1955); it is found that the contribution of the direct interaction term in the low energy limit must be of the form given in equation

(23) up to a correction term of the order of  $(\mu/M)^2$ .

Further, it is also possible to take account of the magnetic moment interaction (see Watson 1952). However, a theoretical treatment which would include this interaction is beyond the scope of this Thesis. Instead, only the result, due to Cini et al (1958), will be quoted:

$$\frac{d\sigma^{\mp}}{d\Omega} = 2 \frac{e^2 f^2}{\mu^2} \frac{q \omega}{(1 + \frac{\omega}{M})^2} \left[ \frac{1}{\sqrt{\omega k}} \left[ (\sigma \cdot \xi) \left( 1 \pm \frac{R(\omega)}{2} \right) + 2 \frac{\sigma \cdot (k-q) q \cdot \xi}{(k-q)^2 + 1} + F(\omega) \right] \right]^2 \quad (27)$$

where the recoil factor is now expressed by

$$1 \pm \frac{1}{2} R(\omega)$$

where

$$R(\omega) = (g_p + g_n) \frac{\omega}{M} \quad (28)$$

in which  $g_p$  and  $g_n$  are the anomalous parts of the proton and the neutron magnetic moments respectively.

On evaluation, equation (27) gives the following differential cross-section at  $90^\circ$  in the centre of mass system near threshold :

$$\frac{d\sigma^{\mp}}{d\Omega_{90^\circ}} = 2 \frac{e^2 f^2}{\mu^2} \frac{q/k}{(1 + \frac{\omega}{M})^2} \left[ 1 - \frac{v^2}{2k^2} \pm (g_p + g_n) \frac{\omega}{M} \left( 1 - \frac{v^2}{2} \right) + F(\omega) \right] \quad (29)$$

where  $v$  is the velocity of the pion. Hence :

$$\frac{d\sigma^-}{d\sigma^+} = \frac{1 - \frac{v^2}{2k^2} + (g_p + g_n) \frac{\omega}{M} \left( 1 - \frac{v^2}{2} \right)}{1 - \frac{v^2}{2k^2} - (g_p + g_n) \frac{\omega}{M} \left( 1 - \frac{v^2}{2} \right)} \quad (30)$$

It is noted that the factor  $v^2/2k^2$  was derived from the direct interaction term. The inclusion of this term and the magnetic moment factor is the main difference in the present approach from previous treatments of the theoretical value of the ratio. The relation (30) gives a value of 1.30 at pion threshold for the negative to positive ratio. In the energy region of particular interest (that is, up to photon energies of about 200 MeV), the ratio is constant within 4%. This is in good agreement with Moravcsik (1957a), and with the value of 1.33 obtained from the analysis of Baldin (1958), who compared the experimental total cross-sections of the  $\pi^+$  production of Beneventano et al (1956) and the  $\pi^-$  production results of Adamovich et al (1956), after correcting for the Coulomb effect. It was shown by Baldin (1958) that the  $\pi^-/\pi^+$  ratio for free nucleons was constant in the photon energy range 153 to 193 MeV.

If, now, this theoretical value of 1.30 is assumed to apply to the free nucleon production ratios in the photon energy range up to 200 MeV (at least), then the application of the theoretically derived Coulomb correction to these ratios should result in the expected trend of the  $\pi^-/\pi^+$  ratio with photon energy for deuterium bound nucleons. This procedure is not

so straight forward as appears in the first instance, what we are seeking to do is to correlate a free nucleon process with one involving the deuteron. The effect of this will make the ratios from deuterium slightly different from those expected from the individual nucleons. This can be seen when it is remembered firstly that three body kinematics are involved, and secondly that the ratio  $R$  is a function of pion energy and angle. Therefore, the observed deuterium data will correspond to an average of energies and angles for the individual processes. There is no doubt that some uncertainty is introduced when a comparison is made of single nucleon calculations with deuterium data, considering the lack of knowledge of the photon energy in the laboratory system. However, in view of the accuracy of even the best experimental ratio, it will be assumed that this complicated effect is negligibly small. In the application of Baldin's Coulomb correction, a pion energy (in the laboratory system) was selected, and the energy of the photon responsible for producing the pion was calculated assuming the kinematics of a free nucleon at rest. (This should not introduce a large error, according to the argument of Beneventano et al [1956s]). Thus, the Coulomb correction as a function

of pion energy was determined for energies less than 25 MeV, which was the upper limit of the validity of assumptions involved in the derivation of the correction. This is shown in figure 31, along with the four experimental ratios measured in this energy interval.

The conclusion from this is that the measured  $\pi^-/\pi^+$  ratios from deuterium are compatible, within experimental error, with the theoretical prediction for free nucleons, after the application of a reasonable Coulomb correction. This conclusion is in disagreement with that inferred by Beneventano et al (1956), but concords with Baldin (1958). In other words, the present experimental results together with the previous data have shown that there is no disparity between the observed  $\pi^-/\pi^+$  ratio, effectively from free nucleons, and that expected from well founded theory.

(b) Threshold Relationship between  $r_0$ , P and  $(\lambda_3 - \lambda_1)$

The importance of the negative to positive ratio in pion photoproduction can be seen from its place in the scheme which includes the threshold value of this ratio, the s-wave scattering phase shifts and the Panofsky ratio. That is, the pion production ratio

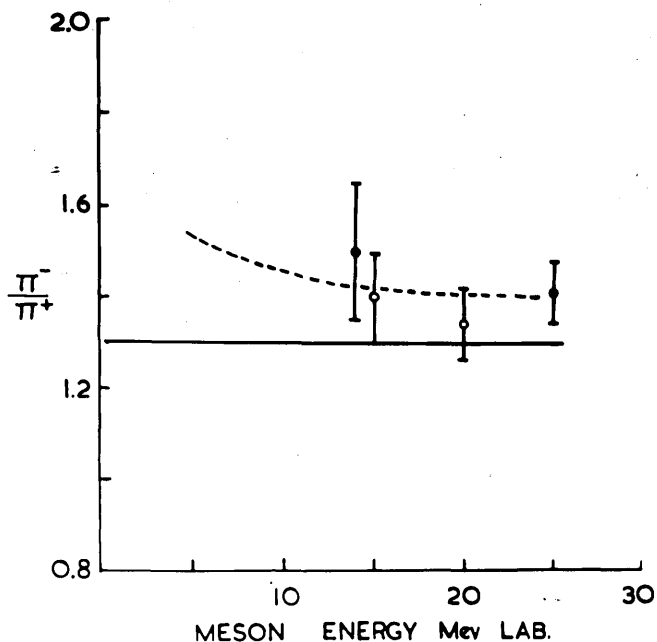


Figure 31.

Solid curve - drawn for  $r = 1.30$ ,  
dashed curve - derived from the solid curve by the  
application of the Coulomb correction of Baldin.

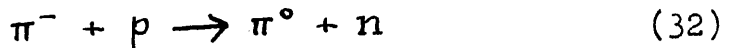
$\pi^-/\pi^+$  ratio from deuterium as a function of meson energy,  
angles measured in the laboratory system,  
 $\times$   $73^\circ$  Sands et al (1954),  $\bullet$   $75^\circ$  Beneventano et al (1956),  
 $\circ$   $75^\circ$  Present Results.

at low energy is one approach to the problem of the s-wave part of the pion-nucleon interaction.

The relationship between the s-wave processes at threshold can be expressed (as given in Appendix 1):

$$P = 3.17 \times 10^{-26} \frac{v^0}{c} \left[ \frac{(\lambda_3 - \lambda_1)^2}{r_0 \cdot \sigma_s^+ / q} \right] \quad (31)$$

This equality is only strictly obeyed at zero pion energy. Therefore, the problem is to extrapolate each measured quantity (which obviously is determined at a positive energy) to threshold. It has been shown, in section (a) of this Chapter, that the theoretical prediction of  $r_0 = 1.3$  is consistent with experiment. In equation (31),  $v^0$  is the velocity of the  $\pi^0$  meson in charge exchange scattering



The value of this parameter can be obtained in the work of Chinowsky and Steinberger (1954):

$$v^0 = (0.20 \pm 0.01) c \quad (33)$$

Cassels et al (1957) quoted a value of  $(0.204 \pm 0.005)$ , as determined by Keuhner et al. However, the former value will be used on the grounds that more details are known about its origin.

The remaining two factors in (31), namely  $(\lambda_3 - \lambda_1)$

and  $\sigma_S^+$ , present more difficulty. The magnitude of  $(\lambda_3 - \lambda_1)$  at positive pion energies is well established; the value assumed is taken from results (valid in the pion energy range 25 to 60 MeV) quoted by Puppi at the C.E.R.N. Conference (1958) :

$$(\lambda_1 - \lambda_3) = 0.283 \pm 0.012 \quad (34)$$

If the Orear (1956) linear extrapolation to threshold is assumed, then (34) is the quantity to be inserted into the relation (31). However, Cini et al (1958) put forward arguments which indicated that  $(\lambda_3 - \lambda_1)$  should be zero in the non-physical region at  $\omega = 0$ , where  $\omega$  is the total pion energy. If this is so, the effect is to cause  $(\lambda_1 - \lambda_3)$  to have a smaller value than (34) at  $\omega = 1$ , (in units of the pion rest mass  $\mu c$ ). Although the form of this extrapolation is not rigorously known, it must be an odd function of  $\omega$ . A linear extrapolation from  $(\lambda_1 - \lambda_3) = 0$  at  $\omega = 0$  to  $(\lambda_1 - \lambda_3) = 0.28$  at 40 MeV gives a value of  $(\lambda_1 - \lambda_3)_{\omega=1} = 0.22$ , while a cubic analysis gives 0.24. It is acknowledged that this introduces a further uncertainty into the analysis, but it is better than using the result (34) at threshold, since this is known to be theoretically unsound. A value of  $(\lambda_1 - \lambda_3) = 0.24 \pm 0.02$  was assumed.

In like manner, Cini et al (1958) dealt with the extrapolation of the positive pion cross-section to threshold, and argued that theoretically it would not be expected that  $A^+/W$  would be constant near threshold (in the notation of equation 17). Between photon energies of 170 and 265 MeV, it has been observed that this quantity was constant, within experimental error. However, Cini et al (1958) have shown that the inclusion of the direct interaction term in the s-wave extrapolation raised the cross-section at threshold by about 20%. Orear (1956) quoted the best experimental value, at that time,

$$\sigma_s^+ = (1.43 \pm 0.02) \times 10^{-28} q \text{ cm}^2 \quad (35)$$

while the new extrapolation gave

$$\sigma_s^+ = (1.87 \pm 0.13) \times 10^{-28} q \text{ cm}^2 \quad (36)$$

Hence, the indirect evaluation of the Panofsky ratio from the positive energy data can be made using the new extrapolations, Table 5.

As well as giving the new value of P, rows (a) and (b) of Table 5 are the data and results of previous work. The difference in row (a) from the information used by Beneventano et al (1956) is the value of  $(\lambda_1, -\lambda_3)$ , which these authors took to be 0.27. It is seen that the Panofsky ratio obtained

	$v^0/c$	$(\lambda_1 - \lambda_3)$	$r_0$	$\sigma_s^+ / q \times 10^{28.2} \text{ cm.}^2$	P
(a)	$0.20 \pm .01$	$0.28 \pm .01$	$1.87 \pm .13$	$1.43 \pm .02$	$1.86 \pm .26$
(b)	$0.20 \pm .01$	$0.28 \pm .01$	1.30	$1.43 \pm .02$	$2.67 \pm .33$
(c)	$0.20 \pm .01$	$0.24 \pm .02$	1.30	$1.87 \pm .13$	$1.50 \pm .18$

Values of the Panofsky Ratio Calculated from Positive Energy Data.

Table 5.

in row (a) is not altogether in disagreement with the observed values of P. However, the value of  $r_0 = 1.87$  is at variance with the theoretical prediction, and it is very difficult to reconcile the difference. Hence, this value of P must be rejected. If now,  $r_0$  is assumed to have the theoretical value, which at that time was not supported by experimental evidence, the value of P obtained, row (b), is about 40% higher than the highest observed ratio. This was calculated from the values of  $(\lambda_1 - \lambda_3)$  and  $\sigma_s^+$  resulting from a linear extrapolation of positive energy data to threshold. From the argument put forward by Cini et al (1958), the values assumed for  $(\lambda_1 - \lambda_3)$  and  $\sigma_s^+$  are those given in row (c). While there is yet no experimental evidence to give support to the new approach, it is believed that the theoretical basis of the paper of Cini et al is sound. Further, if one accepts the Baldin Coulomb correction and the new experimental data from deuterium, then the theoretical value of the threshold  $\pi^-/\pi^+$  ratio has experimental support. Therefore, if all these points are considered, the resulting Panofsky ratio is in good agreement with the experimental data from capture of  $\pi^-$  mesons in hydrogen. In other words, the

discrepancy (which amounted to about 50% at one time) in the relationship between the s-wave parts of pion scattering, photoproduction and absorption has been removed.

It must be acknowledged that there are possible alternative explanations of the discrepancy, as it existed at the beginning of 1958. Either the solution lay in the inaccuracy of the observed data and in fallacies in the relationship between them, or else the problem required re-thinking in terms of basic physics. As evidence for the former supposition, it is to be remembered that in the evaluation of  $(\lambda_3 - \lambda_1)$  from scattering results (by a phase shift analysis), two basic assumptions were involved.

(i) Only s-wave scattering contributed appreciably near threshold.

(ii) Total isotopic spin was a good quantum number. Noyes (1956) considered the second assumption, and this author estimated that the correction required to account for the failure in isotopic spin conservation in the  $(\pi^- + p \rightarrow \pi^0 + n)$  system amounted to about 10% (whereby causing a corresponding decrease in the predicted value of the Panofsky ratio), when the analysis was adjusted using the early value of  $P = 0.94$ .

The appropriate correction should be smaller in view of the higher value of  $P$  now observed, thereby reducing the effect of the radiative transition rate.

Another possibility was the view adopted by Baldin (1958), and Baldin and Kabir (1958) who considered the disparity in the values of the Panofsky ratio to be one reason for thinking in terms of the two-component  $\pi^0$  meson field hypothesis. It was suggested that the neutral mesons which were emitted when  $\pi^-$  mesons were absorbed in hydrogen might not be the usual  $\pi^0$  mesons occurring in symmetric meson theory, but may have isotopic spin  $T = 0$ , the  $\pi_0^0$  meson. From the evidence presented here, the s-wave pion-nucleon interaction has appeared to be given a reasonable explanation in the conventional way, without the additional revolutionary postulate of a second  $\pi^0$  meson. It is acknowledged that this is a negative argument, but it is not possible from photoproduction alone to settle the problem of a  $\pi_0^0$  meson. However, Cini et al (1958) have put forward a few cogent reasons for doubting the existence of the new particle of Baldin's hypothesis. These reasons were based on experimental cross-sections for the charge exchange process, and on the consistency of the experimental Panofsky ratio with the calculated

value from the threshold relationship. In other words, part of the argument of Cini et al was supported by the same conclusion as that found in this Thesis.

(c) Pion-Nucleon Coupling Constant.

As a corollary to the results of the deuterium experiment, it was possible to evaluate the renormalised pion-nucleon coupling constant. This derivation was based on the Kroll - Ruderman theorem, and the method adopted in the calculation was that suggested by Bernardini and Goldwasser (1954).

The differential cross-section, at  $90^\circ$  in the centre of mass system, for charged pion photoproduction at threshold ( $q = 0$ ) can be expressed in the form:

$$\frac{d\sigma^{\mp}}{d\Omega_{90^\circ}} = A^{\mp} \chi \quad (37)$$

where

$$\chi = \frac{q}{k} \left(1 + \frac{\omega}{M}\right)^{-1} \left(1 + \frac{k}{M}\right)^{-1}$$

in the same notation as before. The theorem of Kroll and Ruderman (1954) leads to the expression at threshold:

$$A^{\mp} = \frac{2e^2 f^2}{\mu^2} \left(1 + b \frac{\mu}{M} + \text{higher order terms in } \frac{\mu}{M}\right)$$

Therefore

$$\frac{2e^2 f^2}{\mu^2} = \frac{A^+}{2} \left\{ 1 + \frac{A^-}{A^+} \right\} \quad (38)$$

where  $e^2 = 1/137, f^2$  is the renormalised coupling constant, and  $\mu$  is the pion rest mass. The ratio  $A^-/A^+$  is the observed  $\pi^-/\pi^+$  ratio extrapolated to threshold. This has been shown to have the predicted theoretical value (within experimental error) in section (a) of this Chapter. Previous determinations of  $f^2$  by this method have used the uncorrected ratio from deuterium. In the present calculation, the new value of the s-wave  $\pi^+$  photoproduction amplitude at threshold was used. The new result along with the previous values of  $f^2$  obtained by this method from photoproduction are given in Table 6.

It is interesting to notice that the data used in the present calculation give rise to a slightly higher value of the pion-nucleon coupling constant, although the statistical significance of the result leaves much to be desired. What is now required is a reliable and accurate determination of the  $\pi^+$  cross-section at  $90^\circ$  c.m.s. at a photon energy around 160 MeV. This would verify the theoretical argument of Cini et al (1958), and at the same time give a more accurate value for the coefficient  $A^+$  in the relation (37).

The above values of  $f^2$  can be compared to 0.08

Reference	$A^+ \times 10^{29}$	$A^-/A^+$	$f^2$
Bernardini and Goldwasser (1954)	1.51 $\pm$ 0.14	1.51 $\pm$ 0.10	0.066 $\pm$ 0.008
Leiss et al (1955)	1.57 $\pm$ 0.05	1.40 $\pm$ 0.10	0.069 $\pm$ 0.004
Present results	1.83 $\pm$ 0.13	1.30 $\pm$ 0.10	0.073 $\pm$ 0.007

Renormalised Pion - Nucleon Coupling Constant.

Table 6.

---

which has been determined with great apparent reliability by several procedures, all agreeing well (for example, see Haber-Schaim 1956 and Goldwasser 1957). The significant conclusion to be drawn from Table 6 is that the value of the renormalised pion-nucleon coupling constant is gradually approaching the value obtained from pion scattering, as the experimental data are improved and as the theoretical treatment becomes more refined.

leches long (the surface was varnished to prevent oxidation) was exposed to the photon beam of mean energy  $130 \pm 10$  MeV. Neutrons emitted at  $90^\circ$  to the beam were detected in nuclear emulsions. The plates used in the experiments were Ilford G5 and G2 nuclear emulsions of 100 microns thickness and total area  $4" \times 2"$ . The geometry employed is shown in fig 2.

## Chapter VII.

The Photoproduction of Charged Pions from Calcium.

In this second investigation, it was decided to study the variation of the  $\pi^-/\pi^+$  ratio with meson energy at a fixed angle for calcium, the last stable symmetric nucleus. The detector used was nuclear emulsions, and the study was undertaken in co-operation with D. Sinclair of the Nuclear Plate Group of this Laboratory, the work of scanning and analysis of results being shared.

## (a) Experimental Arrangement.

A cylinder of calcium of one inch diameter and two inches long (the surface was varnished to prevent oxidation) was exposed to the photon beam of maximum energy  $330 \pm 10$  MeV. Mesons emitted at  $90^\circ$  to the beam were detected in nuclear emulsions. The plates used in the experiment were Ilford G5 and C2 nuclear emulsions of 100 microns thickness and total area of 4" x 2". The geometry employed is shown in figure 32 ; the top edge of each plate was 6.4 cm. from the centre of the calcium target and the copper absorber was 2.20 cm. thick.

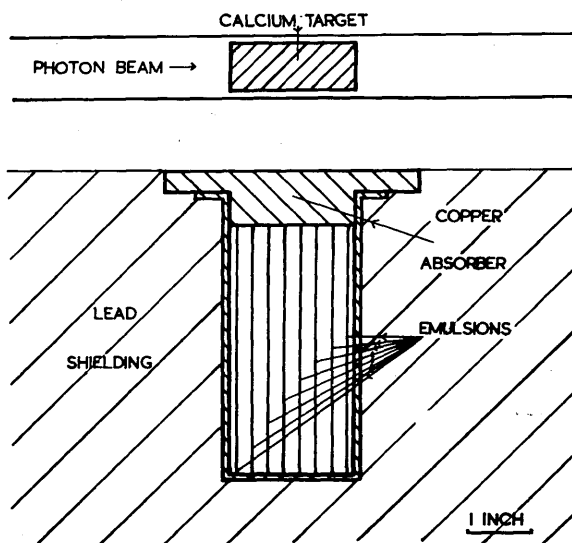


Figure 32.  
Experimental arrangement for calcium investigation.

To provide a homogeneous medium for stopping the mesons, eight plates were spaced at regular intervals in a 2" thick piece of glass of the same composition as that used as a backing for the emulsions. Thus the emulsions were used to sample the number of mesons stopping in the glass as a function of distance from the target.

With this geometry, the top edges of the plates received mesons with a maximum angular spread of  $\pm 37^\circ$  and a probable angular spread of  $\pm 11^\circ$  about the normal to the photon beam, while the corresponding figures for the bottom edges were  $\pm 15^\circ$  and  $\pm 5^\circ$  respectively. The kinetic energies of the mesons were obtained from range-energy relationships for the materials traversed i.e. calcium, copper and glass. Mesons in the energy interval 60 - 120 MeV could be detected with the apparatus.

It was found that those parts of the G5 plates which were nearer the target, and hence exposed to a large background of charged particles, were unusable even although these plates were exposed for a time shorter by a factor of  $2\frac{1}{2}$  than that for C2 plates, all of which could be scanned. The development of the plates was such that minimum ionising particles were not observable

in either type of plates with the result that the decay electrons and positrons from the  $\mu$  mesons could not be detected.

(b) Collection of Data.

The plates were scanned for meson endings with one or more secondary tracks, and the position and nature of each event was noted. Microscopes with X20 objectives were used for searching and all possible meson events were examined under X40 oil-immersion objectives. The total area scanned was 88.65 cm<sup>2</sup> and the scanning time took three months. Several areas of each plate were scanned by each observer to determine the efficiency of scanning. This varied between 60% for one-pronged events to over 90% for stars, depending on the type of plate, the background, and the experience of the scanner. The efficiency values obtained are indicated by comparing the figures given in columns 3 and 5 of Table 7 with those in columns 4 and 6.

Altogether, the number of meson events observed was 927 of which 699 were of the one-pronged type. The meson events were divided into five energy groups according to their position in the emulsions from the

(1)	(2)	(3)	(4)	(5)	(6)	(7)	(8)	(9)
62-83	80.2	146±12	218±26	63±7.9	70.5±9.3	1.05±.21	0.78±.15	0.86±.17
82-89	87.6	183±14	246±22	67±8.2	76.6±10.1	1.00±.18	0.74±.13	0.83±.15
88-98	94.2	175±13	237±28	57±7.6	68.8±11.1	0.92±.21	0.68±.15	0.77±.17
97-106	103.0	104±10	123±15	27±5.2	31.8±6.5	0.80±.21	0.60±.15	0.69±.18
106-119	111.9	91±10	109±14	14± 3.7	16.4±4.6	0.43±.14	0.33±.10	0.39±.11

(1) Pion energy interval MeV. (2) Mean pion energy MeV. (3) Observed number of one-prongs.  
(4) Corrected number of one-prongs  $\sigma_1$ . (5) Observed number of stars. (6) Corrected number of stars  $\sigma_n$ . (7) Uncorrected  $\pi^-/\pi^+$  ratio using data of row (c) of Table 8. (8) Uncorrected  $\pi^-/\pi^+$  ratio using (b) of Table 8. (9)  $\pi^-/\pi^+$  ratio, using (b) of Table 8, corrected for absorption.

Experimental Data of Calcium Experiment.

Table 7.

target. The number of mesons in each of these groups from the different plates was normalised for the area scanned, the exposure to the bremsstrahlung beam, the solid angle and the energy interval of the mesons under consideration. From this, the total yield of charged pions at  $90^\circ$  (laboratory co-ordinates) from calcium was found as a function of meson energy and is given in figure 33. Due to uncertainties in the beam calibration, the absolute scale of the differential cross section has an estimated error of  $\pm 10\%$ .

The analysis of the observations was based on the number of one -pronged meson events and on those with more than one secondary track, the ratio of  $\pi^-/\pi^+$  mesons was determined from these numbers together with established data of other authors on the prong frequency of  $\pi^-$  mesons in nuclear emulsion. The results of prong frequency measurements, in which the same convention was used to define a track length as in the present work, are shown in Table 8. From this, it is evident that there is a lack of consistency in the values obtained, and to illustrate the effect on the result of the  $\pi^-/\pi^+$  ratio, two ratios have been determined from two different sets of values of prong frequencies. If the

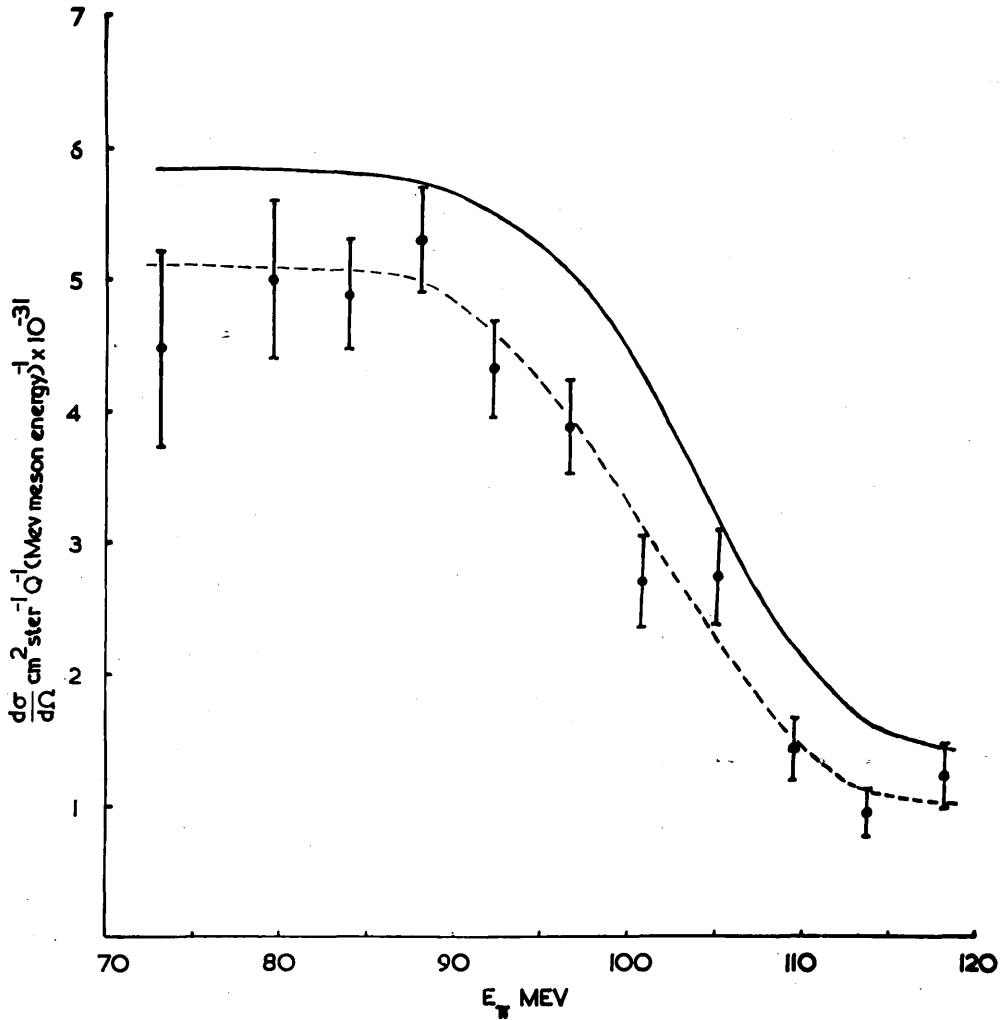


Figure 33.  
 Energy distribution of charged pions from calcium,  
 measured at  $90^\circ$  in the laboratory system.  
 Dashed curve - visual fit,  
 solid curve - corrected for absorption.

Reference	Number of Prongs						Track Length	Pions Observed
	N <sub>0</sub>	N <sub>1</sub>	N <sub>2</sub>	N <sub>3</sub>	N <sub>4</sub>	N <sub>5</sub>		
(a) Cheston and Goldfarb (1950)	18.9 +2.3	29.6 +2.3	21.9	18.9	8.8	1.9	0 $\mu$	429
(b) Menon et al (1950), Adelman and Jones (1950), and Adelman (1952)	26.8 +2.1	23.7 +0.7	23.9 +0.7	16.3 +0.6	7.7 +0.4	1.4 +0.1	3 $\mu$	3366
(c) Demeur et al (1956)	34.9 +2.5	26.0 +1.3	17.8 +1.1	13.2 +0.9	6.6 +0.6	1.6 +0.3	2 $\mu$	1038

Prong Frequency of  $\pi^-$  Mesons in Nuclear Emulsions.

Table 8.

fraction of  $\pi^-$  mesons ending in emulsions with two or more secondary tracks is  $f_n$  and if the corresponding fraction for one-pronged events is  $f_1$ , and since all  $\pi^+$  mesons produce single pronged events (viz.  $\pi^+-\mu^+$  decays), then the ratio of  $\pi^-$  to  $\pi^+$  mesons in a given number of events is 
$$\frac{N^-}{N^+} = \frac{\sigma_n}{f_n \sigma_1 - f_1 \sigma_n}$$
 where  $\sigma_n$  is the observed number of meson stars and  $\sigma_1$  are those with only one secondary track. This method of separation overcomes the uncertainties involved in distinguishing  $\mu$  mesons from  $\pi^-$  mesons with no secondary track, and  $\pi^+-\mu^+$  decays from  $\pi^-$  mesons with only one secondary track.

The data for the analysis of the  $\pi^-/\pi^+$  ratio are contained in Table 7 ; and the ratio as a function of pion energy is shown in figure 34, where the errors shown are statistical standard deviations and include statistical errors arising from the efficiency determinations. The solid curves show the results when corrected for meson absorption. These corrections, although small ( $\sim 10\%$ ), are somewhat uncertain. The method is therefore given in Appendix 2. It is to be noted that the absolute value of the  $\pi^-/\pi^+$  ratio depends on the data used for the percentage of one-pronged

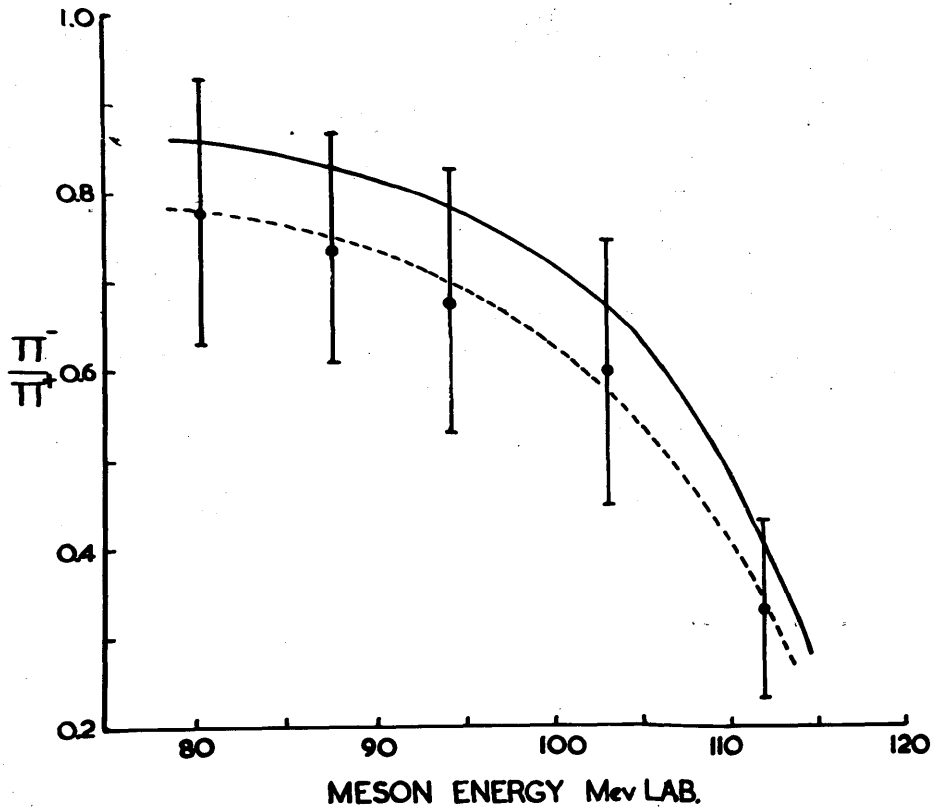


Figure 34.  
 $\pi^-/\pi^+$  ratio from calcium as a function of pion energy,  
 measured at  $90^\circ$  in the laboratory system.  
 Dashed curve - visual fit,  
 solid curve - corrected for absorption.

events and of stars in observed  $\pi^-$  events ending in emulsion.

(c) Interpretation of Results.

The first point to note is that the energy distribution of mesons obtained in the present work is consistent with a description in which the production arises from an interaction of the photon with a single nucleon in the nucleus. As stated in Chapter I, the production process from a complex nucleus, compared to that from a free nucleon is modified in the following way; there exists no unique photon energy corresponding to a given energy and angle of emission of the meson due to the spread in the momentum of the nucleons in the target nucleus. Instead, there corresponds a band of photons available for meson production, and the position of the band of photons in the bremsstrahlung spectrum depends on the binding energies of the target nucleons, and the interactions of the recoiling nucleons and mesons with the product nucleus.

Secondly, the rapid change in the  $\pi^-/\pi^+$  ratio above 95 MeV can be explained in terms of the differing positions in the bremsstrahlung spectrum of the bands of photons available for the production of

the  $\pi^-$  and  $\pi^+$  mesons respectively, and the existence of a cut-off in the spectrum at 330 MeV.

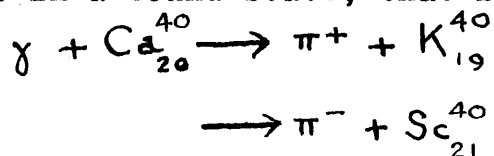
As an illustration, consider the factors influencing the production of  $\pi^-$  and  $\pi^+$  mesons emitted at  $90^\circ$  to the photon direction, with energies of 90 and 100 MeV. In the case of meson production from the surface of the nucleus, Butler (1952) has estimated that the bands of photons are about 50 MeV wide. It is further assumed that, on the average, the photon energy required for the production of the  $\pi^-$  meson is 10 MeV greater than that for the production of the  $\pi^+$ . A difference in energy of this magnitude would appear reasonable when considering the differences in the binding energies of the last added neutron and proton in the  $\text{Ca}^{40}$  nucleus. Thus, a  $\pi^-$  meson, emitted at  $90^\circ$  to the photon beam with a kinetic energy of 90 MeV, has available for its production a range of photon energies in the bremsstrahlung spectrum from about 290 MeV to the cut-off at 330 MeV, while for the  $\pi^+$  meson of the same kinetic energy and angle of emission the photon energies available are 280 to 330 MeV. At a higher kinetic energy of the pion, for example 100 MeV, the photon energies available for the production of the

$\pi^-$  and the  $\pi^+$  mesons are respectively 320 to 330 MeV and 310 to 330 MeV. Thus a variation of the  $\pi^-/\pi^+$  ratio with pion energy of the type observed would result in this way.

Any theoretical predictions concerning the photoproduction of charged pions at complex nuclei must be consistent with the following experimental observations; firstly, for a given nucleus, the cross-section per nucleon for the photoproduction of pions is considerably less than the corresponding cross-section for the free nucleon case. The observed pion yield shows an  $A^{2/3}$  dependence on the atomic mass number  $A$ , for values of  $A$  greater than 20 (for a full bibliography, see Imhof et al 1957). Secondly, there is evidence for a strong correlation between the structure of the nucleus and the  $\pi^-/\pi^+$  ratio for complex nuclei, as indicated by the relationship between the  $\pi^-/\pi^+$  ratio, the mass difference of the nearest isobars to the target nucleus ( $M_{Z-1} - M_{Z+1}$ ), and the atomic number  $Z$  of this nucleus, (see Littauer and Walker 1952, and Motz et al 1955b).

This correspondence between  $\pi^-/\pi^+$  ratios and ( $M_{Z-1} - M_{Z+1}$ ) values can be illustrated by photoproduction at the calcium nucleus; in charged pion photoproduction, a nucleon changes from a proton to a

neutron, or vice versa. In the calcium nucleus, the pion production can be considered to leave the calcium nucleus in a bound state, that is



The transformation into  $\text{Sc}_{21}^{40}$  involves a much greater energy increase than into  $\text{K}_{19}^{40}$  because of the substantial Coulomb energy. There is, therefore, a bias towards  $\pi^+$  production. This preference for the transformation into  $\text{K}_{19}^{40}$  is a characteristic of the calcium nucleus; it would not be expected that an even-even nucleus would have a Z value of 20, but rather one with  $N > Z$  where N is the number of neutrons in the nucleus. This exception is explained by the Shell Model of the nucleus, in which 20 is a magic number. This predicts that there would be a strong preference in a reaction involving the calcium nucleus to form a product nucleus by the transformation of a proton into a neutron. This suggests that the  $\pi^-/\pi^+$  ratio from calcium would be less than unity.

(d) Discussion.

Theoretically, two types of mechanisms of pion photoproduction from complex nuclei have been suggested; the first of these is volume production, in which it is

assumed that pions can be produced with equal probability throughout the nucleus. Secondly, surface production, that is production from the nuclear surface, outside the nuclear radius.

The view that only nucleons at the nuclear surface contributed to pion production was adopted by Butler (1952). The main points of this argument were as follows; from a general consideration of pion production, it was postulated that some of the pions would be absorbed before they escaped from the nucleus. Since absorption of a meson produced in the core of a nucleus was more probable than for one produced at the surface, this led to the  $A^{2/3}$  dependence of the total pion yield. The absorption mean free path, however, of pions in nuclear matter appeared too small to account for the  $A^{2/3}$  law as due only to meson absorption. Wilson (1952) postulated that suppression of meson production from the nuclear core could be understood in terms of a competing photodisintegration process, due to meson exchange effects between strongly interacting nucleons within the nucleus.

A surface production model similar to that of Butler, was assumed by Laing and Moorhouse (1957), who considered the production of charged pions on the

basis of a simple independent particle model with a square well potential. These authors extended the calculations of surface production to include the effects of meson scattering and absorption on the surface. In particular, calculations of cross-sections and  $\pi^-/\pi^+$  ratios were carried out for photoproduction of pions from calcium. The results indicated that the cross-sections obtained from their surface production model were inconsistent with the experimental data, but that volume production accounted for the main contribution to the cross-section.

A useful experimental contribution to this field was that of Belousov et al (1956) who investigated the dependence on atomic mass number of the  $\pi^-$  and  $\pi^0$  photoproduction cross-sections from different nuclei using a bremsstrahlung beam of a maximum energy, firstly of 200 MeV and then of 265 MeV. These authors noted that in the experiment of Littauer and Walker (1952), the charged pions detected had energies of 65 MeV, at which a pion energy the cross-section for inelastic interaction with the nucleus was comparable to the geometric cross-section, so that nuclear absorption of the pion in the core would not be

unexpected. Hence, they investigated the photo-production of pions with energies less than 20 MeV, where the nucleus is mainly transparent. The result of the  $\pi^0$  experiment was that a linear dependence of the cross-section on  $A^{2/3}$  was obtained for the two different maximum energies of bremsstrahlung used. Now, in going from a maximum energy of 265 MeV to 200 MeV in the photon spectrum, the peak pion energy shifted from about 65 to 20 MeV. This fact together with the observation, that the absorption cross-section decreases with pion energy, suggested that if the pions were produced by photons in the entire nuclear volume, the  $\pi^0$  cross-section should have shown a different dependence on  $A$  when the peak pion energy was 65 MeV than when it was 20 MeV. The experimental result indicated that the observed cross-section could not be explained by the reabsorption of mesons produced inside the nucleus. This was the conclusion reached by Baldin and Lebedev (1958) who considered the interaction of pions with nuclei in which the pion wavelength exceeded the size of the nucleus.

On the other hand, Francis and Watson (1953a) and (1953b) claimed that the  $A$  dependence of the photo-production, and scattering, cross-sections was not

inconsistent with the optical model. They postulated that it was unnecessary to consider any suppression process of pion production from the core. Instead, these authors took the view that there was still sufficient uncertainty in the values of the mean free path, for the interaction of pions in nuclear matter, not to exclude pion reabsorption and scattering as being the reasons for the observed suppression (for example, see Stork 1954). The experimental test of the optical model was carried out by Imhof et al (1957), who investigated the dependence of positive photopion production on atomic number for a range of nuclei. If effects of the Coulomb potential and the potential arising from the pion-nucleon interaction were taken into account, then it was found that there was fair agreement with the optical model. It was observed that while the results of this experiment were consistent with a surface production model, such as that of Butler, it was unnecessary to think in terms of such a model, with its additional assumptions, because of the agreement with the optical model.

(e) Conclusions.

The present state of the interpretation of experimental results of photoproduction of pions from complex nuclei can be summarised as follows; the

argument put forward by Butler (1952), for surface production was based on the observation that volume production gave too large a pion production cross-section, and that this was difficult to explain in terms of reabsorption of the pions. This is in agreement with the experimental results of Belousov et al (1956), and the analysis of Baldin and Lebedev (1958). The mechanism of the suppression of pion production from the nuclear core was proposed by Wilson (1952) and (1956). This surface production model was supported by George (1956), by evidence from experiments on the photoproduction of stars and pions in nuclear emulsions. In contrast to this, Francis and Watson (1953a) showed that the experimental results of the photoproduction of pions from complex nuclei could be explained in terms of the optical model. Imhof et al (1957) produced experimental support of this, after a full investigation. The above illustrates the complexity of the problem of the mechanism of photoproduction from nuclei of high atomic number. It is concluded, that it is difficult to fit both the observed cross-sections and the  $\pi^-/\pi^+$  ratios simultaneously, and also to say with certainty which theoretical predictions are model independent.

Regarding the experimental results of this present work, the three most interesting points can be summarised thus; the calcium experiment shows in a qualitative way the mechanism of charged pion photo-production from the calcium nucleus, namely that the production process involves individual nucleons. Secondly, whereas the previous results of the  $\pi^-/\pi^+$  ratio from calcium referred to one energy range of the pions at a given angle, the above results are of interest in showing the variation of the ratio with pion energy. Finally, the way in which the observed trend of the  $\pi^-/\pi^+$  ratio could be explained by the position in the bremsstrahlung spectrum of the bands of photons responsible for the  $\pi^-$  and the  $\pi^+$  meson production and by the cut-off in this spectrum, supports the explanation of the strong dependence of the  $\pi^-/\pi^+$  ratio on  $(M_{Z-1} - M_{Z+1})$  found by Littauer and Walker (1952). This was due to the fact that the pions they detected (65 MeV at  $135^\circ$  to the photon beam) were produced by bands of photons near the cut-off in the bremsstrahlung spectrum, where the influence of binding energy effects would be most apparent.

Appendix.

1. Derivation of the Panofsky Ratio  $P$  from the  $\pi^-/\pi^+$  Deuterium Ratio at Threshold and the S-wave Scattering Lengths.

Pion-nucleon scattering data can be analysed on the assumption that isotopic spin behaves as a quantised angular momentum vector in isotopic spin space. In the scattering of mesons by protons, the orientation of the isotopic spin vectors is mixed (spin up and spin down) and both isotopic spins  $3/2$  and  $1/2$  are involved. It follows that the scattering features at any given energy will be determined by the phase shifts of the different states of given isotopic spin, orbital and total angular momenta. If it is assumed that only s- and p- states are important, there will be six phase shifts at each energy. These correspond to the possible values of  $3/2$  and  $1/2$  of the isotopic spin, and for each of these values to the s-wave phase shift and to the phase shifts of the two p-waves of angular momentum  $3/2$  and  $1/2$ . These are designated:

	$I = 3/2$	$I = 1/2$
s-waves : $\ell = 0, j = 1/2$	$\alpha_3$	$\alpha_1$
p-waves : $\ell = 1, j = 1/2$	$\alpha_{31}$	$\alpha_{11}$
$\ell = 1, j = 3/2$	$\alpha_{33}$	$\alpha_{13}$

Such a phase shift analysis of charge exchange scattering gives the following expression for the centre of mass angular distribution:

$$\frac{d\sigma(\pi^- \rightarrow \pi^0)}{d\Omega_{c.m.}} = \frac{\lambda^2 v_0}{18 v_-} \left\{ |a + b \cos \theta|^2 + |c|^2 \sin^2 \theta \right\} \quad (A1)$$

where  $\lambda$  is the de Broglie wavelength of the pion,

$$\begin{aligned} a &= e^{2i\alpha_3} - e^{2i\alpha_1} \\ b &= 2 e^{2i\alpha_{33-}} - 2e^{2i\alpha_{13+}} - e^{2i\alpha_{31}} - e^{2i\alpha_{11}} \\ c &= e^{2i\alpha_{33-}} - e^{2i\alpha_{31}} - e^{2i\alpha_{13+}} + e^{2i\alpha_{11}} \end{aligned} \quad (A2)$$

The main interest in this is the application to the nuclear absorption of  $\pi^-$  mesons from the K-shell in hydrogen. In this energy region the p-wave phase shifts are negligible, for example in the pion energy range 25 to 65 MeV, the Rochester results (Barnes et al 1958) are

$$\begin{aligned} \alpha_{31} &= (-0.044 \pm 0.005) q^3 & \alpha_{13} &= (-0.049 \pm 0.061) q^3 \\ \alpha_{11} &= (-0.017 \pm 0.011) q^3 & \alpha_{33} &= (+0.234 \pm 0.019) q^3 \end{aligned}$$

where it is noted that the p-wave phase shifts increase proportionally by the third power of the centre of mass pion momentum  $q$ . Hence, neglecting p-wave phase shifts and taking  $\sin \alpha \sim \alpha$ , one obtains

$$\frac{d\sigma(\pi^- \rightarrow \pi^0)}{d\Omega_{c.m.}} = \frac{2}{9} \lambda^2 \frac{v_0}{v_-} (\alpha_3 - \alpha_1)^2 \quad (A3)$$

where  $v_0/v_-$  is the ratio of the velocities of the incident  $\pi^-$  and the emitted  $\pi^0$  meson in the centre of mass system. Here  $v_0/v_-$  is a kinematic factor to

account for the  $(\pi^- - \pi^0)$  mass difference which cannot be neglected at low energies.

On integration, the total cross-section is found:

$$\sigma(\pi^- \rightarrow \pi^0) = \frac{8\pi\lambda^2}{9} \cdot \frac{V_0}{V_-} (\alpha_3 - \alpha_1)^2 \quad (A4)$$

Alternatively, this can be expressed in terms of the scattering lengths:

$$\sigma(\pi^- \rightarrow \pi^0) = \frac{8\pi}{9} \cdot \frac{V_0}{V_-} \lambda_c^2 (\lambda_3 - \lambda_1)^2 \quad (A5)$$

where  $\lambda_c$  is the pion Compton wavelength.

As already stated in Chapter I, the Panofsky ratio P can be used to connect the positive energy s-wave cross-sections for pion-proton scattering and pion photoproduction (Anderson and Fermi 1952). This relationship between positive energy and zero energy processes can be established if it is assumed that the transition rate for these low energy pion processes is proportional to the square of the modulus of the pion wave function at the position of the proton. If, further, Coulomb effects are neglected, it follows that the absorption cross-sections at very low positive energies (e.g. in the pion photoproduction, the momentum of the photon in the centre of mass system is assumed to be constant) obey the "1/v law",

$$\sigma = K/v \quad (A6)$$

where  $q$  is the pion momentum in terms of  $\mu c$ , being the pion rest mass. The constant  $K$  is given by the k-shell absorption rate  $w$  as follows:

$$w = c \frac{K}{\pi b_0^3} \quad (\text{A7})$$

where  $b_0$  is the Bohr radius calculated for the reduced pion mass. (See Born 1952). Hence, for the application to the Panofsky ratio, it is permissible to write

$$w = A \sigma \quad (\text{A8})$$

where  $A$  is a constant.

If this is applied to equation (A5), the following transition rate is obtained

$$w(\pi^- \rightarrow \pi^0) = \frac{8\pi}{9} \cdot \frac{V_0}{V_-} A \lambda_c^2 (\lambda_3 - \lambda_1)^2 \text{sec}^{-1} \quad (\text{A9})$$

By definition, we have

$$R_0 = \left[ \frac{\sigma(\gamma + d \rightarrow \pi^- + 2p)}{\sigma(\gamma + d \rightarrow \pi^+ + 2n)} \right]_{\omega=1} \quad (\text{A10})$$

and

$$r_0 = \left[ \frac{\sigma(\gamma + n \rightarrow \pi^- + p)}{\sigma(\gamma + p \rightarrow \pi^+ + n)} \right]_{\omega=1} = CR_0 \quad (\text{A11})$$

where  $C$  is the value of the Coulomb correction,  $0 < C < 1$ , and  $\omega$  is the pion energy in the centre of mass system, in units of the pion rest mass.

Now by the principle of detailed balancing

$$\sigma(\pi^- + p \rightarrow n + \gamma) = 2 \frac{p_\gamma^2}{p_\pi^2} \sigma(\gamma + n \rightarrow \pi^- + p) \quad (\text{A12})$$

where  $p_\gamma$  is the photon momentum } in the centre of  
and  $p_\pi$  is the pion momentum } mass system.

Therefore,

$$\sigma(\pi^- + p \rightarrow n + \gamma) = 2 r_0 \frac{p_\gamma^2}{p_\pi^2} \sigma(\gamma + p \rightarrow \pi^+ + n) \quad (\text{A13})$$

At threshold

$$P_\gamma = \mu c \frac{\left(1 + \frac{\mu}{2M}\right)}{\left(1 + \frac{\mu}{M}\right)} \quad (\text{A14})$$

where  $M$  is the nucleon mass.

$$\text{Hence, } \omega(\pi^- \rightarrow \gamma) = 2A r_0 \frac{P_\gamma^2}{P_\pi^2} \sigma(\gamma + p \rightarrow \pi^+ + n) \text{ sec}^{-1} \quad (\text{A15})$$

The Panofsky ratio is obtained by combining (A9) and (A15) :

$$P = \frac{\omega(\pi^- \rightarrow \pi^0)}{\omega(\pi^- \rightarrow \gamma)} = \frac{4\pi}{9} \chi_c^2 \frac{\left(1 + \frac{\mu}{M}\right)^2}{\left(1 + \frac{\mu}{2M}\right)^2} \cdot \frac{v_0}{c} \cdot \frac{(\lambda_3 - \lambda_1)^2}{r_0 \cdot \sigma_s^+ / q} \quad (\text{A16})$$

where  $\sigma_s^+$  is the s-wave contribution to the total cross-section for the process  $\gamma + p \rightarrow \pi^+ + n$  at threshold.

If it can be experimentally verified that  $CR_0 = r_0$ , where  $r_0$  is the theoretical prediction for the ratio, then it is possible to express the Panofsky ratio in terms of the measurable quantities (determined at positive energies) :  $R_0$ ,  $(\lambda_3 - \lambda_1)$ ,  $\sigma_s^+$ , and  $v_0$ .

Equation (A16) can be evaluated to give:

$$P = 3.17 \times 10^{-26} \frac{v_0}{c} \left[ \frac{(\lambda_3 - \lambda_1)^2}{r_0 \cdot \sigma_s^+ / q} \right] \quad (\text{A17})$$

This is equivalent to equation (15) in Chapter II, where  $v_0/c$  was taken to have the value of 0.20 in accordance with the measurements of Chinowsky and Steinberger (1954).

## 2. Absorption of Mesons.

The number of pions  $dN$  absorbed in a thickness of absorber  $dx$  is given by the relation

$$\frac{dN}{N} = -n \sigma dx \quad (\text{A18})$$

where  $n$  is the number of nuclei in unit volume of the absorber and  $\sigma$  is the absorption cross-section. The difference in the absorption of positive and negative pions is given by

$$\frac{dN^-}{N^-} - \frac{dN^+}{N^+} = -n(\sigma^- - \sigma^+) dx \quad (\text{A19})$$

where the superscripts refer to the charge of the meson.

There have been many measurements of the mean free paths of  $\pi^-$  and  $\pi^+$  mesons in various materials, including nuclear emulsions. If it is verified that the quantity  $(\sigma^- - \sigma^+)$  for a given absorber is independent of the kinetic energy of the meson in a particular energy interval, then equation (A19) may be integrated to give the result

$$\frac{N_0^-}{N_0^+} = \frac{N^-}{N^+} \exp\left\{n(\sigma^- - \sigma^+) x\right\} \quad (\text{A20})$$

where  $N_0$  is the flux of mesons at the source, and  $N^-/N^+$  is the observed ratio.

Now, consider the application of (A20) to the results of the calcium experiment. Bernardini et al (1951), Bernardini and Levy (1951), and Ferretti and Manaresi (1955) have measured the mean free paths of charged pions in nuclear emulsions. The combined results of these workers indicated that the quantity  $(\sigma^- - \sigma^+)$  was independent of pion energy in the range 20 to 90 MeV. An average of the results of these authors gave a value of 0.26 barns for  $(\sigma^- - \sigma^+)$ , where  $\sigma$  is the cross-section for star production together with inelastic scattering by the nuclei of an emulsion, excluding hydrogen. Since the average geometric cross-section of the elements in the glass was 0.67 of that for the complex nuclei in an emulsion, the quantity  $(\sigma^- - \sigma^+)$  for glass was taken to be  $0.67 \times 0.26$ , that is 0.17 barns. This has a large experimental error (about 30%). For copper  $(\sigma^- - \sigma^+) = 0.46$  barns, a value found experimentally by Cassels (reported by Burcham 1955). Other measurements, however, of the absorption of pions in copper would tend to give a smaller value for  $(\sigma^- - \sigma^+)$ , see Chedester et al (1951), and Martin (1952). A change of even 30%, however, in  $(\sigma^- - \sigma^+)$  altered the  $\pi^-/\pi^+$  ratio for calcium by only 5%.

Publications.

1. The Photoproduction of Charged Mesons from Calcium,  
by W.R. Hogg and D. Sinclair. Philosophical  
Magazine 1, 466, 1956.
2. The Photoproduction of Charged Pions from Deuterium,  
by W.R. Hogg and E.H. Bellamy. Proceedings of the  
Physical Society 72, 895, 1958.

## References.

Abbreviations: Physical Review - P.R., Nuovo Cimento - N.C., Nuovo Cimento Supplement - N.C.S., Proceedings of the Physical Society Section A - P.P.S.A, Review of Scientific Instruments - R.S.I., and Bulletin of the American Physical Society - B.A.P.S.

Adamovich, M.I., Veksler, V.I., Kuzmicheva, G.V.,  
Larionova, V.G., and Kharlamov, S.P., (1956),  
C.E.R.N. Symposium.

Adelman, F.L., (1952), P.R. 85, 249.

Adelman, F.L., and Jones, S.B., (1950), Science 111, 226.

Alston, M.H., Evans, W.H., Fidecaro, M., Newport, R.W.,  
Von Gierke, G., and Williams, P.R., (1956) P.P.S.A  
69, 798.

Anderson, H.L., and Fermi, E., (1952), P.R. 86, 794.

Atkinson, J.R., McFarlane, W., Reid, J.M., and Swinbank,  
P., (1957), Nuclear Instruments, 1, 152.

Baldin, A., (1958), N.C. 8, 569.

Baldin, A.M., and Kabir, P.K., (1958), N.C. 9, 547.

Baldin, A.M., and Lebedev, A.I., (1958), Soviet  
Physics, J.E.T.P., 6, 940.

- Barnes, S.W., Rose, B., Giacomelli, G., Ring, J., and Miyake, K., (1958), University of Rochester, Dept. of Physics Report NYO-2170.
- Belousov, A.S., Popova, V.M., Semashko, N.G., Shitov, E.V., Tamm, E.I., Veksler, V.I., and Iagudina, F.R., (1956), C.E.R.N. Symposium.
- Beneventano, M., Bernardini, G., Carlson-Lee, D., Stoppini, G., and Tau, L., (1956), N.C. 4, 323; (1956s), N.C.S. 2, 926.
- Beneventano, M., Carlson-Lee, D., Stoppini, G., Bernardini, G., and Goldwasser, E.L. (1954), N.C. 12, 156.
- Bernardini, G., and Goldwasser, E.L., (1954), P.R. 95, 857.
- Bernardini, G., and Levy, F., (1951), P.R. 84, 610.
- Bernardini, G., Booth, E.T., and Lederman, L., (1951), P.R. 83, 1075.
- Bethe, H.A., and de Hoffmann, F., (1955), "Mesons and Fields", Volume II - Mesons; Row, Peterson and Company, New York.
- Bishop, A.S., Steinberger, J., and Cook, L.J., (1950), P.R. 80, 291.
- Bodansky, D., Sachs, A.M., and Steinberger, J., (1953), P.R. 90, 997; (1954), P.R. 93, 1367.

- Born, M., (1952), "Atomic Physics" page 351; Blackie and Son, Ltd., London and Glasgow.
- Brueckner, K.A., (1950), P.R. 79, 641.
- Brueckner, K.A., and Case, K.M., (1951), P.R. 83, 1141.
- Brueckner, K.A., and Goldberger, M.L., (1949), P.R. 76, 1725.
- Brueckner, K.A., and Watson, K.M., (1952), P.R. 86, 923.
- Burcham, W.E., (1955), Nature 176, 371.
- Butler, S.T., (1952), P.R. 87, 1117.
- Carlson-Lee, D., (1958), B.A.P.S. 3, 334.
- Carlson-Lee, D., Stoppini, G., and Tau, L., (1955), N.C. 2, 162.
- Cassels, J.M., Fidecaro, G., Wetherell, A.M., and Wormald, J.R., (1957), P.P.S.A 70, 405.
- Chedester, C., Isaacs, P., Sachs, A., and Steinberger, J., (1951), P.R. 82, 958.
- Cheston, W.B., and Goldfarb, L.J.B., (1950), P.R. 78, 683.
- Chew, G.F., (1953), P.R. 89, 591; (1954), P.R. 94, 1748; (1954), P.R. 95, 1669.
- Chew, G.F., and Low, F.E., (1956), P.R. 101, 1579.
- Chew, G.F., Goldberger, M.L., Low, F.E., and Nambu, Y., (1957), P.R. 106, 1345.
- Chinowsky, W., and Steinberger, J., (1954), P.R. 93, 586.

- Cini, M., Gatto, R., Goldwasser, E.L., and Ruderman, M., (1958), Preprint.
- Cook, L., (1951), R.S.I. 22, 1006.
- Crowe, K.M., (1957), N.C. 5, 541.
- Crowe, K.M., Friedman, R.M., and Hagerman, D.C., (1955), P.R. 100, 1799. (See Hagerman et al 1957).
- Demeur, M., Huleux, A., and Vanderhaeghe, G., (1956), N.C. 4, 509. (See Vanderhaeghe and Demeur 1956).
- De Sabbata, V., Manaresi, E., and Puppi, G., (1953), N.C. 10, 1704.
- Dunoyer, L., (1926) "Vacuum Practice"; Bell and Sons Ltd., London.
- Edwards, M.H., (1956), American Journal of Physics, 24, 43.
- Ferretti, L., and Manaresi, E., (1955), N.C. 1, 512.
- Fischer, J., March, R., and Marshall, L., (1958), P.R. 109, 533.
- Francis, N.C., and Watson, K.M., (1953a), P.R. 89, 328; (1953b), American Journal of Physics, 21, 659.
- Gell-Mann, M., and Watson, K.M. (1954), Annual Review of Nuclear Science, 4, 219.
- George, E.P., (1956), P.P.S.A 69, 110.
- Goldwasser, E.L., (1957), High Energy Nuclear Physics Conference, Rochester.

- Haber-Schaim, U., (1956), P.R. 104, 1113.
- Hagerman, D.C., Crowe, K.M., and Friedman, R.M. (1957),  
106, 818.
- Igo, G., and Eisberg, R.M., (1954), R.S.I. 25, 450.
- Imhof, W., Knapp, E.A., Easterday, H., and Perez-Mendez,  
V., (1957), P.R. 108, 1040.
- Jakobson, M., Schulz, A., and Steinberger, J., (1951),  
P.R. 81, 894.
- Jenkins, T.L., Luckey, D., Palfrey, T.R., and Wilson,  
R.R., (1954), P.R. 95, 179.
- Kaplon, M.F., (1951), P.R. 83, 712.
- Klein, A., (1955), P.R. 99, 998.
- Knapp, E., Imhof, W., Kennedy, W., and Perez-Mendez, V.,  
(1957), P.R. 107, 323.
- Kroll, N.M., and Ruderman, M.A., (1954), P.R. 93, 233.
- Kuehner, J.A., Merrison, A.W., and Tornabene, S., (1956),  
C.E.R.N. Symposium, (also reported by Cassels et  
al 1957).
- Laing, E.W., and Moorhouse, R.G., (1957), P.P.S.A 70, 629.
- Land, R.H., (1956), C.E.R.N. Symposium.
- Landau, L., (1944), Journal of Physics, (U.S.S.R.)  
8, 201.
- Landecker, K., and Gray, A.J., (1954), R.S.I. 25, 1151.
- Lax, M., and Feshbach, H., (1951), P.R. 81, 189.

Lebow, I.L., Feld, B.T., Frisch, D.H., and Osborne,  
L.S., (1952), P.R. 85, 681.

Leiss, J.E., Robinson, C.S., and Penner, S., (1955),  
P.R. 98, 201.

Leonard, S.L., and Stork, D.H., (1954), P.R. 93, 568.

Lindenfeld, P., Sachs, A., and Steinberger, J., (1953),  
P.R. 89, 531.

Littauer, R., (1958), R.S.I. 29, 178.

Littauer, R.M., and Walker, D., (1952), P.R. 86, 838.

Low, F.E., (1955), P.R. 97, 1392.

McFarlane, W., Barden, S.E., and Oldroyd, D.L., (1955),  
Nature, 176, 666.

McMillan, E.M., Peterson, J.M., and White, R.S., (1949),  
Science, 110, 579.

Machida, S., and Tamura, T., (1951), Progress of  
Theoretical Physics, 6, 572.

Malmberg, J.H., and Robinson, C.S., (1958), P.R.  
109, 158.

Marshak, R., (1952), "Mesons Physics"; McGraw-Hill  
Book Company Inc., New York.

Martin, R.L., (1952), P.R. 87, 1052.

Menon, M.G.K., Muirhead, H., and Rochat, O., (1950),  
Philosophical Magazine, 41, 583.

- Moravcsik, M.J., (1956), P.R. 104, 1451; (1957a),  
P.R. 105, 267; (1957b), P.R. 107, 600;  
(1958), N.C. 7, 442.
- Motz, H., Crowe, K.M., and Friedman, R.M., (1955a),  
P.R. 98, 268; (1955b), P.R. 99, 673.
- Nagle, D.E., (1955), P.R. 97, 480.
- Nagle, D.E., Hildebrand, R.H., and Plano, R.J.,  
(1957), P.R. 105, 718.
- Nicolai, V.O., (1955), R.S.I. 26, 1203.
- Noyes, H.P., (1956), P.R. 101, 320.
- Oakley, D.C., and Walker, R.L., (1955), P.R. 97, 1283.
- Orear, J., (1954), P.R. 96, 176; (1956), N.C. 4, 856.
- Orear, J., Lord, J.J., and Weaver, A.B., (1954a),  
P.R. 93, 575.
- Orear, J., Slater, W., Lord, J.J., Eilenberg, S.L.,  
and Weaver, A.B., (1954b), P.R. 96, 174.
- Palfrey, T.R., Luckey, D., and Wilson, R.R., (1953),  
P.R. 91, 468.
- \*  
Perry, J.P., and Angell, C.E., (1953), P.R. 91, 1289.
- Puppi, G., (1958), reported at the C.E.R.N. Conference.
- Rinehart, M.C., Rogers, K.C., and Lederman, L.M. (1955),  
P.R. 100, 883.
- Rogers, K.C., and Lederman, L.M., (1957), P.R. 105, 247.
- Saito, Y., Watanabe, Y., and Yamaguchi, Y., (1952),  
Progress of Theoretical Physics 7, 103.

- Sands, M., Teasdale, J.G., and Walker, R.L., (1954),  
P.R. 95, 592; (1954), P.R. 96, 849.
- Spry, W.J., (1954), P.R. 95, 1295.
- Squire, C.F., (1953), "Low Temperature Physics";  
McGraw-Hill Publishing Company Ltd., London.
- Steinberger, J., and Bishop, A.S., (1950), P.R. 78, 494.
- Stork, D.H., (1954), P.R. 93, 868.
- Swenson, C.A., and Stahl, R.H., (1954), R.S.I. 25, 608.
- Tinlot, J., and Roberts, A., (1954), P.R. 95, 137.
- Tollestrup, A.V., Keck, J.C., and Worlock, R.M., (1955),  
P.R. 99, 220.
- Tracy, J.F., (1953), P.R. 91, 960.
- Vanderhaeghe, G., and Demeur, M., (1956), N.C.S. 2, 931.
- Walker, R.L., Teasdale, J.G., Peterson, V.Z., and Vette,  
J.I., (1955a), P.R. 99, 210.
- Walker, R.L., Oakley, D.C., and Tollestrup, A.V.,  
(1955b), P.R. 97, 1279.
- Waters, J.R., (1957), B.A.P.S. 2, 195.
- Watson, K.M., (1952), P.R. 85, 852.
- Watson, K.M., Keck, J.C., Tollestrup, A.V., and Walker,  
R.L., (1956), P.R. 101, 1159.
- Whalin, E.A., and Reitz, R.A., (1955), R.S.I. 26, 59.
- Whetstone, S.L., and Stork, D.H., (1956), P.R. 102, 251.
- White, R.S., Jacobson, M.J., and Schulz, A.G., (1952),  
P.R. 88, 836.

Wilson, R.R., (1952), P.R. 86, 125; (1956), P.R.  
104, 218.

Woolley, H.W., Scott, R.B., and Brickwedde, F.G.,  
(1948), Journal of Research of the National  
Bureau of Standards 41, 379.

\* Panofsky, W.K.H., Aamodt, R.L., and Hadley, J., (1951),  
P.R. 81, 565.